

# **The Role of EF-G in Translational Reading Frame Maintenance on the Ribosome**

**Dissertation**

for the award of the degree

**“Doctor rerum naturalium” (Dr.rer.nat.)**

of the Georg-August-Universität Göttingen

within the doctoral program:

GGNB Biomolecules: Structure – Function -Dynamics  
of the Georg-August University School of Science (GAUSS)

submitted by

**Bee-Zen Peng**

From Taichung, Taiwan

Göttingen 2018

## **Members of the Thesis Committee**

Prof. Dr. Marina Rodnina  
Department of Physical Biochemistry  
Max Planck Institute for Biophysical Chemistry, Göttingen Germany

Prof. Dr. Holger Stark  
Department of Structural Dynamics  
Max Planck Institute for Biophysical Chemistry, Göttingen Germany

Prof. Dr. Ralf Ficner  
Department of Molecular Structural Biology  
Institute for Microbiology and Genetics  
Georg-August-Universität Göttingen, Göttingen Germany

## **Members of the Examination Board**

Prof. Dr. Marina Rodnina (1<sup>st</sup> Referee)  
Department of Physical Biochemistry  
Max Planck Institute for Biophysical Chemistry, Göttingen Germany

Prof. Dr. Holger Stark (2<sup>nd</sup> Referee)  
Department of Structural Dynamics  
Max Planck Institute for Biophysical Chemistry, Göttingen Germany

## **Further members of the Examination Board**

Prof. Dr. Ralf Ficner  
Department of Molecular Structural Biology  
Institute for Microbiology and Genetics  
Georg-August-Universität Göttingen, Göttingen Germany

Prof. Dr. Wolfgang Wintermeyer  
Department of Physical Biochemistry  
Max Planck Institute for Biophysical Chemistry, Göttingen Germany

Dr. Alexis Caspar Faesen  
Department of Biochemistry of Signal Dynamics  
Max Planck Institute for Biophysical Chemistry, Göttingen Germany

Dr. Juliane Liepe  
Department of Quantitative and Systems Biology  
Max Planck Institute for Biophysical Chemistry, Göttingen Germany

**Date of the oral examination:** September 14<sup>th</sup>, 2018

## **Affidavit**

I hereby declare that the presented dissertation entitled "The Role of EF-G in Translational Reading Frame Maintenance on the Ribosome" has been written independently and with no other sources and aids than quoted.

Göttingen, June 29<sup>th</sup>, 2018

Bee-Zen Peng



## **Publications**

1. Klimova, M., Senyushkina, T., Samatova, E., **Peng, B.Z.**, Pearson, M., Peske, F., and Rodnina, M.V. (2019). EF-G–induced ribosome sliding along the noncoding mRNA. *Science Advances* 5, eaaw9049.



# Table of Contents

<b>ABSTRACT .....</b>	<b>1</b>
<b>1. INTRODUCTION.....</b>	<b>3</b>
1.1. Ribosome.....	3
1.2. Overview of translation .....	7
1.3. The elongation cycle.....	9
1.3.1. Decoding .....	10
1.3.2. Peptide bond formation .....	12
1.3.3. Translocation .....	13
1.3.4. The fidelity of elongation.....	15
1.3.5. Programmed -1 ribosomal frameshifting .....	17
1.4. Reading frame maintenance during translation .....	19
1.4.1. The role of tRNAs .....	19
1.4.2. The contributions of the ribosome .....	21
1.5. Elongation factor G .....	22
1.6. Scope of the thesis .....	25
<b>2. RESULTS.....</b>	<b>27</b>
2.1. Generation of EF-G mutants.....	27
2.2. GTP hydrolysis by EF-G mutants.....	28
2.3. Establishment of the reading frame maintenance assay .....	29
2.4. Effects of EF-G mutants on reading frame maintenance.....	31
2.5. Kinetics of translocation.....	35
2.5.1. Monitoring of mRNA translocation by fluorescence-labeled mRNA.....	35
2.5.2. Measurement of tRNA translocation by time-resolved Pmn assay.....	37
2.6. Correlation between the speed of translocation and frameshifting .....	39
2.7. Effects of EF-G mutants on the trajectory of translocation.....	40
<b>3. DISCUSSION .....</b>	<b>51</b>
3.1. Maintenance of reading frame during translation.....	51
3.2. Effects of EF-G mutants on the SSU dynamics .....	54
3.3. Conclusion and perspective .....	56
<b>4. MATERIALS AND METHODS .....</b>	<b>57</b>
4.1. Chemicals .....	57
4.2. Buffers and Media .....	57
4.3. Cell culture media.....	62
4.4. mRNAs .....	62
4.5. DNA primers.....	62

4.6.	Fluorophores .....	63
4.7.	Instruments and software .....	63
4.8.	Preparation of EF-G.....	65
4.8.1.	Expression and purification of EF-G .....	65
4.8.2.	Labeling of EF-G .....	65
4.9.	Preparation of fluorescence-labeled ribosome .....	66
4.9.1.	Expression and purification of L7/12.....	66
4.9.2.	Labeling and purification of L7/12 .....	67
4.9.3.	Depletion and reconstitution .....	68
4.10.	Turnover GTP hydrolysis.....	68
4.11.	Preparation of ribosome complexes.....	69
4.12.	Reading frame maintenance assay .....	69
4.13.	Rapid kinetics assay .....	70
4.13.1.	mRNA translocation .....	70
4.13.2.	Time-resolved puromycin assay .....	70
4.13.3.	Global fitting of translocation.....	71
<b>5.</b>	<b>REFERENCES .....</b>	<b>73</b>
<b>6.</b>	<b>APPENDIX .....</b>	<b>85</b>
6.1.	Abbreviations.....	85
6.2.	List of figures: .....	87
6.3.	List of Tables .....	89
	<b>ACKNOWLEDGEMENTS.....</b>	<b>91</b>
	<b>CURRICULUM VITAE .....</b>	<b>93</b>



## Abstract

Translation of an mRNA by the ribosome is the final step of gene expression. During translation initiation, the ribosome establishes the mRNA reading frame with the help of initiator tRNA binding to the start codon. This reading frame is maintained during the entire process of translation. The interactions between the codon-anticodon duplex and elements of the ribosome decoding site ensure tight binding of tRNAs to their respective codons and are essential for fast and correct decoding. However, during the tRNA–mRNA translocation step, the interactions between the mRNA-tRNA complex and the ribosome have to be disrupted to allow the movement of the ribosome along the mRNA. This is when reading frame maintenance faces the greatest challenge during the elongation. Ribosome slippage into an alternative reading frame usually leads to the synthesis of inactive, misfolded or even toxic proteins that increase not only the energetic cost of translation but also compromise the cellular fitness. Maintaining the translational reading frame is one of the most important task for the ribosome in the translation, but the mechanisms are poorly understood.

Here we examine the mechanism of reading frame maintenance using a fully-reconstituted translation system from *Escherichia coli*. We have selected an mRNA sequence that allows significant frameshifting and analyzed the roles of the ribosome and elongation factor G (EF-G) in this process. Based on crystal and cryo-EM structures of the ribosome–EF-G complexes, residues at the tip loops of domain IV of EF-G were replaced to examine the role of EF-G on reading frame maintenance. We show that the ribosome is highly prone for spontaneous frameshifting on a slippery sequence, whereas EF-G suppresses frameshifting. Single amino acid exchanges in key positions of domain IV of EF-G greatly increase frameshifting. Kinetic experiments indicate that the ability of EF-G to suppress spontaneous frameshifting correlates with the speed of translocation. Using the toolbox of fluorescence reporters, we identify how the trajectories of translocation and motions of the ribosome alter with the EF-G mutants. Our results suggest that the potential interactions between the residues at the tip of domain IV of EF-G and the mRNA-tRNA complex are essential during translation. Disruption of these interactions interferes with the dynamics of the SSU head and body domains movements, slow down the late translocation events, and open the kinetic window that allows the ribosome to shift into an alternative reading frame. Our work demonstrates the contribution of EF-G on reading frame maintenance during translocation.



## 1. Introduction

Protein synthesis is the fundamental process in all living cells to express the genetic information from the messenger RNA (mRNA) into the sequence of amino acids in proteins. Three bases in mRNA constitutes a codon, and each codon specify one of the twenty standard amino acid incorporated into the protein. The genetic information is decoded by the ribosome with the help of the aminoacyl-transfer RNA (aa-tRNA), which binds specifically with its anticodon to the codon on the mRNA. Studying the ribosome does not only reveal the mechanisms of its fundamental function in gene expression, but also provides important insights into clinically relevant problems such as disease and drug designs. The more detailed knowledge is gained, the more information can be applied to improve our daily life.

### 1.1. Ribosome

The ribosome is a complex molecular machine that carries out protein synthesis. It provides the platform to decode and translate the genetic information into polypeptide chains. Regardless of the size and molecular mass, the key components of the ribosomes are similar across all three kingdoms of life in archaea, bacteria, and eukarya (Korobeinikova et al., 2012). The ribosome is composed of two unequal subunits, the large subunit (LSU) and the small subunit (SSU), and each subunit consists of one or more ribosomal RNA (rRNA) molecules and several different ribosomal proteins (r-proteins) (Table 1-1). The eukaryotic ribosome is an 80S (S, sedimentation coefficient) complex with about 4.2 MDa molecular mass. The small 40S subunit includes an 18S rRNA and 33 r-proteins while the large 60S subunits contains 3 rRNAs and 49 r-proteins. The prokaryotic ribosome is slightly smaller than eukaryotic ribosome. The small 30S subunit and the large 50S subunit form the complete 70S ribosome with about 2.5 MDa molecular mass. The 30S subunit consist of the 16S rRNA together with 21 r-proteins while the 50S subunit is composed of the 23S rRNA, the 5S rRNA, and 31 r-proteins. A third type of ribosome, the mitochondrial ribosome, is 55S and is formed by the small 28S subunit and large 39S subunit with 3 rRNAs and 82 r-proteins. The mitochondrial ribosome has a smaller sedimentation coefficient but higher molecular mass than prokaryotic ribosome because of a different rRNA to r-protein ratio. The mitochondrial ribosome is composed of 25% rRNA and 75% r-proteins whereas the prokaryotic ribosome contains 65% of rRNA and 35% of r-proteins.

The ratio of rRNA to the r-protein in eukaryotic ribosome is about 1 (Amunts et al., 2015; Greber and Ban, 2016; Kurland, 1960; Ramakrishnan, 2014; Wilson and Doudna Cate, 2012).

**Table 1-1. The composition of ribosomes**

	<b>Size</b>	<b>rRNAs</b>	<b>r-Proteins</b>
<b>Eukaryotic ribosomes</b>	80S (4.2 MDa)		
<b>SSU</b>	40S (1.4 MDa)	18S rRNA	33 r-Proteins
<b>LSU</b>	60S (2.8 MDa)	28S rRNA 5.8S rRNA 5S rRNA	49 r-Proteins
<b>prokaryotic ribosomes</b>	70S (2.5 MDa)		
<b>SSU</b>	30S (0.9 MDa)	16S rRNA	21 r-Proteins
<b>LSU</b>	50S (1.6 MDa)	23S rRNA 5S rRNA	31 r-Proteins
<b>Mitochondrial ribosomes</b>	55S (2.7 MDa)		
<b>SSU</b>	28S	12S rRNA	30 r-Proteins
<b>LSU</b>	39S	16S rRNA CP tRNA	52 r-Proteins

With the progress of high-resolution structural studies, atomic resolution structures of SSU, LSU, and of functional 70S complex were solved in 2000 (Ban et al., 2000; Harms et al., 2001; Schluenzen et al., 2000; Wimberly et al., 2000; Yusupov et al., 2001). Since then, high-resolution structures of ribosomes obtained from X-ray crystallography and cryogenic electron microscopy (cryo-EM) provide increasingly deeper insights into the interactions with translation factors and the conformational rearrangements during translation (Frank, 2017; Ling and Ermolenko, 2016; Voorhees and Ramakrishnan, 2013)

The landmarks of the large 50S subunit are the peptidyl transferase center (PTC), the L1 stalk, and the L10-L7/L12/L11 stalk (Figure 1-1). The PTC catalyzes the two essential chemical reactions during translation: (1) the peptide bond formation between aminoacyl-tRNA and peptidyl-tRNA during elongation and (2) the hydrolysis of the nascent peptide chains during termination. The growing polypeptide chain passes through the exit tunnel, which connects the PTC and the cytoplasmic side of the subunit where the peptide emerges into the cell. The surface residue within the exit tunnel can interact with the nascent peptide chain and allow the co-translation folding of the growing peptides.

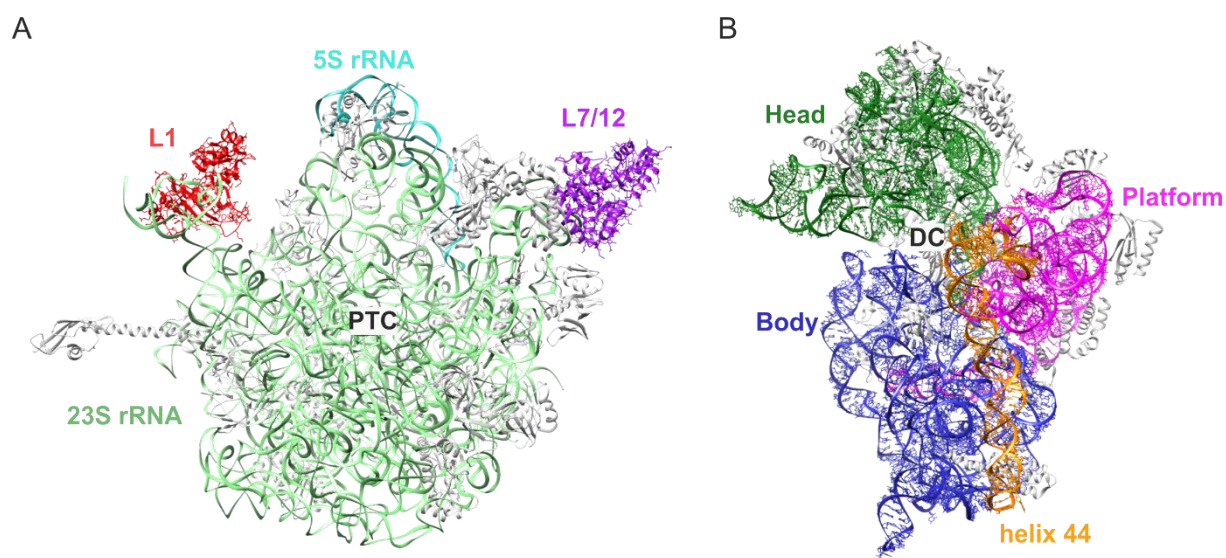


### Figure 1-1. Structure of the 50S and 30S subunits

(A) View of the 50S subunit from the interface site. The 23S rRNA and 5S rRNA are in light green and cyan, respectively. The peptidyl transferase center (PTC) is composed of by the 23S rRNA. The L1 stalk (red) is involved in the dissociation of deacylated-tRNA and the L7/12 stalk (purple) assists the recruitment of translation factors. Other r-proteins are in light grey. (B) View of the 30S subunit from the interface site. The 30S subunit can be divided into three domains: the head (green), the platform (magenta), the body (blue). Helix 44 (yellow) contains key functional residues A1493 and A1492 of the 16S rRNA that monitor the quality of codon-anticodon interaction in the decoding center (DC). Images based on PDB files 4V4P (Jenner et al., 2005) and 4OX9 (Dunkle et al., 2014).

The catalytic activity of the PTC is mediated by the 23S rRNA suggesting that the ribosome is a ribozyme. Most of the r-proteins act as scaffold proteins and neutralize the charge of large rRNA molecules. However, some r- proteins have an important role as well. The L1 stalk is composed of helices H76-78 and the protein L1 (Yusupov et al., 2001). The L1 stalk is a highly dynamic element that has an open and a close conformation during translation. When the L1 stalk is oriented away from the ribosome it assumes the so-called open conformation which allow the departure of the deacylated-tRNA whereas the exit path of deacylated-tRNA is blocked in the close conformation of L1 when the L1 stalk contacts the E-site tRNA (Cornish et al., 2009). By that, it acts as the gate for the leaving tRNA at the exit. By interacting with the deacylated-tRNA, the L1 stalk also contributes to the movement of the tRNAs during translocation (Bock et al., 2013; Brilot et al., 2013; Fischer et al., 2010).

The L7/12 is located on the opposite side of the L1 and has a crucial role in the recruitment of translation factors and their GTPase activity (Diaconu et al., 2005; Kothe et al., 2004; Mohr et al., 2002). The difference between L7 and L12 is the acetylated N-terminus. L7/12 forms dimers and exists in total in four copies in *E. coli* ribosome. The number of L7/12 copies can differ between four and eight copies depending on the organism (Davydov et al., 2013; Diaconu et al., 2005).

The small 30S subunit consists of 3 domains, the head, the body, and the platform (Figure 1-1). The mRNA binds between the SSU head and body and the genetic information is decoded in the decoding center of the 30S subunit. The decoding center is composed of parts of helices 18, 34, 44 of the 16S rRNA. The interaction of the first two base pairs of a codon-anticodon duplex, which is crucial for the accuracy of decoding, is monitored by the bases A1493 and A1492 of helix 44 (Ogle et al., 2001).

With the help of RNA-RNA, RNA-protein, and protein-protein interactions, the 50S subunit and the 30S subunit associates to yield the complete 70S ribosome (Yusupov et al., 2001) (Figure 1-2). The functional ribosome contains three stable tRNA binding sites: the aminoacyl (A) site, the peptidyl (P) site, and the exit (E) site. The tRNA-binding elements of the A site and P site are formed by both the 30S and the 50S subunit, whereas the E site is mainly confined to the 50S subunit. As indicated by their names, the A sites binds the incoming aminoacyl-tRNA (aa-tRNA); the P site holds the peptidyl-tRNA with the growing peptide chain as well as

deacylated-tRNA after peptide bond formation; and the E site harbors the deacylated-tRNA on its transit out of the ribosome.

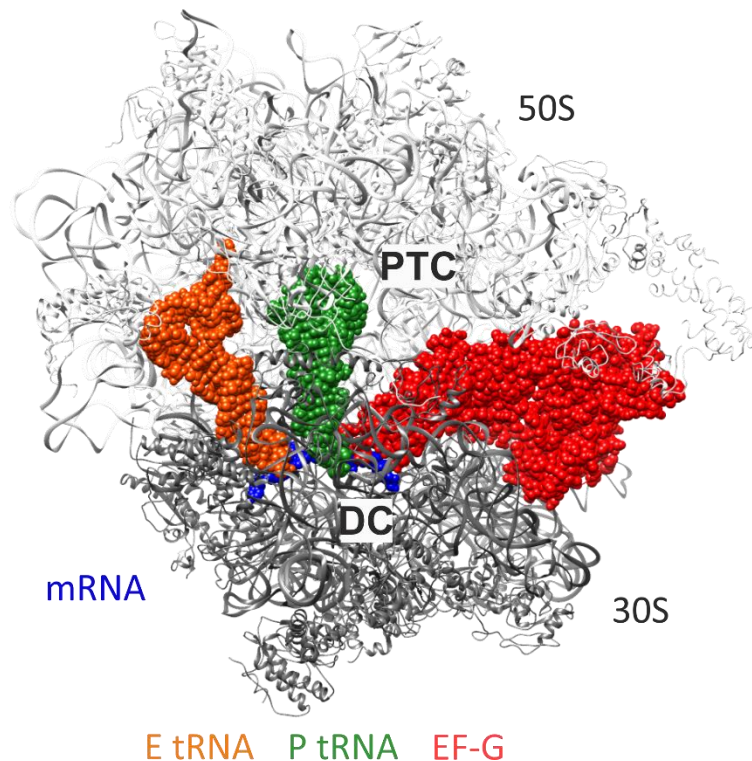


### Figure 1-2. Structure of 70S ribosome

The 70S ribosome is composed of two subunits: the large 50S subunit (LSU, light grey) and the small 30S subunit (SSU, dark grey). The LSU includes the peptidyl transferase center (PTC), while the SSU contains the decoding center (DC). The mRNA (blue) together with deacylated-tRNA (orange) in the E site and peptidyl-tRNA (green) in the P site indicate that this is an overall view of a non-rotated post-translocation complex with EF-G (red) in the A site. Image based on PDB file 4V5F (Gao et al., 2009).

## 1.2. Overview of translation

Translation proceeds in four phases: initiation, elongation, termination, and ribosome recycling (Dunkle and Cate, 2010) and all phases of protein synthesis require the assistance of translation factors (Figure 1-3) (Rodnina and Wintermeyer, 2009). Several translation factors are GTPase that couple their functional cycles to GTP hydrolysis.

Translation initiation is the most regulated step of translation. It requires initiation factors (IFs) and results in the recognition of AUG start codon, which defines the open reading frame on the

mRNA. In the first step, the mRNA coding for the protein to be made binds to the 30S subunit together with the IFs and the initiator tRNA (fMet-tRNA<sup>fMet</sup>). The factor recruitment to the 30S preinitiation complex (PIC) begins with the binding of IF3, followed by IF2 and IF1. The initiator tRNA is last to be recruited and the mRNA binding is independent of the components in the 30S PIC (Milon et al., 2012). The start codon AUG is guided to the P site by the Shine-Dalgarno sequence which is located upstream of the start codon and base pairs to the complementary sequence at the 3' end of the 16S rRNA. The initiator tRNA is then positioned at the start codon in the P site resulting in the formation of a stable 30S initiation complex (IC). The functional 70S IC is completed by the docking of the large 50S subunit with the assistance of IF2 and the dissociation of all IFs. The formation of a stable 70S IC is highly modulated by all three IFs (Gualerzi and Pon, 2015; Milon et al., 2012) .

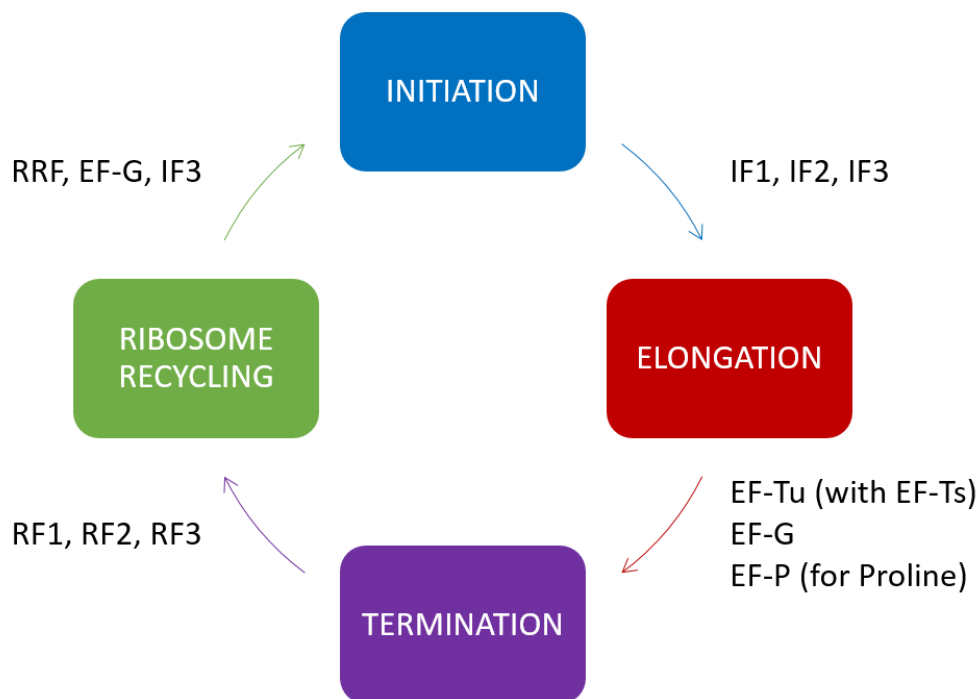


### Figure 1-3. Overview of translation cycle

The process of translation entails four steps, initiation, elongation, termination, and ribosome recycling. Each step is carried out with the help of translation factors. The elongation factor EF-P is needed to synthesize the stretches of consecutive prolines.



The elongation phase comprises repetitive cycles of amino acid additions to the growing peptide. In the first step of elongation, which is called decoding, an amino acid is delivered to the ribosome by aminoacyl-tRNA in a ternary complex with elongation factor Tu (EF-Tu) and GTP. Aminoacyl-tRNA binds to the vacant A site according to the codon presented there. In the second step, the peptide bond formation between the aminoacyl-tRNA in the A site and peptidyl-tRNA in the P site is facilitated by the environment of the PTC. This reaction results in a peptidyl-tRNA in the A site and a deacylated-tRNA in the P site. In the final step of elongation cycle, the two tRNAs and the mRNA move together from the A and P site to the P and E site, respectively, and deacylated-tRNA leaves the ribosome. The movement of the mRNA-tRNA complex is called translocation. It is promoted by elongation factor G (EF-G) and requires the hydrolysis of GTP by the factor. The dissociation of the E-site tRNA and the vacant A site prepare the ribosome for the next cycle of elongation.

The elongation cycle continues until the ribosome reaches one of the three termination codons in the mRNA. The UAG and UAA codons are recognized by release factor (RF) 1 and the UGA and UAA codons are recognized by RF2. Once a termination codon in the A site is recognized, RF1 or RF2 induces the hydrolysis of the phosphodiester bond in peptidyl-tRNA and release the newly synthesized protein from the ribosome. Then, RF3 assists the dissociation of RF1 or RF2. Finally, the ribosome dissociates into subunits with the assistance of ribosome recycling factor (RRF) and EF-G. RRF and EF-G disrupt subunit bridges between the SSU and LSU, causing the separation of the two subunits. The ribosomal subunits are now ready for the next round of translation.

### **1.3. The elongation cycle**

Translation elongation is the central phase of translation. Elongation is a repetitive process and encompasses three steps, decoding, peptide bond formation, and mRNA-tRNA translocation (Figure 1-4). The overall rate of elongation is quite high, about 10-25 amino acid per second incorporated into nascent peptide chain in *E. coli*, and is mostly limited by the delivery of cognate aa-tRNA into the A site (Bremer and Dennis, 2008). The differences of translation rates result from the abundance of tRNA, the codon context of an mRNA, the secondary structure elements in the mRNA, and other factors that may cause pausing and stalling of the

ribosome. In the following section, the three steps of elongation and their role in fidelity of translation will be discussed.

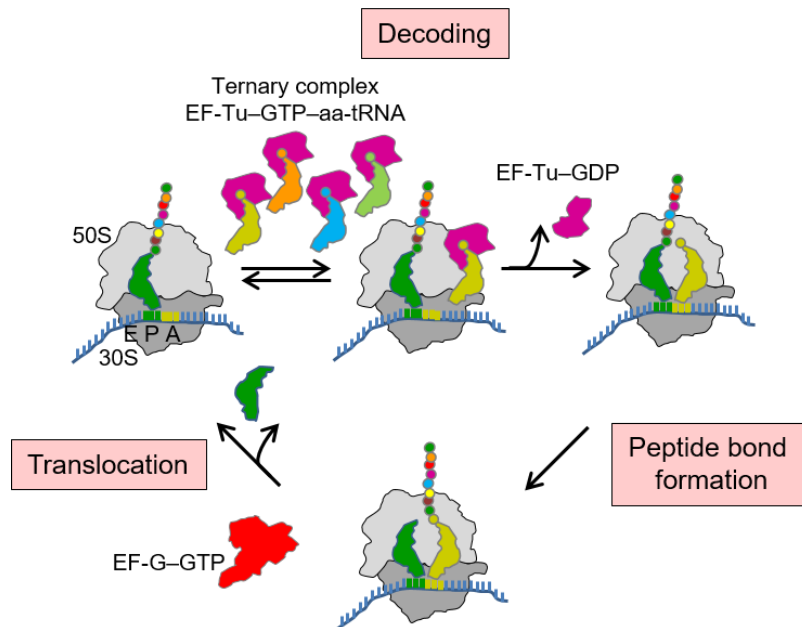


#### Figure 1-4. Overview of the elongation cycle

Elongation phase entails three steps, decoding, peptide bond formation, and the translocation. During decoding, the aa-tRNA is delivered in the ternary complex (aa-tRNA-EF-Tu-GTP) to the A site. After the rigorous selection of aa-tRNA during decoding, the cognate aa-tRNA (lime) accommodates in the A site. This is followed by the formation of the peptide bond leading to peptidyl transfer from the peptidyl-tRNA in the P site to the aa-tRNA in the A site. This reaction is catalyzed by the PTC in the 50S subunit. The newly formed peptidyl-tRNA and the deacylated-tRNA translocate to the P site and E site, respectively, with the help of EF-G (red) and at the cost of GTP hydrolysis. After the release of peptidyl-tRNA from the E site, the A is vacant and ready for the next round of elongation. Figure modified from (Rodnina, 2016).

### 1.3.1. Decoding

Decoding is the process in which the ribosome selects an aa-tRNA corresponding to the codon presented on the mRNA in the A site (cognate aa-tRNA) from the pool of total tRNAs. The fidelity of protein synthesis during decoding is controlled by the two selection stages. The first step is the initial selection at which near-cognate and non-cognate aa-tRNAs are rejected prior the GTP hydrolysis. The second step is aa-tRNA proofreading after GTP hydrolysis, here

incorrect aa-tRNAs dissociate from the ribosome before they can accommodate in the A site, and thus before the incorporation of the amino acid to the peptide chain (Figure 1-5) (Pape et al., 1999; Rodnina and Wintermeyer, 2001, 2016).

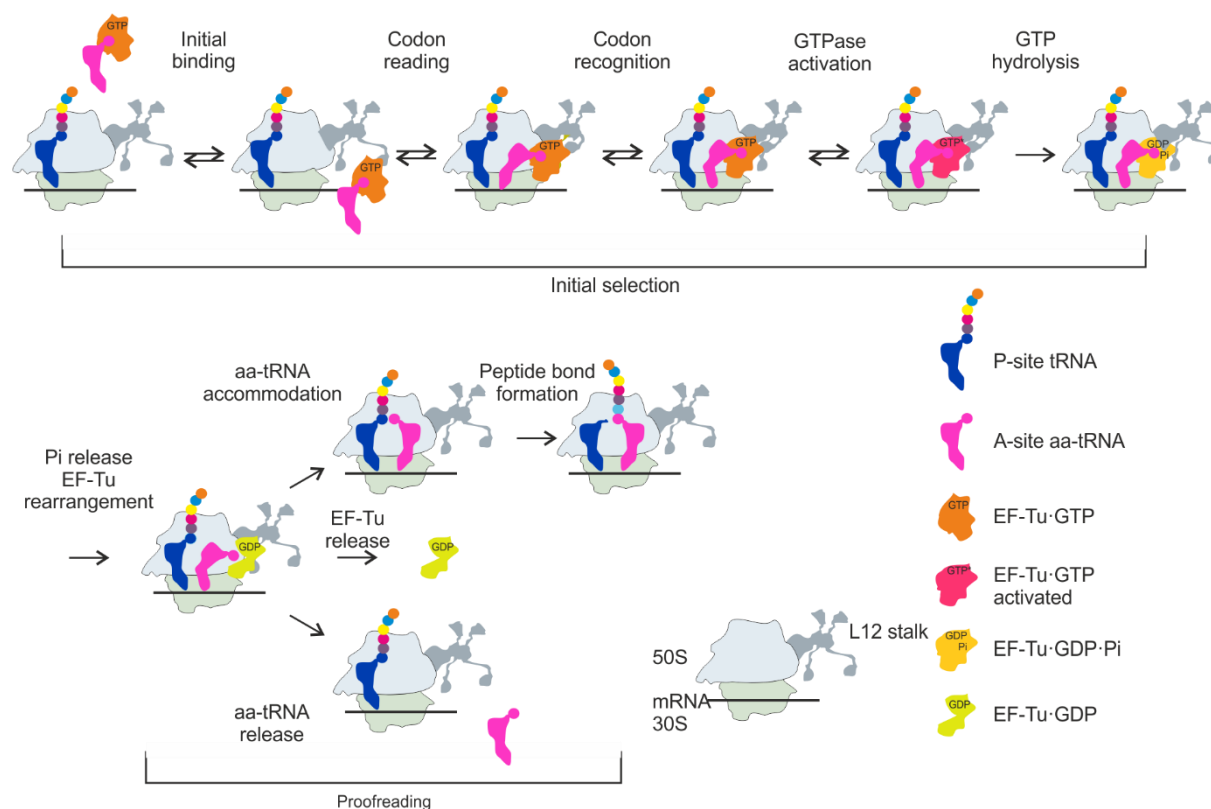


### Figure 1-5. Mechanism of aa-tRNA selection during decoding

The fidelity of decoding is controlled by two selection steps, initial selection and proofreading. During initial selection, the cognate tRNA binds to the ribosome whereas near-cognate and non-cognate tRNAs are rejected due to different reaction rates. The processes of initial selection is reversible until the GTP hydrolysis step by EF-Tu. In the proofreading stage, incorrect tRNAs have a higher chance of dissociating from the ribosome before they can accommodate in the A site and before the incorrect amino acid is incorporated into the peptide chain. Figure modified from (Rodnina and Wintermeyer, 2016).

The decoding process starts with the initial binding of the ternary complex (aa-tRNA-EF-Tu-GTP) through the L7/12 stalk. (Diaconu et al., 2005; Kothe et al., 2004). The selectivity of correct aa-tRNA is due to higher reaction rates of the forward reactions for cognate aa-tRNA

prior the GTP hydrolysis. The stability of the near and non-cognate codon-anticodon interaction is also lower compared to the cognate codon-anticodon duplex (Gromadski et al., 2006). The inappropriate interaction of an incorrect codon-anticodon duplex slows down the reaction leading to the rejected by the ribosome (Gromadski et al., 2006; Gromadski and Rodnina, 2004; Kothe and Rodnina, 2007).

The formation of the cognate codon-anticodon duplex causes conformational changes of the 30S subunit, particularly of bases G530, A1492, and A1493 in helix 44 of the 16S rRNA (Fischer et al., 2016; Loveland et al., 2017; Ogle et al., 2001). This results in a closed conformation of the 30S subunit compared to the structure when the A site is unoccupied. The reversible step of initial selection ends with the GTP hydrolysis by EF-Tu that controls both rate and fidelity of decoding (Wohlgemuth et al., 2011). Although most of the incorrect aa-tRNAs are rejected during initial selection, it is still possible that a near-cognate or a non-cognate aa-tRNA successfully bind to the A site of the ribosome. At this point, the second control mechanism is carried out. The incorrect aa-tRNA has a higher dissociation rate from the ribosome compared to a cognate aa-tRNA.

### **1.3.2. Peptide bond formation**

The formation of peptide bond is carried out by the attack of the nucleophilic  $\alpha$ -amino group of the aa-tRNA in the A site to the carbonyl group of the ester bond of the peptidyl-tRNA in the P site. The nascent peptide chain is subsequently transferred to the tRNA in the A site resulting in a one amino acid longer peptidyl-tRNA. This reaction is catalyzed by the PTC that is located on the 50S of the ribosome. Because the PTC is composed of rRNA, the catalytic activity relies on the limited repertoire of active groups of RNA. With extensive mutational studies of the catalytic core of the ribosome and the analysis of effects of pH changes on peptide bond formation, it was shown that ionizing groups of ribosome do not contribute peptide bond formation (Ban et al., 2000; Beringer et al., 2003; Beringer et al., 2005; Bieling et al., 2006; Rodnina, 2013; Youngman et al., 2004).

The mechanism of peptide bond formation entails two steps. The first step is the rate-limiting step that includes the formation of a zwitterionic tetrahedral intermediates and the transfer of a proton. The attack of the  $\alpha$ -amino group of the A-site tRNA on the carbonyl group of the P-site tRNA results in the formation of an eight-membered transition state in which it receives a proton from the P-site tRNA. The second step is relatively fast and leads to the formation of the reaction product, i.e. the peptide bond (Hiller et al., 2011; Kuhlenkoetter et al., 2011; Satterthwait and Jencks, 1974). It is worth noting that peptide bond formation with proline is particularly slow compared to other amino acids (Pavlov et al., 2009; Wohlgemuth et al., 2008). The slow rate of peptide bond formation of proline can lead to ribosome stalling especially when multiple proline residues have to be incorporated (Doerfel et al., 2013; Ude et al., 2013). To obtain rapid translation with several proline residues in a row, an additional elongation factor, EF-P, is required. EF-P binds to the E site of the ribosome and assists the positioning of the proline tRNA (Pro-tRNA<sup>Pro</sup>) in the PTC to accelerate the reaction (Doerfel et al., 2013; Doerfel et al., 2015; Elgamal et al., 2014; Ude et al., 2013).

### **1.3.3. Translocation**

After the peptide bond formation, the newly formed peptidyl-tRNA in the A site and the deacylated-tRNA in the P site move synchronously to the P site and E site, respectively, with the help of EF-G. The translocation of the mRNA-tRNA complex is the most dynamic step in elongation. After peptide bond formation, the two tRNAs are present either in the classical state or hybrid state due to the fluctuation of the tRNAs and the ribosome. In the classical state both the 3' end and the anticodon region of the peptidyl-tRNA and the deacylated-tRNA are located in the A site (A/A) and P site (P/P), respectively. The 3' acceptor arms of both tRNAs can shift spontaneously toward the P site (A/P) and E site (P/E) to form the hybrid state (Adio et al., 2015; Agirrezabala et al., 2008; Blanchard et al., 2004; Cornish et al., 2008; Julian et al., 2008; Moazed and Noller, 1989).

EF-G can bind both to the classical state and hybrid state and stabilizes the hybrid state (Holtkamp et al., 2014b; Li et al., 2015; Lin et al., 2015; Sharma et al., 2016). GTP hydrolysis by EF-G causes a conformational change of the 30S subunit and forms the so-called unlocked state of the ribosome. This relaxes the interactions between the codon-anticodon complex and

the ribosome and gives the flexibility need for the movement of the mRNA-tRNA complex (Rodnina et al., 1997; Savelsbergh et al., 2003). At the same time, the head and body domains of the 30S subunits rotate back to the original position and the ribosome relocks (Belardinelli et al., 2016a). The translocation cycle ends with the peptidyl-tRNA in the P site and a vacant A site for next translation codon (Figure 1-6).

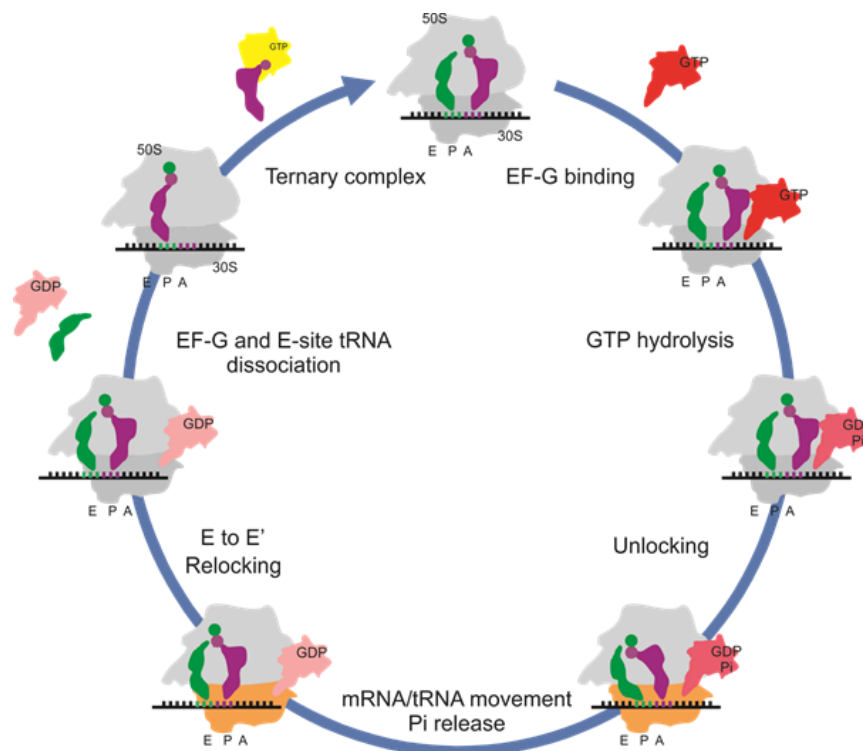


**Figure 1-6. Scheme of translocation cycle.**

Three different states of EF-G are indicated in red (GTP-bound), rose (GDP·Pi-bound), and pink (GDP-bound). EF-G binds to the PRE complex (only the classical state is shown) and promotes the translocation of the mRNA-tRNA complex at the cost of GTP hydrolysis. Conformational changes of the 30S subunit result in the unlocked state (yellow 30S) of the ribosome which allows the movement of the mRNA-tRNA complex. After translocation, the ribosome is relocked and the deacylated-tRNA (green) and EF-G dissociate from the ribosome. The peptidyl-tRNA (purple) is now located in the P site and the ribosome is ready for the next round of elongation (Rodnina and Wintermeyer, 2011).

However, the translocation can also occur spontaneously, albeit slowly, without the participation of EF-G. Depending on the thermodynamic preference of the tRNAs for the A, P, and E sites, these two attached tRNAs might move in forward or backward directions (Fredrick and

Noller, 2003; Konevega et al., 2007; Semenov et al., 2000; Shoji et al., 2006). Although translocation is always promoted by the EF-G in the cells, it is still important to understand the mechanism of spontaneous translocation, as it reveals the fundamental principles of the movement on the ribosome (Bock et al., 2013; Fischer et al., 2010).

#### **1.3.4. The fidelity of elongation**

Protein synthesis is a fundamental and important process that consumes a lot of energy and resources of the cell. Hence, the accuracy of translation is crucial for the cellular survival. Incorrect mRNA decoding may lead to inactive, misfolded or toxic proteins that not only increase the energetic cost of translation, but also compromise the cellular fitness. To avoid a waste of resources and potential crisis, the ribosome has evolved to generate proteins with high efficiency and accuracy. It is difficult to estimate the error frequency of translation initiation due to the low incidence. Even if fMet-tRNA<sup>fMet</sup> initiator tRNA is occasionally replaced by another hydrophobic amino acid, it may not be detrimental for translation. Meanwhile, false termination of translation by RFs is also infrequent, the error frequency is less than  $10^{-5}$  *in vivo* (Jorgensen et al., 1993). However, the ribosome is still an error prone polymerase compared to DNA and RNA polymerases, the translation error frequency is about  $10^{-5}$  to  $10^{-3}$  (Fijalkowska et al., 2012; Kurland, 1992; Traverse and Ochman, 2016). In other words, most mistranslation events occur during the elongation phase.

The fidelity of elongation is mainly controlled by three different selection steps. As described above in Section 1.3.1, the first selection step rejects the incorrect ternary complexes containing non-cognate aa-tRNA prior to GTP hydrolysis in EF-Tu. The second selection step is the proofreading step after GTP hydrolysis; most of the near-cognate aa-tRNAs are rejected in this step (Rodnina and Wintermeyer, 2001) (Figure 1-5). The third selection step is called retrospective editing and acts after peptide bond formation. The erroneously formed peptidyl-tRNA is prematurely terminated by the release factors (Zaher and Green, 2009a, b) (Figure 1-7).

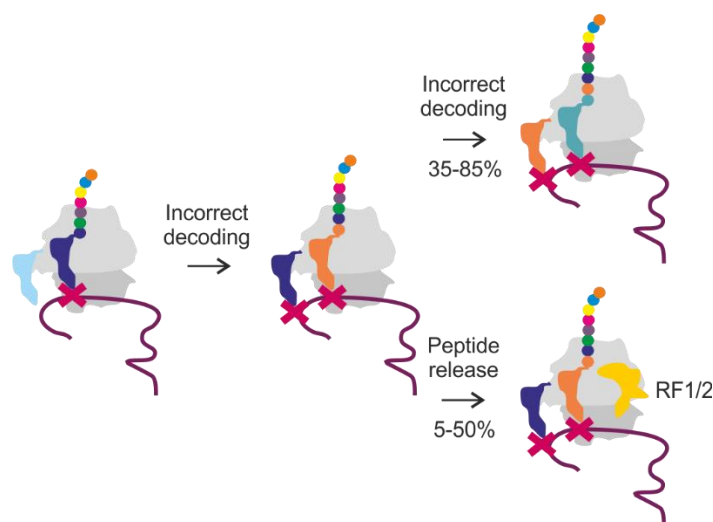


### Figure 1-7. Retrospective editing

The incorporation of an amino acid via a non-cognate tRNA into the newly formed peptide chain results in the retrospective quality control reaction, which leads to a general loss of specificity in the A site leading to the propagation of errors and eventually causing the termination of protein synthesis. IF3 is essential for the reaction but the exact mechanism remains unclear (Zaher and Green, 2009a, b). Figure from (Rodnina, 2012)

Together, these mechanisms achieve the overall frequency of missense errors in the range of  $10^{-5}$  to  $10^{-3}$  per codon depending on the type of measurements, the type of aa-tRNA, and the context of mRNA sequence (Drummond and Wilke, 2009; Kramer and Farabaugh, 2007). Although the error frequency of elongation is higher than the one of initiation and termination, missense errors may be more readily tolerated than other errors. In most cases, a single or even multiple amino acid exchanges do not affect cell viability, which is evident from numerous examples of highly-expressed mutant protein, unless the error appears at the catalytic site of the protein (Lind et al., 2010).

In addition to missense errors which occur during decoding, translocation can also lead to errors. This type of error is due to the change of reading frame, i.e. frameshifting. Frameshifting refers to the movement of the mRNA coding sequence towards the 5' or the 3' end, i.e. – or + frameshifting, respectively. Although the frequency at which ribosomes switch the reading frame is less than  $10^{-5}$  (Farabaugh and Björk, 1999), it is considered to be more harmful than others. If the reading frame is not maintained and the ribosome continues translation in the wrong reading frame, will result in the production of a protein that is completely different from



the original 0-frame. Unlike programmed frameshifting that shifts the reading frame on purpose to regulate gene expression (Brierley and Dos Ramos, 2006), spontaneous frameshifting is a purely unwelcome event and has to be avoided by the cell.

### 1.3.5. Programmed -1 ribosomal frameshifting

Although reading frame maintenance is the one of the most critical task that the ribosome has to deal with during translocation, the ribosome might abandon the principle of mRNA-protein co-linearity and decode an mRNA in an alternative frame. Programmed ribosomal Frameshifting (PRF) is a recoding event that leads to the shift of the reading frame and thereby yield more than one protein from the same mRNA (Atkins et al., 2016; Gesteland and Atkins, 1996; Tinoco et al., 2013). Compared to spontaneous frameshifting ( $<10^{-5}$ ), the efficiency of PRF can reach up to 80% (Fayet and Prère, 2010). The reading frame might shift in + or - direction depending on the frameshifting site. The classic example of -1PRF require two elements in the mRNA, a slippery sequence and a downstream secondary structure element (Brierley et al., 1989; Jacks et al., 1988). The slippery sequence is usually a heptameric sequence with the pattern X\_XX.Y\_YY.Z, where XXY and YYZ are the codons in 0 frame whereas XXX and YYY are the codons in -1 frame. Secondary structures like pseudoknots or a stem-loops are common structures that can be found 5-8 nucleotides after the slippery sequence (Brierley et al., 2010; Fayet and Prère, 2010). Furthermore, the stacked guanine-tetrads (G-quadruplexes), Shine-Dalgarno like element upstream of slippery sequence, and long-distance base-pairing can also stimulate -1PRF (Howard et al., 2004; Larsen et al., 1994; Miller and Giedroc, 2010; Yu et al., 2014). Kinetic analysis of a modified frameshifting sequence of avian infectious bronchitis virus (IBV) *Ia/Ib* revealed the mechanism of -1PRF (Caliskan et al., 2014) (Figure 1-8); it was shown that -1PRF takes place during the translocation process of the second codon of slippery sequence.

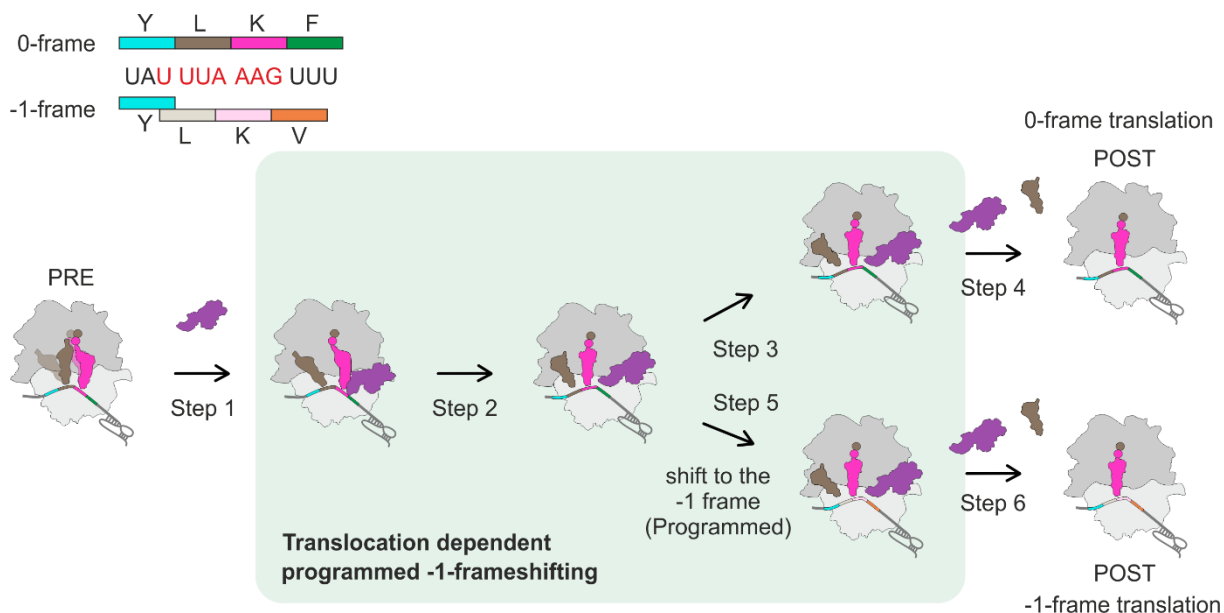


### Figure 1-8. Kinetic model of programmed -1 ribosomal frameshifting (-1PRF)

-1PRF occurs during translocation when the ribosome encounters a slippery sequence and a downstream secondary structure on the mRNA, e.g. a pseudoknot. Binding of EF-G to the PRE-complex (step 1) promotes translocation of the tRNAs (step 2). However, further movements are hindered by the pseudoknot and the deacylated-tRNA moves on the 50S subunit while the distance to the 30S subunit is not changed (step 3 and 5 in -1 frame). Afterwards, the deacylated-tRNA and EF-G dissociate and the ribosome re-locks thereby the respective reading frame is fixed (step 4 and 6). The decoding rate in the 0-frame is limited by the slow movement of deacylated-tRNA (step 3 and 4). By contrast, the process is relatively faster when the ribosome shifts to the -1-frame (step 5 and 6). Figure modified from (Caliskan et al., 2014)

This model is supported by the other -1PRF studies of dnaX using the single-molecule fluorescence resonance energy transfer (smFRET) technique (Kim et al., 2014; Kim and Tinoco, 2017). However, another smFRET study on -1PRF in dnaX suggested that -1PRF occurs during or after translocation of the first slippery codon in the P site (Chen et al., 2014). In addition to -1PRF, -2, +1, and even +2PRF may occur according to the pausing of hungry codon or thermodynamics stability of the codon-anticodon interactions (Caliskan et al., 2017; Yan et al., 2015). Although there are still disagreements on the timing of -1PRF, a delay of the dissociation of the deacylated-tRNA and the extended residence time of EF-G on the ribosome were observed in all cases. Multiple EF-G binding and dissociation events may impair translocation and facilitate the conformational changes of the ribosome during the translocation process leading to frame shifting (Caliskan et al., 2014; Chen et al., 2014; Kim and Tinoco, 2017).

## 1.4. Reading frame maintenance during translation

As a result of translation initiation, the mRNA reading frame is established by binding of the initiator tRNA to the start codon. Upon decoding, the interactions between the codon-anticodon complex and the elements of the ribosome decoding site ensure the maintenance of the mRNA reading frame. However, during the translocation phase, the interactions between the mRNA-tRNA complex and the ribosome have to be interrupted at some point during translocation to allow the movement of the mRNA and both attached tRNAs through the ribosome, which is the moment where the ribosome is prone to slippage. Thus, the chance of losing the reading frame is given at every round of elongation.

In theory, if the ribosome cannot maintain the reading frame, it may shift in either 5' or 3' direction which results in – or + frameshifting. Because the A site is occupied by EF-G during translocation, it is less likely for the tRNAs to move back to the A site, i.e. to undergo the + frameshifting. In contrast, the probability of spontaneous – frameshifting that shifts the reading frame towards to the 5' end is higher, particularly if the codon-anticodon interaction in the E site has been resolved. The impacts of losing reading frame are much more severe than of other translation errors. Cells must have evolved sophisticated control mechanisms to assure that the correct reading frame is maintained.

### 1.4.1. The role of tRNAs

The tRNAs are the molecules that bring the amino acids to the ribosome in translation. To form the highly conserved secondary and tertiary structure, certain modifications of nucleotide in the tRNA core region are necessary. More than 100 different modified nucleosides have been found and characterized in tRNAs so far (Cantara et al., 2011). The abundance of modified nucleosides in tRNAs from all organisms suggests that these modifications not only rearrange the global tRNA structure but also have a pivotal role in the function of tRNAs, i.e. in the efficiency and accuracy of translation. Although the modified nucleosides can be found at many different positions within the tRNA, the two most frequently found positions are 34 (the wobble position) and 37 (3'-adjacent to the anticodon). Both positions are located in the anticodon region suggesting that the modifications of nucleosides may play a role in reading frame

maintenance. Defects in tRNA modification can affect the reading frame maintenance in three different ways (Figure 1-9). In the first scenario, the binding of defective cognate aa-tRNA to the A site is too slow, which allows the near-cognate aa-tRNA to enter the A site. During translocation of the near-cognate tRNA to the P site, the reading frame might shift, because the codon-anticodon duplex is too weak and is disrupted. If the defective tRNA successfully binds to the A site, the reading frame might slip during or after translocation due to the weakened interactions between tRNA and ribosome. The third scenario can occur during the pause of ribosome caused by defective tRNA. The single peptidyl-tRNA in the P site might move in both forward and backward direction while waiting for the binding of the next tRNA.

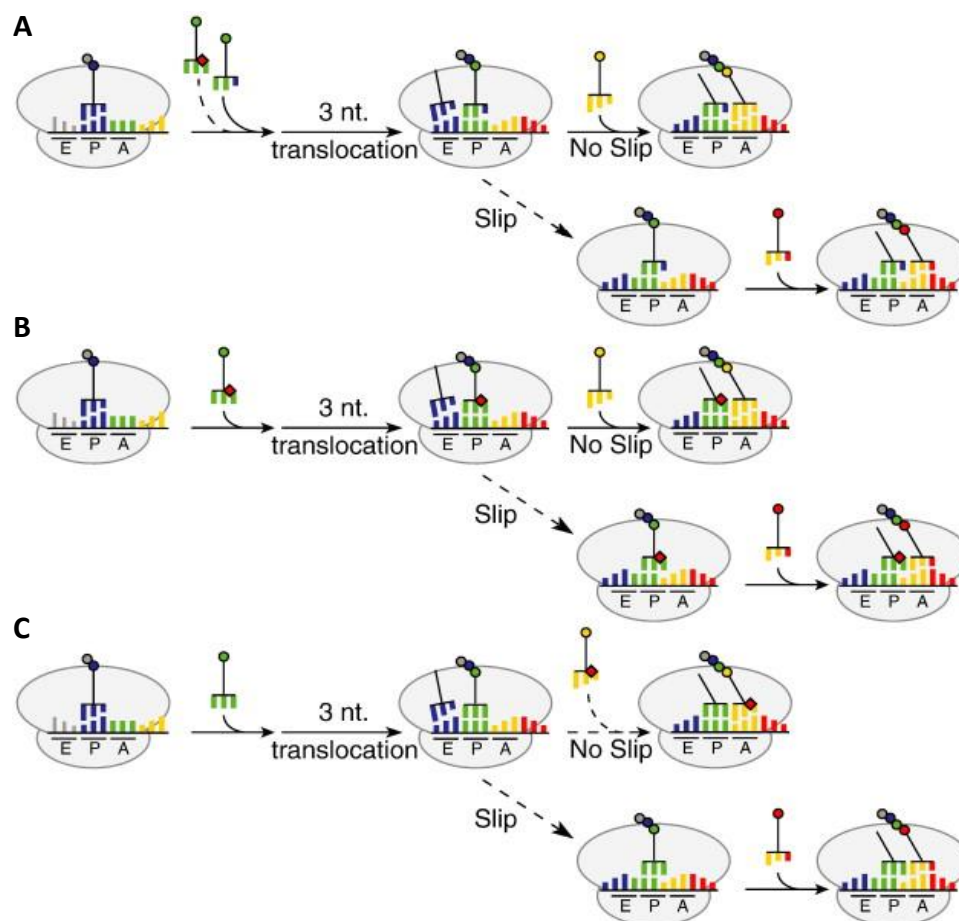


### Figure 1-9. Mechanisms of induced frameshifting via defective tRNA

Defects in tRNA modification can induce the change of reading frame in three different ways. The mRNA reading frame might slip due to (A) the near-cognate tRNA in the P site, (B) the defective tRNA in the P site, and (C) the stalling of ribosome caused by defective cognate tRNA. The defective cognate tRNA are shown in purple, with a black diamond on the tRNA, and the near-cognate tRNA is in pink. The broken arrows indicates slow reaction. Figure reproduced from (Näsvalld et al., 2009).

Studies of hypomodified tRNAs indicated that reading frame maintenance is more rigorous in the presence of all modifications (Bjork et al., 1999; Gamper et al., 2015; Koh and Sarin, 2018). The frequencies of +1 frameshifting are increased in mutants defective in tRNA modification. The modifications at position 34 and 37 shorten the pause in the A site and prevent the slippage of peptidyl-tRNA (Urbonavičius et al., 2001). A high-resolution crystal structure of tRNA<sup>Phe</sup><sub>GAA</sub> indicated that a hypermodified nucleoside at position 37 stabilizes the codon-anticodon interactions in all three tRNA binding sites of the ribosome. Meanwhile, the continuous base stacking network formed between tRNA modifications, 16S rRNA, and protein S3 also helps the ribosome maintaining the reading frame during elongation (Jenner et al., 2010).

#### **1.4.2. The contributions of the ribosome**

As the major component responsible for translation, the ribosome has to hold the mRNA reading frame from the beginning to the end of the open reading frame. As discussed, tRNAs have several different ways to avoid the loss of reading frame. However, codon-anticodon interactions are maintained not only by the tRNA alone but also assisted by the ribosome. The P site is the only tRNA binding site that always contains a tRNA during the entire translation of an mRNA. The initiator tRNA binds to the P site and establishes the mRNA reading frame and the peptidyl-tRNA waits at the P site for the next amino acid. R-protein S9 contacts the P site tRNA in both the P/P classical and the P/E hybrid state suggesting that S9 might help to stabilize the tRNA in place and subsequently prevents the loss of reading frame (Näsvalld et al., 2009). The interactions between S9 and the nucleosides at positions 32-34 of the peptidyl-tRNA form the "ribosomal grip" which appears to hold the reading frame. The deletion of the S9 C-terminal SKR (Ser, Lys, and Arg) tail reduces reading frame maintenance which results in a higher propensity of +1 and -1 frameshifting.

A similar behavior was also observed in a mutational study of ribosomal protein S7 which is located at the E site. The deletion of an S7  $\beta$ -hairpin stimulates both +1 and -1 frameshifting, but the frequency of misreading or stop codon readthrough is not increased. These data suggest that the interactions between the S7  $\beta$ -hairpin, mRNA, and the E site tRNA contribute to reading frame maintenance during elongation (Devaraj et al., 2009). Previous data also suggest that the presence of the E-site tRNA avoids slippage on the mRNA by codon-anticodon interaction.

Mutations at the anticodon region of tRNAs reduce the codon-anticodon interaction and increase the challenge on reading frame maintenance for +1 frameshifting when these tRNAs are in the E site (Sanders et al., 2008; Wilson and Nierhaus, 2006).

In addition to the r-proteins, mutations of 16S and 23S rRNAs also leads to the change of reading frame. Helix 34 (h34) of 16S is located in the head domain of SSU and forms part of the decoding region. Mutations in h34 increase the stop codon readthrough as well as the +1 and -1 frameshifting both *in vitro* and *in vivo* (Kubarenko et al., 2006; Moine and Dahlberg, 1994; Prescott and Kornau, 1992). The interaction between C2394 of 23S rRNA and A76 of tRNA is essential for the binding of deacylated-tRNA to the E site (Bocchetta et al., 2001; Lill et al., 1988). Mutation at this position, the C2394G, leads to higher frequencies of stop codon readthrough and -1 frameshifting due to incorrect translocation (Sergiev et al., 2005). Although the modifications of tRNAs play a role in reading frame maintenance, it is generally believed that the ribosome is the most responsible component for holding the reading frame in the proper position.

### 1.5. Elongation factor G

EF-G is one of the essential factors in translocation. It is a five domain GTPase and promotes translocation at the cost of GTP hydrolysis (Aevarsson et al., 1994; Rodnina et al., 1997). Translocation of the peptidyl-tRNA from the A to the P site can also occur in the absence of EF-G, but the rate of spontaneous translocation is very low, about  $10^{-3} \text{ s}^{-1}$  (Katunin et al., 2002; Peske et al., 2004), rather than  $20 \text{ s}^{-1}$  with EF-G (Holtkamp et al., 2014a). Domain I is also referred to as the G domain that binds GTP or GDP. Mutations in domain I inhibit the ability of GTP hydrolysis (Cunha et al., 2013). Domain II is conserved among translational GTPases. Domain III to V are specific for EF-G. The ribosome recruits EF-G through interactions with ribosomal protein L7/12 (Diaconu et al., 2005). The conformation of ribosome-free EF-G mainly adopts to compact form (Figure 1-10A) that the domain III-V are close to the domain I-II (Salsi et al., 2015). Although the compact form of EF-G is less stable, it can avoid the steric clash with the anticodon stem loop of the A-site tRNA during binding to the ribosome. Binding of EF-G to the ribosome induces a conformational change of EF-G to the elongated form (Figure 1-10B). The domain IV is oriented away from domain I-II and points to the A site to

facilitate the unidirectional translocation process. The translocation rate is accelerated by  $10^4$  to  $10^6$  fold in the presence of EF-G (Katunin et al., 2002).

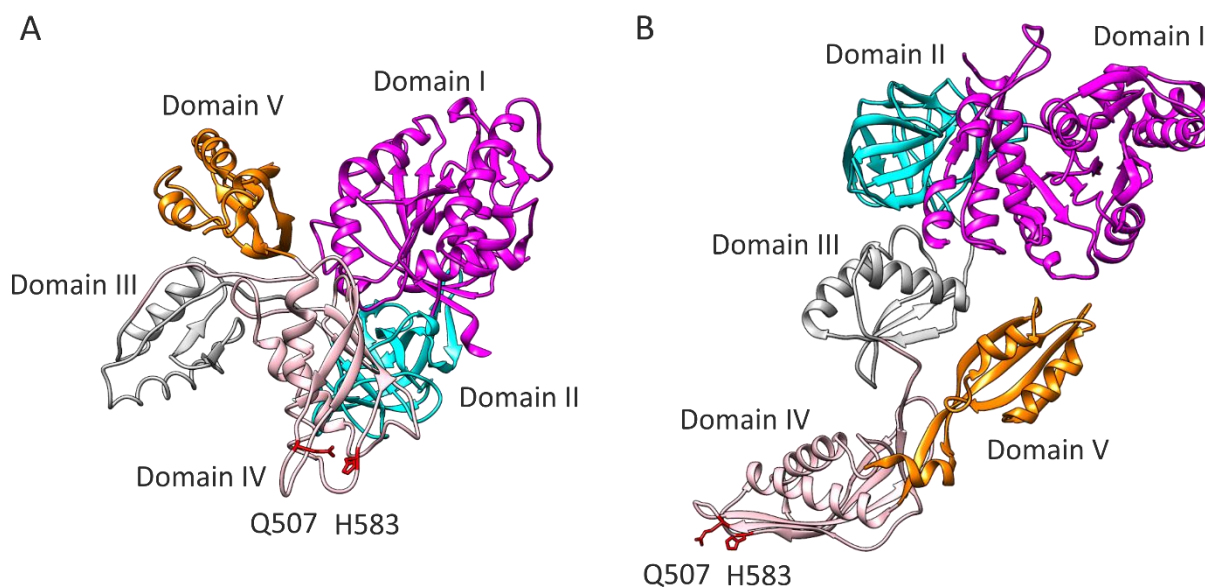


**Figure 1-10. The structure of EF-G.**

EF-G is a five-domain protein that contains a G domain for GTP hydrolysis. Domain I and II are conserved in all translational GTPases, such as EF-Tu, RF2 and RF3. Domains III to V are specific for EF-G. (A) Compact form of EF-G (B) Elongated form of EF-G. Images based on PDB files 4WPO (Lin et al., 2015) and 4V7D (Brilot et al., 2013).

Domain IV of EF-G plays a crucial role in translocation. Deletion of domain IV or domain IV and V not only slows down translocation to the order of  $10^{-2} \text{ s}^{-1}$  but also interferes with the dissociation of EF-G (Rodnina et al., 1997; Savelsbergh et al., 2000). Even a single point mutation in domain IV, for instance a replacement of the histidine at position 583 (*E. coli* nomenclature) with lysine can reduce the rate of translocation by 20-fold (Holtkamp et al., 2014a; Savelsbergh et al., 2000). The reason why the deletion or mutation of domain IV are so deleterious is probably due to potential interactions between the tip loops of domain IV and the peptidyl-tRNA. Deletion or mutation of domain IV impairs the translocation activity of EF-G without affecting EF-G binding or GTP hydrolysis (Liu et al., 2014; Rodnina et al., 1997; Savelsbergh et al., 2000). Especially loop I and loop II at the tip of domain IV interact with the decoding center to trigger the translocation reaction and 30S head domain swiveling (Liu et al.,

2014).

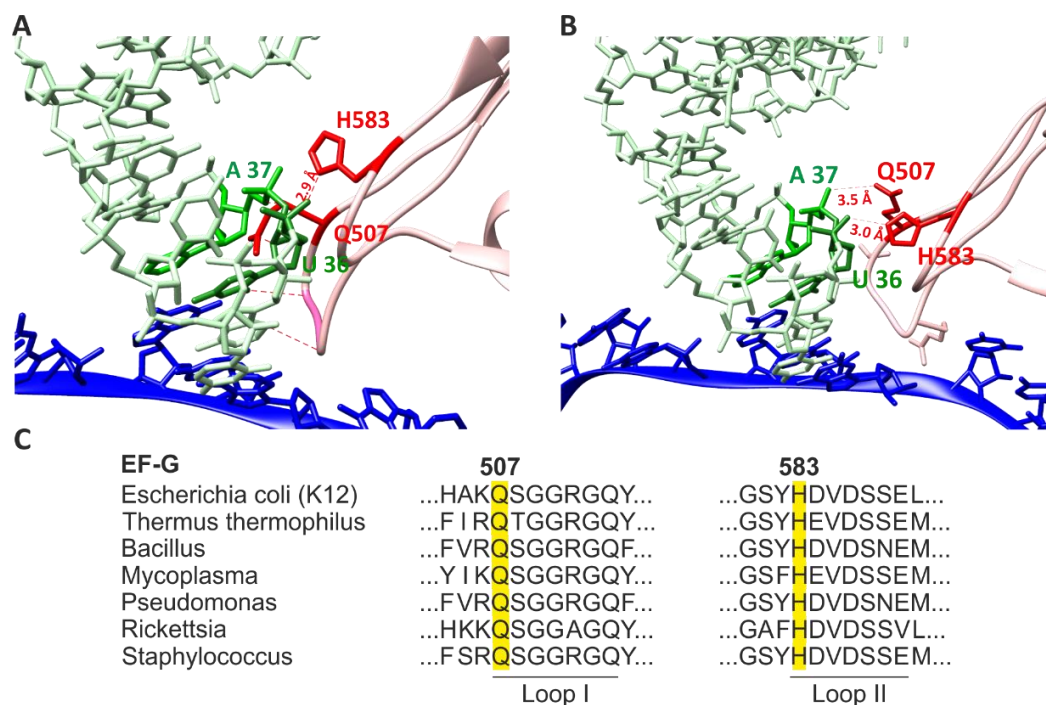


### Figure 1-11. Interactions between the loops at the tip of domain IV of EF-G and peptidyl-tRNA

Details of the interactions between domain IV of EF-G and the peptidyl-tRNA in the P site in the (A) intermediate state of translocation and (B) the post translocation state. The mRNA is in blue, the peptidyl-tRNA is in light green, EF-G is in pink, and amino acids Q507 and H583 are in red. In the intermediate state of translocation, the acceptor stem of the peptidyl-tRNA moves towards the P site, whereas the anticodon loop is still between the A site and the P site. Image based on PDB 4V7B (Ramrath et al., 2013). In the post translocation state, residues Q507 and H583 form a network of interactions with the peptidyl-tRNA (position 36 and 37, green). Q500 and H573 in *T. thermophilus* structure. Image based on PDB 4V5F (Gao et al., 2009). (C) Evolutionary conservation of Q507 and H583 among bacterial species.

With the progress of crystallization and cryo-EM technology, the network of interactions between the tip loops of domain IV, especially of Q507 and H583, and the peptidyl-tRNA have been revealed in both intermediate state and post-translocation state (Brilot et al., 2013; Gao et al., 2009; Ling and Ermolenko, 2016; Ramrath et al., 2013; Zhou et al., 2014). (Figure 1-11A, B). According to the structural studies, the two conserved residues in domain IV of EF-G, Q507 in loop I and H583 in loop II (*E. coli*), are can form the network of interactions with the peptidyl-



tRNA in the post-translocation state (Gao et al., 2009). In addition, these two residues are highly conserved in prokaryotes (Figure 1-11C). These structures illustrate the conformational changes of EF-G and the interaction rearrangements between EF-G, ribosome, and the two tRNAs. It suggests that these interactions might exist already at the beginning of translocation and contribute to maintaining the mRNA reading frame throughout the process of translocation. The contacts of the tip residues of domain IV with the peptidyl-tRNA and the mRNA might not only accelerate translocation but also play a role in reading frame maintenance.

## **1.6. Scope of the thesis**

The reading frame on the mRNA is established during initiation and it is maintained throughout the entire process of elongation. The correct 0-frame codon-anticodon interactions, once established at the decoding step of elongation, are stabilized by the interactions with the ribosome except during translocation of the tRNA–mRNA. EF-G promotes translocation and may interact with the codon-anticodon duplex, but the role of EF-G in reading frame maintenance during translocation has not been studied. Using mutational analysis, we screened for specific residues in EF-G involved in reading frame maintenance. Using model mRNAs that allow spontaneous –1-frameshifting in the absence of stimulatory elements, we identified single amino acid exchanges that have a severe effect on frameshifting. We then used a toolbox of fluorescence reporters for studying ribosome dynamics to identify the steps of translocation at which EF-G contributes to reading frame maintenance. Our results suggest that residues at the tip of domain IV of EF-G control the coupling between mRNA-tRNA movement and the dynamics of the 30S head and body; disruption of this coupling results in ribosome slippage and the change of reading frame. This work contributes to the understanding of ribosome dynamics in maintaining accurate mRNA translation.



## 2. Results

Translocation is a multi-step process including EF-G binding and dissociation, conformational rearrangements of the ribosome, GTP hydrolysis by EF-G, and the movement of mRNA-tRNA complex. Translocation requires all these processes to function with high efficiency and accuracy. To examine the role of EF-G on reading frame maintenance, an *in vitro* reconstituted translation system with EF-G mutants was used. The contribution of EF-G is determined by the composition of translated 0- and -1-frame peptides. To understand how EF-G mutants change the motion of ribosomes during translocation, rapid kinetics techniques such as stopped flow and quench flow were applied to monitor the reactions in real time. The pre-steady kinetics provides the opportunity to observe the transient intermediates and to estimate the rate constants based on the formation and consumption of these intermediates.

### 2.1. Generation of EF-G mutants

To examine the importance of these interactions and the role of EF-G in reading frame maintenance, the conserved glutamine (Q) at position 507 or the histidine (H) at position 583 were replaced by an amino acid that differ in their chemical nature, charge, or size (Table 2-1). The mutations were introduced into the EF-G-coding plasmid by site-directed mutagenesis. The EF-G mutants were then overexpressed in *E. coli* BL21 (DE3) and purified by affinity chromatography on a Protino gravity column using a C-terminal oligo histidine tag on EF-G. In total, 9 different EF-G mutants were constructed and used in the following experiments to reveal the role of EF-G on reading frame maintenance.

**Table 2-1. List of EF-G mutations**

<b>Position</b>	<b>Natural amino acid</b>	<b>Substitution</b>	<b>Side chain feature</b>
507	Glutamine (Q)	Alanine (A)	Small, uncharged side chain, only one methyl group
		Aspartate (D)	Negative charge, one methyl group less
		Glutamate (E)	Negative charge, same length of the side group
		Phenylalanine (F)	Aromatics
		Histidine (H)	Positive charge, aromatics
		Asparagine (N)	One methyl group less
583	Histidine (H)	Serine (S)	Hydroxyl group
		Alanine (A)	Small uncharged side chain, only one methyl group
		Lysine (K)	Positive charge, linear side chain

## 2.2. GTP hydrolysis by EF-G mutants

Mutations in proteins, including individual point mutations, can affect the folding and structure of the protein. Thus, a loss of function might not be the result of the function of a specific side chain, but reflect an altered structure of the protein. A simple assay to test the ability of EF-G to bind to the ribosome and to turnover is the GTPase activity test. GTP hydrolysis in free EF-G is negligible and is stimulated by the ribosome; thus, the ability of EF-G to hydrolyze GTP can be used as an indicator of the functional activity of EF-G in binding to the ribosome and to dissociate after GTP hydrolysis. The ability of mutant EF-G to hydrolyze GTP was examined by incubating vacant ribosomes together with EF-G and GTP. Control experiments were performed by mixing either vacant ribosome or EF-G with GTP to measure the background GTP hydrolysis of the system. After 30 min incubation, about 60-80% of GTP was converted to GDP (Figure 2-1). Although some small effect was observed with EF-G Q507D and EF-G

H583A, in general, there was efficient GTP hydrolysis for all EF-G mutants. Thus, all EF-G variants were functional with respect to ribosome binding and dissociation.

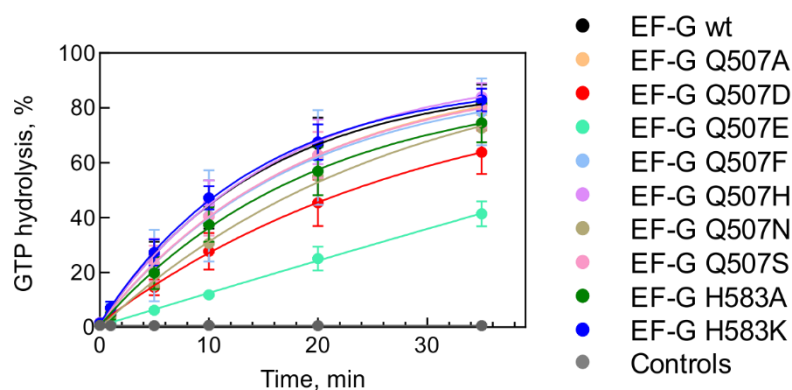


### Figure 2-1. GTP hydrolysis by EF-G

The rate of GTP hydrolysis by the wt and mutant EF-G was measured under turnover conditions. The GTP (1 mM) was incubated with vacant ribosome (0.5  $\mu$ M) and EF-G (1  $\mu$ M). The educt GTP and product GDP were analyzed via thin-layer chromatography. Error bars represented standard deviation (SD) obtained from three independent experiments.

### 2.3. Establishment of the reading frame maintenance assay

To examine the effects of EF-G on reading frame maintenance we established an experimental system that would allow us to detect the product of the 0- and  $-1$  frame. The design of the mRNAs has to fulfil two requirements. First, the mRNA has to contain either a tetrameric (X\_XX.Y) or a heptameric (X\_XX.Y\_YY.Z) slippery motif but do not have any other elements, e.g. a secondary structure, that might stimulate frameshifting. The slippery sequence is a major determinant of frameshifting; we deliberately omitted the secondary structure element downstream of the slippery sequence, which is a characteristic regulator of the programmed ribosome frameshifting, in order to monitor the intrinsic shiftiness of translation. Second, it should be feasible to separate the peptides translated from these mRNAs by HPLC, especially the 0-frame and the  $-1$ -frame products. The two different mRNAs are referred to as mRNA4S for the mRNA contained the tetrameric slippery motif and mRNA7S for the mRNA included the heptameric slippery motif (Figure 2-2A, B).

Both mRNAs were designed based on the AAA and AAG codons coding for lysine (K). One of the reasons why lysine has been chosen is that these two codons are decoded by the same tRNA<sup>Lys</sup>. Second, tRNA<sup>Lys</sup> has the highest propensity to frameshift among different tRNAs in *E. coli* and can be found frequently in the slippery site of programmed frameshifting sites. In addition, it is very common to have an A nucleobase before the AAA or AAG codon *in vivo* (Dr. Iakov Davydov, personal communication). About 10,800 cases have been found among the reading frames of the *E. coli* genome (K12) where an A base precedes a lysine codon. This number is higher than estimated by simulation analysis for the randomly distribution of all four nucleobases. The overrepresented of the A base upstream of lysine codons indicated that the slippery motif used in the model mRNA, especially the tetrameric slippery motif, is a common situation that the ribosome faces during translation.

The mRNA4S encodes MEKF for 0-frame and MEKV for -1-frame; the mRNA7S encodes MGKF for 0-frame and MGKV for -1-frame. In both cases, the peptide sequences differ in the last amino acid only. However, this does not mean that the reading frame is lost in the last round of translation. The translated peptides were then separated by the reverse phase HPLC due to the differences of hydrophobic character of amino acids. The elution time points and the amounts of translated peptides were determined and quantified by the radioactivity labeled f[<sup>3</sup>H]Met and [<sup>14</sup>C]Lys. The amino acid (M), dipeptides (ME or MG), and tripeptides (MEK or MGK) cannot be separated, which is not crucial for the purpose of this study. The 0-frame products, MEKF or MGKF, eluted at 19 min and the -1-frame products, MEKV or MGKV, eluted at 15 min (Figure 2-2C, D). The resolution and elution time points might slightly differ due to different HPLC columns, but this does not affect the separation of 0-frame and -1-frame products. By using this assay, the effects of mutations of EF-G on reading frame maintenance could be tested with the *in vitro* reconstituted translation system consisting of purified components from *E. coli*. The -1-frame products, MEKV or MGKV, will be observed when the mRNA reading frame is not maintained by the ribosome properly and slips to the -1-frame position.

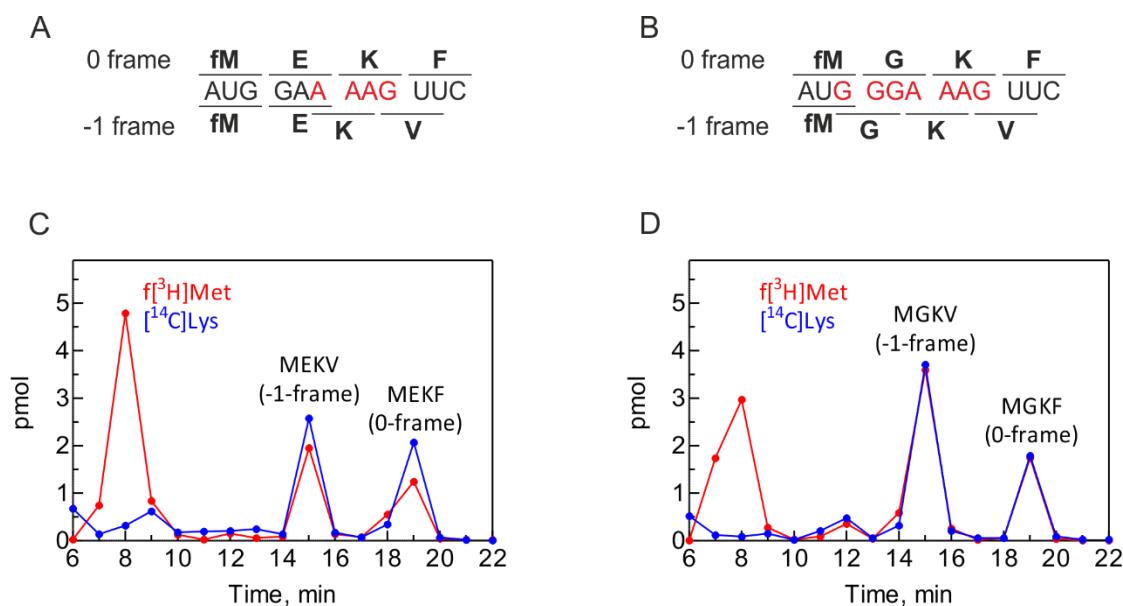


### Figure 2-2. Sequence and HPLC separation profile of mRNA4S and mRNA7S

The mRNA sequence of the (A) mRNA4S and (B) mRNA7S. The slippery motif of each mRNA construct is indicated in red and the encoded 0- and -1-frame peptides are shown next to the nucleotide sequence. The HPLC separation profiles of the translation products of (C) mRNA4S and (D) mRNA7S quantified by radio activity counting. In both cases, the 0-frame products are eluted at 19 min and the -1-frame products at 15 min. Peptides that appear before 10 min are the free amino acids, dipeptides, and tripeptides. The resolution and elution time points might have  $\pm 1$  min variation due to different columns.

## 2.4. Effects of EF-G mutants on reading frame maintenance

To test the effect of the mutations in EF-G, ribosomes were programmed with mRNA4S and mRNA7S and initiation complexes (IC) were purified. Translation was started by mixing IC ( $0.1 \mu\text{M}$ ) with ternary complexes contained corresponding aa-tRNA (Glu or Gly/Lys/Phe/Val) and with saturating concentrations of wt EF-G or variants of EF-G ( $2 \mu\text{M}$ ) in the presence of GTP. The reaction reactions were stopped after 5 min and the products were analysed (Figure 2-3A). On both mRNAs 0- and -1-frame products were observed showing that the reading frame was not maintained but that a fraction of ribosomes slipped to the -1-frame. (Figure 2-3B, C). The total amount of product was the same in all cases independent of the EF-G variant used.

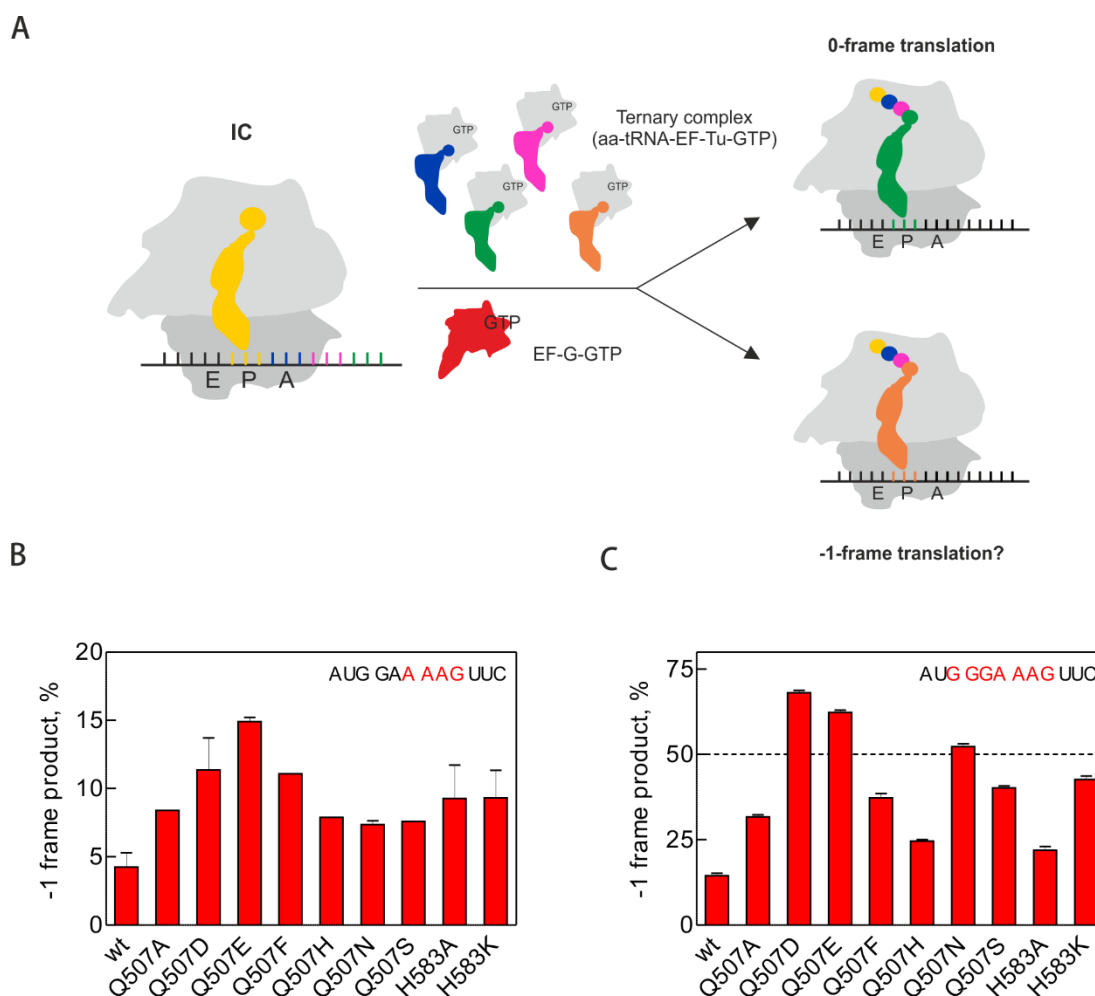


### Figure 2-3. Effects of EF-G mutants on reading frame maintenance

(A) Experimental scheme to examine the effects of EF-G on reading frame maintenance. Purified IC with either the mRNA4S or mRNA7S (0.1  $\mu$ M) were mixed with ternary complex and EF-G (2  $\mu$ M) in the presence of EF-G. The formations of 0- and -1-frame product were then analysed by the HPLC. The percentage of -1-frame product of the total product is shown for mRNA4S (B) mRNA7S (C). Error bars represented standard deviation (SD) obtained from three independent experiments.

On mRNA4S the frameshifting efficiency was about 4% in the presence of wt EF-G. The frameshifting efficiency was higher when the EF-G variants were used instead of the wt EF-G. The same trend was observed with mRNA7S, but here the fraction of -1-frame product was much higher. For wt EF-G the frameshifting efficiency was about 10%. For EF-G Q507D, EF-G Q507E and EF-G Q507N, the major product was the -1-frame one, up to 70% with EF-G Q507D. The increase of frameshifting efficiency with wt EF-G is similar for mRNA4S and



mRNA7S. Because frameshifting efficiency, and hence the dynamic range of the experiments was larger with mRNA7S,, all further experiments were done only with that mRNA.

Despite strong effects of EF-G mutants on frameshifting efficiency, it is still difficult to elucidate the role of EF-G on reading frame maintenance. To understand whether the increase of -1-frame product is due to effects on the factor's affinity to the ribosome or an effect on the turnover, we repeated the experiments at different EF-G concentrations. The purified IC (0.1  $\mu$ M) programmed with mRNA7S was incubated with TC(Gly/Lys/Phe/Val) and EF-G wt or variants (1 nM – 2  $\mu$ M) in the presence of GTP, the reaction was stopped after 5 min and the products were analysed by HPLC. The frameshifting efficiency was then plotted against the concentration of EF-G. For all factors, the loss of reading frame decreases with higher EF-G concentrations. Only EF-G Q507D shows a high and constant level of frameshifting (Figure 2-4A). Remarkably, very high frameshifting efficiency was observed at low EF-G concentrations and the extrapolation of zero EF-G concentration yielded the same value for all proteins (Figure 2-4B). The frameshifting curves were analysed according to the formula (Table 2-2):

$$Y = (FS_{\text{noEF-G}}) - ((\text{Amp}_{\text{FS}} * X) / ([\text{EF-G}]_{\text{FS1/2}} + X))$$

The parameters X, Y,  $FS_{\text{noEF-G}}$ ,  $\text{Amp}_{\text{FS}}$ , and  $[\text{EF-G}]_{\text{FS1/2}}$  indicate the concentration of EF-G, the frameshifting efficiency at given EF-G concentration, , frameshifting efficiency in the absence of EF-G, the difference of -1-frame product between no EF-G and saturated condition of EF-G, and the concentration of EF-G at which the half maximum value of the frameshifting efficiency is achieved.

Depending on the ratio of EF-G to the ribosome, the observed effects can be assigned to two different translocation regimes. When the ratio of EF-G to the ribosomes is larger than one, that is, the concentration of EF-G is more than 100 nM in this study, the frameshifting efficiency is independent of EF-G concentration. Frameshifting efficiency is about 65%, 40%, 20% and 15% with EF-G Q507D, EF-G H583K, EF-G H583A, and wt EF-G, respectively. The differences in the frameshifting efficiency are due to the mutations in EF-G.

When the concentration of EF-G is lower than 100 nM, i.e. the ratio of EF-G to the ribosome is less than one, the formation of -1-frame product is increased with decreasing concentration of EF-G, except the EF-G Q507D. When the concentration of EF-G is extrapolated to zero,

frameshifting efficiency reaches about 65-70% for wt EF-G and EF-G mutants ( $FS_{noEF-G}$ , Table 2-2). In other words, without EF-G the reading frame is maintained only on 30-35% of ribosomes programmed with mRNA<sub>7S</sub>. There is a 60% of difference in the amounts of -1-frame product formation ( $Amp_{FS}$ ) between translation with and without the participation of wt EF-G. In this concentration regime, the formation of -1-frame products depends on the concentration of EF-G. With EF-G Q507D, frameshifting efficiency is 65%, regardless of the concentration.

These results suggest that the propensity for frameshifting on the slippery sequence is the property of the ribosome itself. At low concentrations of EF-G the time for the ribosomes to encounter an EF-G is increased, thereby opening the time window for the ribosome to slip. In the presence of excess EF-G, EF-G binding is no longer rate limiting, and the time window for slippage is only defined by the relative rates of slippage and translocation. The strong effect of EF-G Q507D indicates that the assistance of EF-G on reading frame maintenance has been completely disrupted by this mutation.

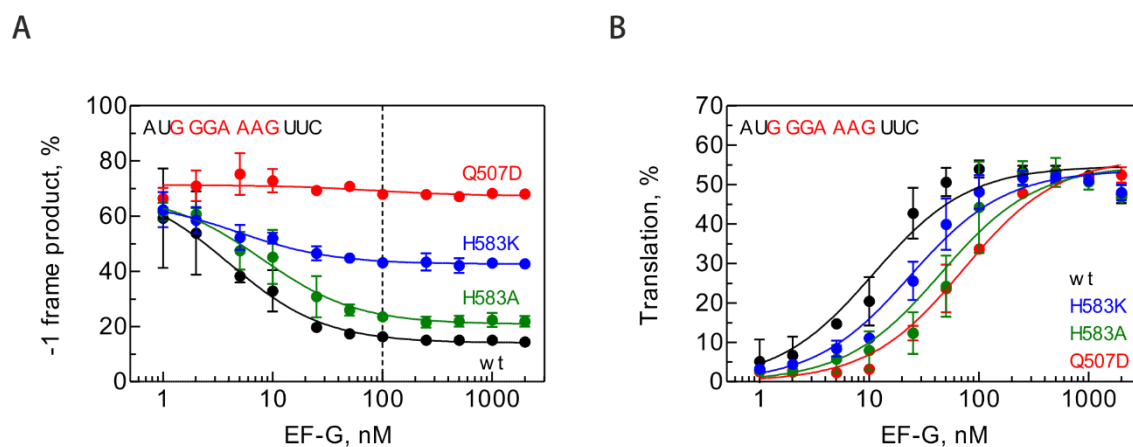


**Figure 2-4. Dependence of reading frame maintenance on EF-G concentration**

(A) Wt EF-G, EF-G H583A, EF-G H583K, and EF-G Q507D are indicated in black, green, blue, and red, respectively. The concentration (100 nM) at which EF-G and pre-translocation complexes are equimolar is indicated as a dotted line. Error bars represented standard deviation (SD) obtained from three independent experiments. (B) The translation efficiency with wt and mutant EF-G. Shown is the total product after 5 min incubation at different EF-G concentrations.

**Table 2-2. Dependence of frameshifting efficiency on EF-G concentration**

	<b>FS<sub>noEF-G</sub> (%)*</b>	<b>Amp<sub>FS</sub> (%)**</b>	<b>[EF-G]<sub>FS1/2</sub> (nM) ***</b>
<b>EF-G wt</b>	71 ± 8	57 ± 7	4 ± 2
<b>EF-G Q507D</b>	71 ± 1	4 ± 2	n.d.
<b>EF-G H583A</b>	68 ± 3	47 ± 3	8 ± 2
<b>EF-G H583K</b>	66 ± 3	23 ± 3	5 ± 2

$$Y = (FS_{noEF-G}) - ((Amp_{FS} * X) / ([EF-G]_{FS1/2} + X))$$

\* Formation of –1-frame product in the absence of EF-G

\*\* Difference of –1-frame product between no EF-G (FS<sub>noEF-G</sub>) and saturated condition of EF-G

\*\*\* EF-G concentration at which the -1 product reaches the half maximum

## 2.5. Kinetics of translocation

### 2.5.1. Monitoring of mRNA translocation by fluorescence-labeled mRNA

For all kinetic experiments, ribosomes were programmed with the mMF+14Alx405 mRNA. The movement of the mRNA was monitored by the change of the fluorescence Alexa405 labeled at the 3' end of the mRNA. Equal volumes of purified PRE-complex (0.05 μM) and EF-G (4 μM) were mixed in a stopped-flow apparatus at 37°C (Figure 2-5A). The assay is based on the observation that fluorescence intensity decreases when the mRNA moves toward to the ribosome during translocation. The rate of mRNA translocation was then evaluated by exponential fitting using TableCurve software. This method is relatively robust for the evaluation of kinetic experiment and has been validated in many previous studies (Belardinelli et al., 2016a; Cunha et al., 2013; Holtkamp et al., 2014a).

In our experimental setup, in addition to the downwards phase representing translocation, we also observed an increase of the fluorescence signal upon prolonged incubation, particularly with the EF-G mutants H583A and EF-G Q507D (Figure 2-5B, green and red). The fluorescence changes represent the direction of mRNA movement relative to the ribosome. The translocation is a virtually irreversible process and the non-slippery mMF should not move in the backward direction. One of the explanation for the unexpected traces might be the

contamination of PRE-complex or any other components that used in the experiment. If this is the case, the increasing phase of fluorescence signal should be also observed in the wt EF-G and EF-G H583K case (blue), which is not the case. Alternative, the mutants can favor reverse translocation. Given the ambiguity caused by the unusual effects of EF-G mutants, another method had to be applied for measuring the rate of translocation with the EF-G variants.

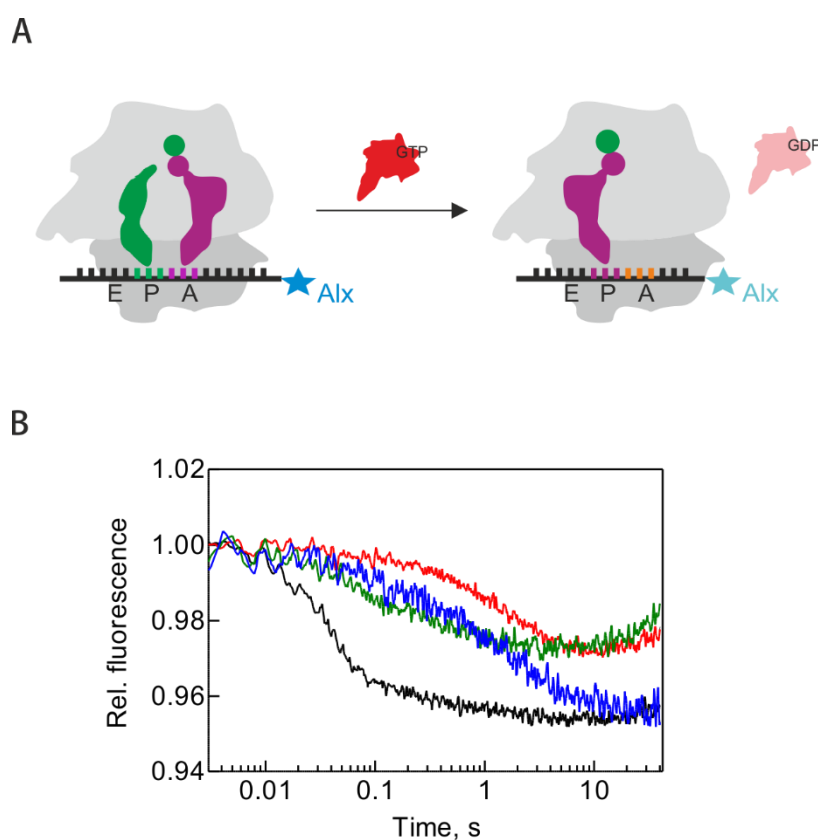


### Figure 2-5. Kinetic of mRNA translocation

(A) Experimental scheme of mRNA translocation. Purified PRE-complex programmed with the Alx405-labeled mMF was mixed with equal volume of EF-G (4  $\mu$ M) in a stopped-flow apparatus. The movement of mRNA is monitored as a change of Alx405 fluorescence. (B) Time course of mRNA movement for wt EF-G (black), EF-G H583A (green), EF-G H583K (blue), and EF-G Q507D (red).

### 2.5.2. Measurement of tRNA translocation by time-resolved Pmn assay

To understand how the mutations in EF-G affect its ability to promote translocation, we used the time-resolved puromycin (Pmn) assay. Pmn is an antibiotic that leads to the premature termination during translation. It enters to the vacant A site and reacts with the peptidyl-tRNA in the P site such that the peptide is transferred to the Pmn. The PRE complex has only a very low Pmn reactivity with Pmn, because the A site is occupied with a peptidyl-tRNA and the antibiotic cannot bind. To obtain efficient Pmn reaction, the peptidyl-tRNA in the PRE complex has to first translocate to the P site. For the POST-complex, the peptidyl-tRNA is already in the P site and can react with Pmn directly. The reaction of Pmn with peptidyl-tRNA is completed on a millisecond time scale, which is comparable of the rate of translocation. Then, the rate of tRNA translocation ( $k_{TL}$ ) is determined from the reaction rate of PRE-complex ( $k_{PRE}$ ) and POST-complex ( $k_{POST}$ ) using the formula  $1/k_{TL}=1/k_{PRE}+1/k_{POST}$  (Holtkamp et al., 2014a).

The time-resolved Pmn assays were performed by mixing the purified PRE-complex (0.2  $\mu$ M) together with EF-G (4  $\mu$ M) and Pmn (10 mM) in the quenched-flow apparatus. The POST complexes were freshly prepared before the experiment and mixed with Pmn only (Figure 2-6A). The apparent constants  $k_{PRE}$  and  $k_{POST}$  were obtained from the time course of the tripeptide fMet-Phe-Pmn formation. The reacted tripeptide fMet-Phe-Pmn and unreacted dipeptide fMet-Phe were separated by HPLC and quantified based on the radioactivity of f[ $^3$ H]Met and [ $^{14}$ C]Phe. The Pmn reaction was defined by the ratio of reacted tripeptide to the sum of reacted and unreacted peptides. The value of Pmn reaction is then plotted against time for the determination of  $k_{PRE}$  and  $k_{POST}$  using single exponential fitting (Figure 2-6B). To minimize the contribution of the Pmn reaction, saturated concentration of Pmn were used. Although the efficiency of reaction is slightly less with EF-G mutants, still roughly 65% of PRE-complexes were able to perform the translocation in the presence of any EF-G and reacted with Pmn. About 75% of fMet-Phe-Pmn were found in the reaction of POST complex. The rate of tRNA translocation with wt EF-G is comparable to the value reported previously, about 20  $s^{-1}$  (Holtkamp et al., 2014a), whereas all EF-G mutants show lower rates of translocation 0.8-11  $s^{-1}$  (Figure 2-6C).

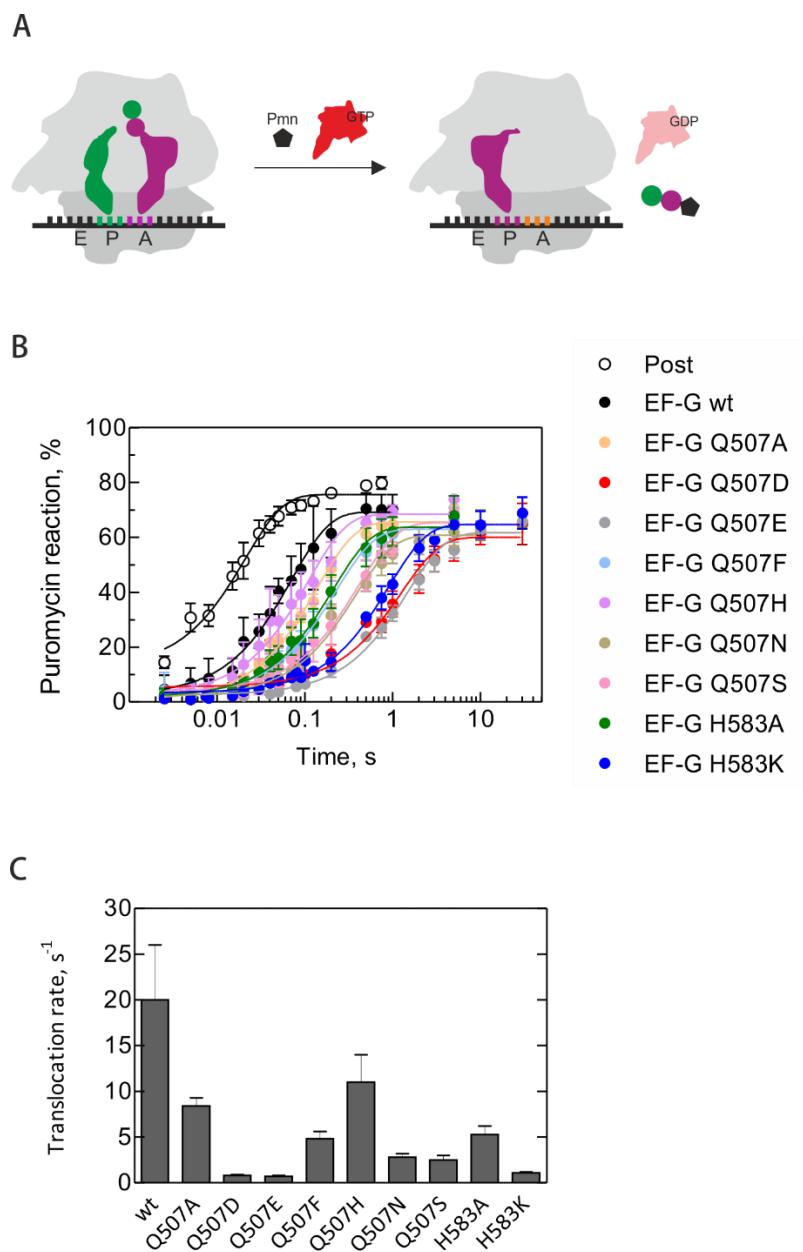


### Figure 2-6. Kinetics of tRNA translocation

(A) Experimental scheme of the time-resolved Pmn assay. The purified PRE complexes (MF) were mixed with EF-G (4  $\mu\text{M}$ ) and Pmn (10 mM) in the quenched-flow machine. (B) PRE (closed circle) or POST complexes (open circle) were rapidly mixed with Pmn and EF-G (black: wt) in the quench-flow apparatus and the time courses of fMet-Phe-Pmn formation were recorded. The apparent rate constants ( $k_{\text{PRE}}$ ,  $k_{\text{POST}}$ ) of the reactions were obtained by one-exponential fitting. (C) The rate of tRNA translocation was obtained by deconvolution of the rate of PRE- and POST-complex reaction ( $1/k_{\text{TL}}=1/k_{\text{PRE}}-1/k_{\text{POST}}$ ). Error bars represented standard deviation (SD) obtained from three independent experiments.

**Table 2-3. Apparent rates and translocation rates of variants of EF-G**

	Apparent rate (s <sup>-1</sup> )	Translocation rate $k_{TL}$ (s <sup>-1</sup> )*
<b>k<sub>POST</sub>:</b>	48 ± 7	
<b>wt:</b>	14 ± 3	20 ± 6
<b>Q507A:</b>	7.2 ± 0.6	8.5 ± 0.9
<b>Q507D:</b>	0.8 ± 0.1	0.8 ± 0.1
<b>Q507E:</b>	0.7 ± 0.1	0.7 ± 0.1
<b>Q507F:</b>	4.4 ± 0.6	4.8 ± 0.8
<b>Q507H:</b>	9 ± 2	11 ± 3
<b>Q507N:</b>	2.6 ± 0.4	2.8 ± 0.4
<b>Q507S:</b>	2.4 ± 0.5	2.5 ± 0.5
<b>H583A:</b>	4.8 ± 0.8	5.3 ± 0.9
<b>H583K:</b>	1.1 ± 0.1	1.1 ± 0.1

\*Translocation rate ( $k_{TL}$ ):  $1/k_{TL}=1/k_{PRE}-1/k_{POST}$

## 2.6. Correlation between the speed of translocation and frameshifting

To understand whether there is a correlation between the observed low rates of translocation and the decrease of reading frame maintenance during translocation, the frameshifting efficiency measured at saturating concentration of EF-G was plotted against to natural logarithm (ln) value of translocation rate. The correlation between these two values was analysed using the linear-correlation coefficient  $r$ . The value of  $r$  ranging from 0 to  $\pm 1$  indicates either no correlation or complete correlation, respectively. Positive values mean positive correlation and negative value means negative correlation. As shown in Figure 2-7, the correlation coefficient  $r$  is  $-0.97$ , which indicates a strong negative correlation between translocation rate and the formation of  $-1$ -frame product. However, the correlation coefficient only describe whether the correlation of two variables or not. To figure out how well the regression model fits to the data and predicted outcome, the coefficient of determination ( $R^2$ ) has to be introduced. A higher  $R^2$  indicates a better goodness of fit for the observation. In this

study, the  $R^2$  has a value of 0.94, which indicated that 94% of the  $-1$ -frame product formation can be explained by the translocation rate. That means frameshifting increased with decreasing rate of translocation. In other words, slow translocation compromises reading frame maintenance.

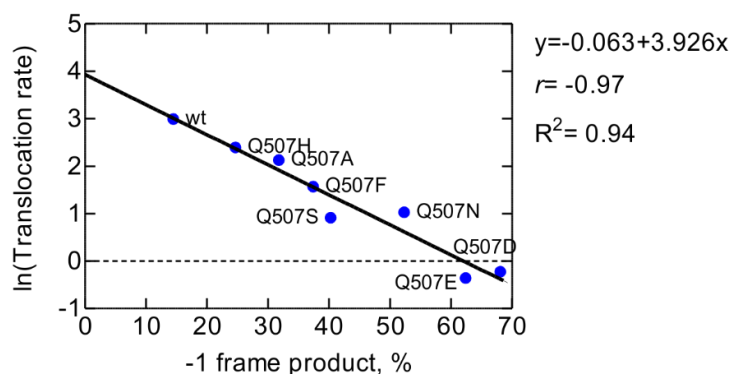


### Figure 2-7. Correlation between the translocation rate and frameshifting

The  $\ln$  value of tRNA translocation rate is plotted against the formation of the  $-1$  frame product under saturated concentration of EF-G. The correlation between the rate of translocation and reading frame maintenance was determined by linear regression. Coefficient of determination  $R^2$  indicates that 94% of the formation of  $-1$ -frame product can be explained by the translocation rate.

## 2.7. Effects of EF-G mutants on the trajectory of translocation

The experiments described above showed that the tRNA translocation is slowed down by all EF-G mutants tested, both at position 507 and 583. However, translocation is a multi-step process and apart from measuring the rate of tRNA movement, a toolbox of fluorescence assay is available to measure different other movements of the ribosome or parts of it during translocation (Figure 2-8). The binding and dissociation of EF-G, small subunit (SSU) dynamic, SSU head swiveling, SSU rotation relative to the large subunit (LSU), and the P-site tRNA movements were monitored, respectively, by FRET between L12 and EF-G, ribosomal protein S13, FRET between S13 and L33, FRET between S6 and L9, FRET between P-site tRNA and L33, and P-site tRNA in real time (Belardinelli et al., 2016a; Caliskan et al., 2014; Sharma et al., 2016). For each reporter, a series of EF-G concentration were applied. As in the previous



experiments, only three mutants the EF-G Q507D, EF-G H583K, and EF-G H583A were selected out of the total of nine mutants.

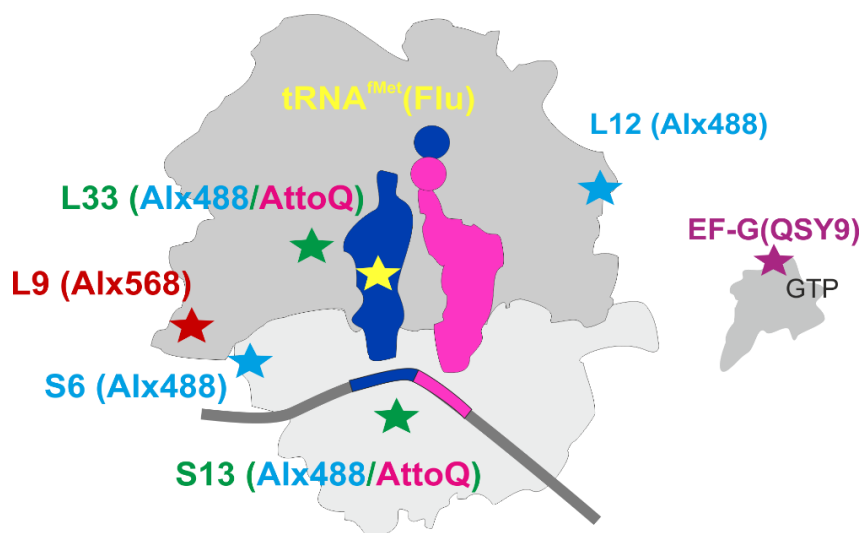


### Figure 2-8. Fluorescence reporters

The overall translocation and SSU rearrangement is monitored by the Alx488-labeled S13. EF-G binding and dissociation is monitored by the FRET pair between Alx488-labeled L7/12 and QSY9-labeled EF-G. The SSU head swiveling is monitored by the FRET pair between AttoQ-labeled S13 and Alx488-labeled L33. The SSU body rotation is monitored by the FRET pair between Alx568-labeled L9 and Alx488-labeled S6. The P site tRNA movement is monitored by fluorescence change of fluorescein-labeled tRNA<sup>fMet</sup> and by the FRET pair between fluorescein-labeled tRNA<sup>fMet</sup> and AttoQ-labeled L33 (Belardinelli et al., 2016a; Caliskan et al., 2014; Sharma et al., 2016).

All experiments were performed by mixing PRE complexes (MF) together with EF-G in a stopped-flow apparatus. The recording time used for wt EF-G and EF-G mutants depends on the rate of translocation. To analyse the data, average fluorescence signals were first normalized to the relative fluorescence values and then plotted against the reaction time (Figure 2-9 to 12). For some reporters such as L12 and EF-G, the difference between low and high concentration of EF-G can be easily distinguished. Even though the changes are relatively small for other reporters, the titration of EF-G concentration of each reporter indicated that the all reactions are concentration-dependent. For better comparison of the effects of EF-G mutations on each fluorescence reporter, the traces obtained at the highest EF-G concentration were combined in

the same graph (Figure 2-13). With wt EF-G, the reaction was completed within a second, as seen from the end level of the fluorescence signals, whereas with the EF-G mutants, roughly the same level was reached only after 10-20 s. EF-G Q507D showed the strongest effects on translocation, followed by the EF-G H583K, and EF-G H583A.

To understand the influence of EF-G mutations on the different sub-steps, an analysis by global fitting is required. Global fitting allows to fit all traces together according to in a single translocation model. Based on previous research on the mechanism of wt EF-G, a linear five-step kinetic model was used (Figure 2-14A) (Belardinelli et al., 2016a). The information about the elemental rate constants of each step (Table 2-4) and the absolute values of the intrinsic fluorescence intensities (IFIs) of each reporter (Figure 2-14B) were obtained by the global fitting analysis based on the numerical integration in KinTek explorer (Johnson, 2009). The IFIs are the characteristic fluorescence signature of the kinetic intermediates for each reporter at each step, which is analogous to the FRET values in the smFRET studies. In addition, the IFIs were calculated in an unbiased way without any previous assumptions of fluorescence changes at each step. Therefore, the direction of motions of each component and the order of the rearrangements monitored with each FRET pair can be demonstrated by the IFIs.

The first reaction in the five-step translocation model is a reversible step accounting for EF-G binding and dissociation. The rest four steps are considered quasi-irreversible, because the overall translocation is strongly committed towards the forward translocation in the presence of EF-G and GTP. As shown in Table 2-4, the elemental rate constants of translocation with wt EF-G are comparable to the previously published values. Comparison between the wt and mutant EF-G show that  $k_1$  values are similar, indicating that EF-G binding to the ribosome is not affected by the point mutations in domain IV of EF-G. The dissociation rate constant  $k_{-1}$  is somewhat lower for EF-G H583K compared to the wt EF-G and other mutants, but given the strong forward commitment of the reaction, the effect is probably not significant, as the effective  $K_M$  for the reaction, defined as  $K_M=(k_{-1}+k_2)/k_1$ , is very similar for all EF-G variants. The value of  $k_2$  is defined by several steps, including GTP hydrolysis, EF-G engagement. This rate constant is similar for the wt and mutant EF-G, consistent with the similar rates of GTP hydrolysis in multiple turnover experiment. The rate constant of the third step,  $k_3$ , is decrease by 3-4 fold for the EF-G Q507D and EF-G H583K mutants or by 2-fold for the EF-G H583A mutant; this step reflects to the movements of mRNA-tRNAs complex from the A site and P site to the P site and E site, respectively. The main effect is observed at the steps 4 and 5, which

entail the movement of the deacylated-tRNA from the P site to the intermediate E-site tRNA binding state (E' state) then into solution and the release of EF-G from the ribosome. The  $k_4$  is reduced by the factor of 4.5 to 13, and  $k_5$  by a factor of 8-30, suggesting a major effect of the mutations of domain 4 are manifested at the late stages of translocation. EF-G Q507D and EF-G H583K have stronger effects than EF-G H583A.

In addition to the kinetic analysis, we also explored whether IFIs change for EF-G mutants (Figure 2-14B). The normalized IFI for the interaction of EF-G with L12 are very similar for the wt EF-G and the mutants, suggesting similar location of the G-domain of EF-G to the L12 ribosome upon recruitment and during tRNA translocation. Also the release of the P-site tRNA through the E site towards the dissociation from the ribosome followed a similar pathway. Notably, the dissociation of both EF-G and tRNA is slower, although it proceeds through the same intermediates. The most prominent changes are in the IFIs that reflect the swiveling of SSU head, the rotation of SSU body and the position of the tRNA elbow region in the A site. For wt EF-G, the SSU body starts to rotate in the backward direction at step 2 and the SSU head starts to swivel backward during step 3. Both SSU body and head continues their gradual rotation in the backward direction until the release of deacylated-tRNA and EF-G. Similar trajectories of SSU body and head motions were observed in the presence of EF-G H583A. However, for the EF-G Q507D and EF-G H583K, the backward movement of SSU head and body were observed mainly in step 5.

**Table 2-4. Elemental rate of sub-step of translocation**

	$k_1(\mu\text{M}^{-1}\text{s}^{-1})$	$k_{-1}(\text{s}^{-1})$	$k_2(\text{s}^{-1})$	$k_3(\text{s}^{-1})$	$k_4(\text{s}^{-1})$	$k_5(\text{s}^{-1})$
<b>wt*</b>	55 ± 6	65 ± 10	85 ± 10	43 ± 2	15 ± 1	4 ± 1
<b>wt</b>	40 ± 11	60 ± 15	72 ± 22	32 ± 6	11 ± 2	3.6 ± 0.1
<b>Q507D</b>	44 ± 6	45 ± 7	43 ± 6	12 ± 2	0.82 ± 0.01	0.12 ± 0.03
<b>H583K</b>	71 ± 6	22 ± 3	52 ± 3	9.0 ± 0.9	1.25 ± 0.03	0.19 ± 0.01
<b>H583A</b>	58 ± 8	48 ± 12	31 ± 6	20 ± 1	2.45 ± 0.07	0.43 ± 0.02

\* From (Belardinelli et al., 2016a)

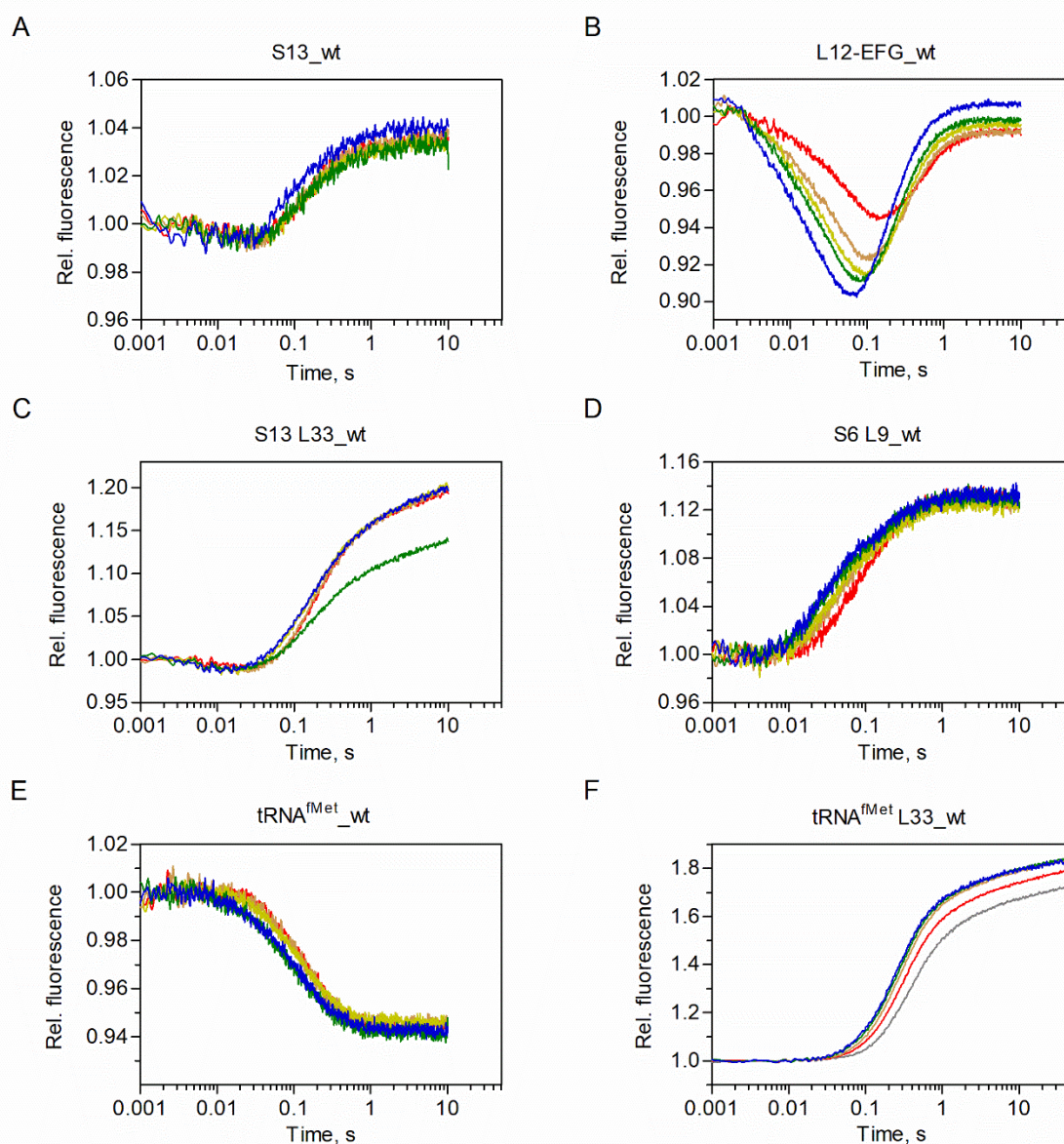


**Figure 2-9. Fluorescence changes of different reporters with wt EF-G**

The PRE-complex (MF) is mixed with 0.2 (grey), 0.5 (red), 1.0 (brown), 1.0 (lime), 2.0 (green), and 4.0 (blue)  $\mu$ M of wt EF-G in the stopped flow apparatus. The fluorescence reporters and what they monitored are: (A) S13: SSU dynamic; (B) L12 and EF-G: EF-G binding and dissociation; (C) S13 and L33: SSU head swiveling; (D) S6 and L9: SSU rotation relative to the LSU; (E) tRNA<sup>fMet</sup>: P-site tRNA movement; (F) tRNA<sup>fMet</sup> and L33: P-site tRNA movement.

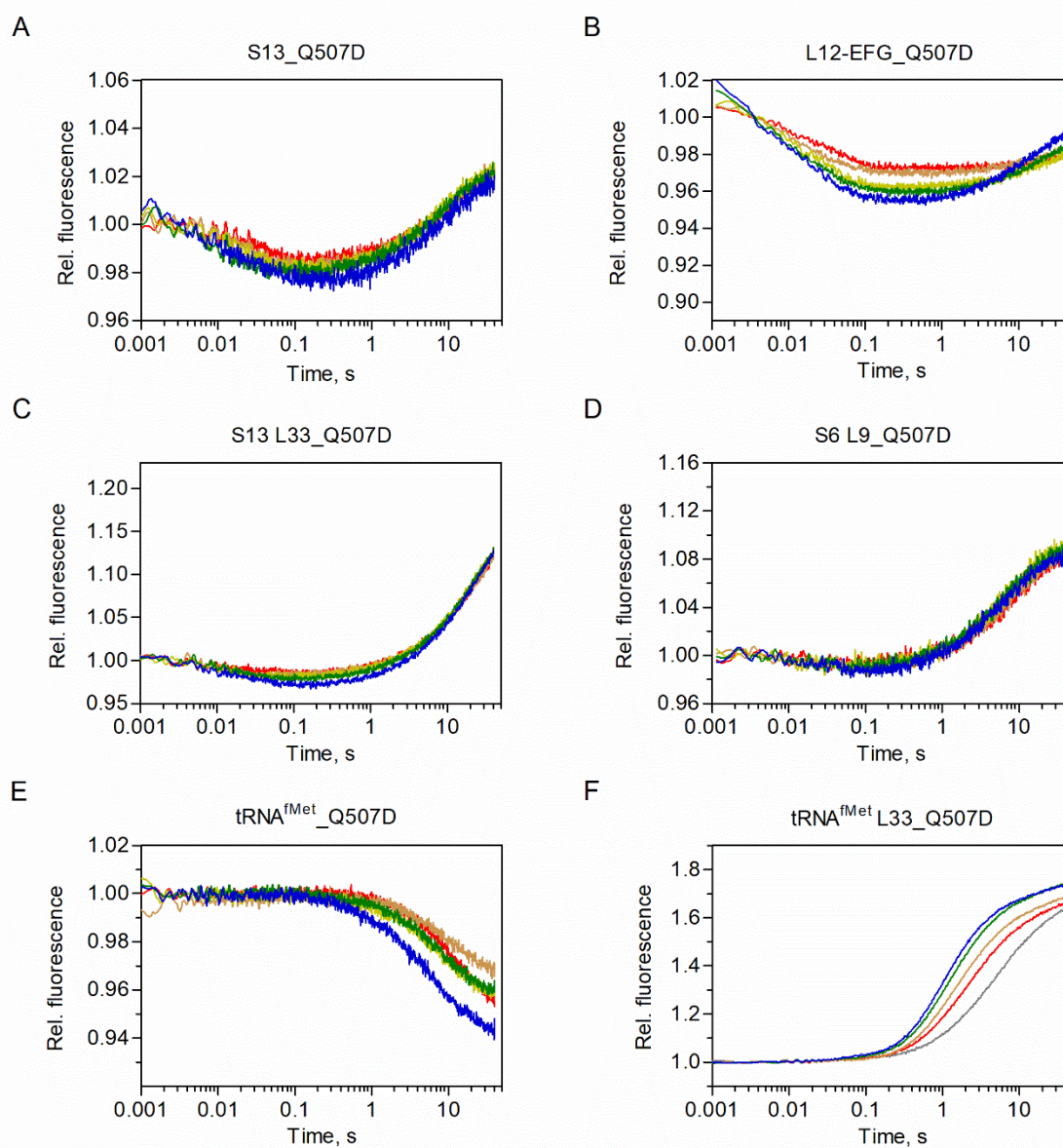


**Figure 2-10. Fluorescence changes of different reporters with EF-G Q507D**  
The experiment settings and color code are the same as for wt EF-G (Figure 2-9).



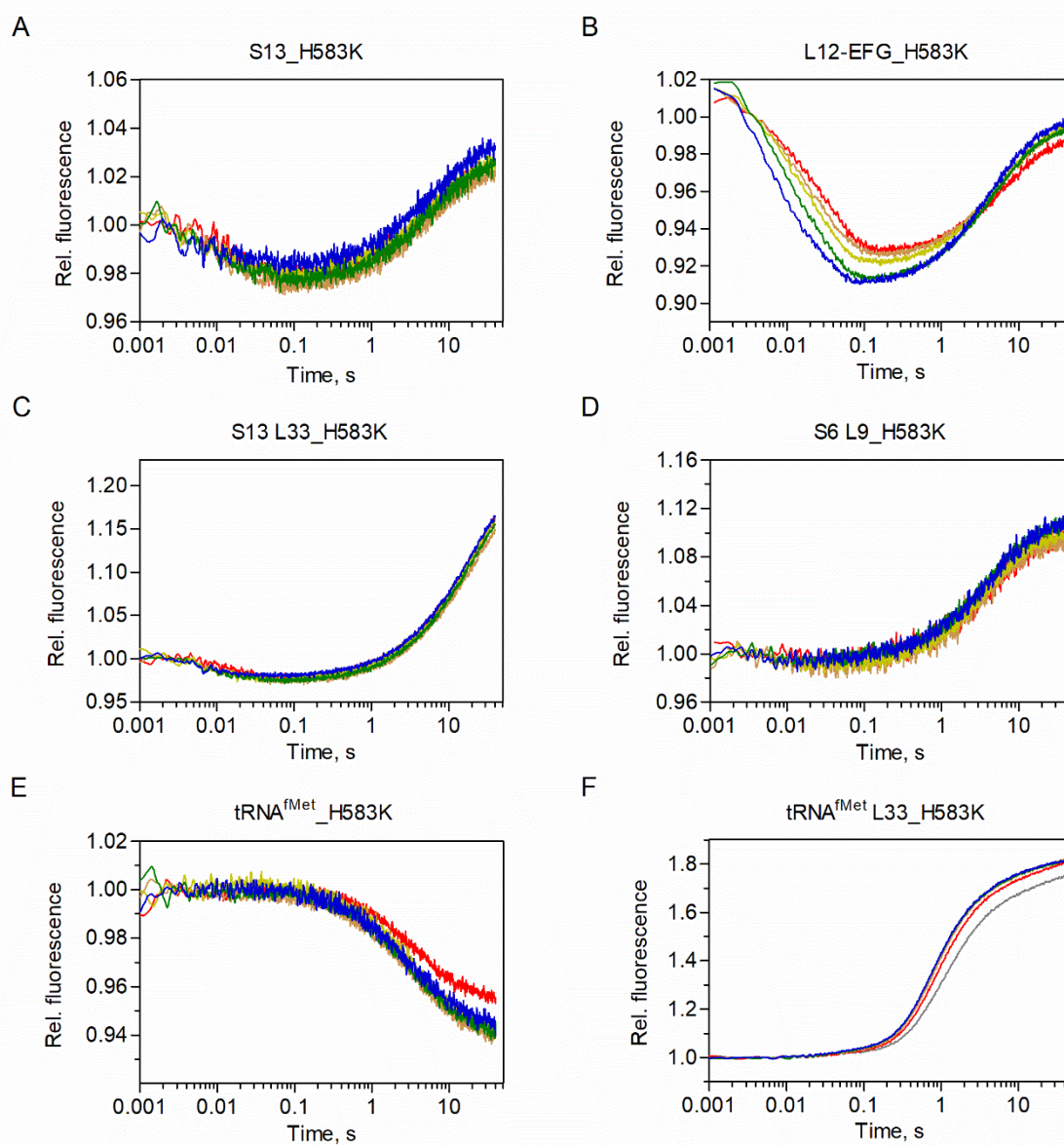


**Figure 2-11. Fluorescence changes of different reporters with EF-G H583K**

The experiment setting and the color code are the same as for wt EF-G (Figure 2-9).

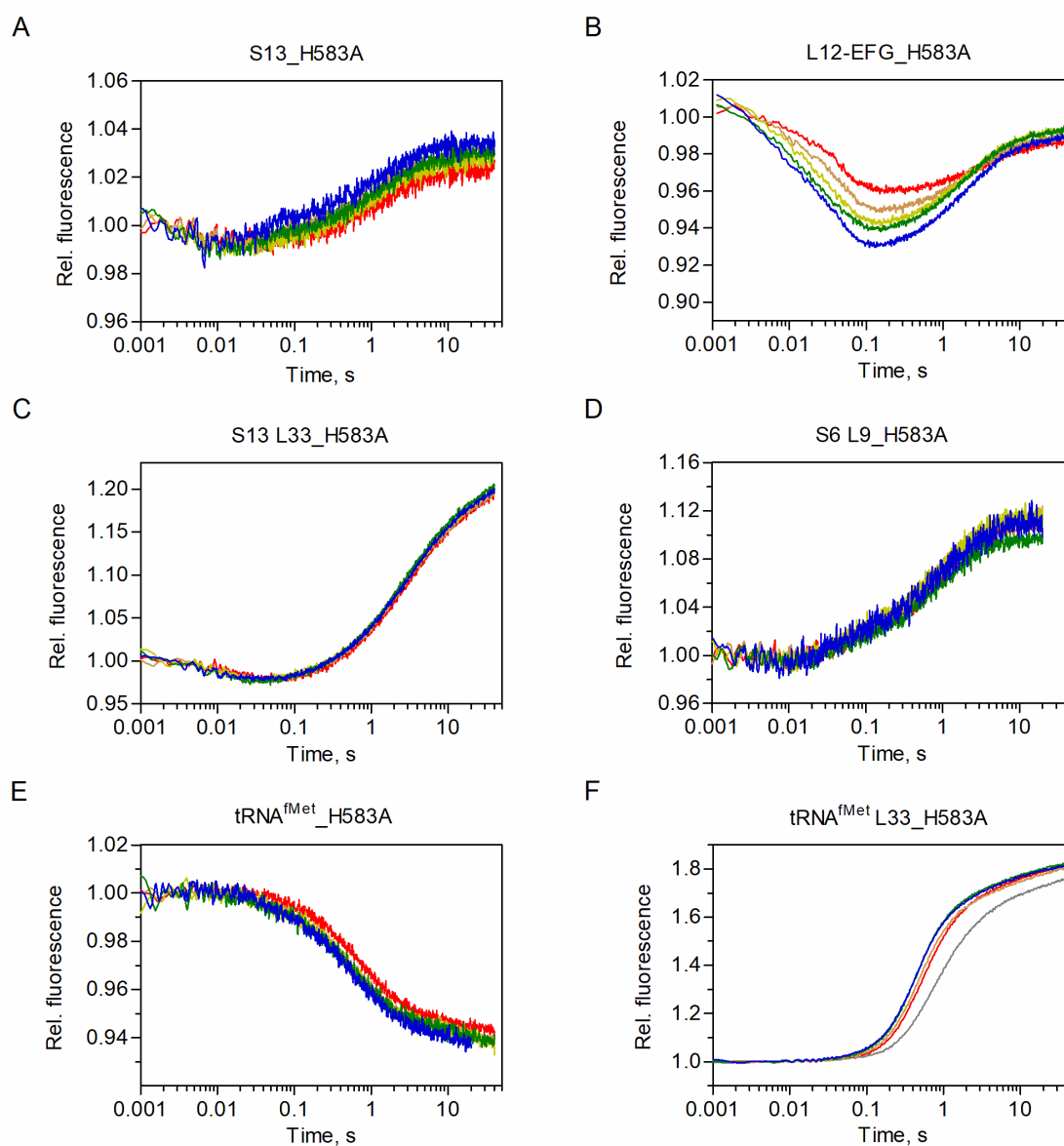


**Figure 2-12. Fluorescence changes of different reporters with EF-G H583A**

The experiment setting and the color code are the same as for wt EF-G (Figure 2-9).

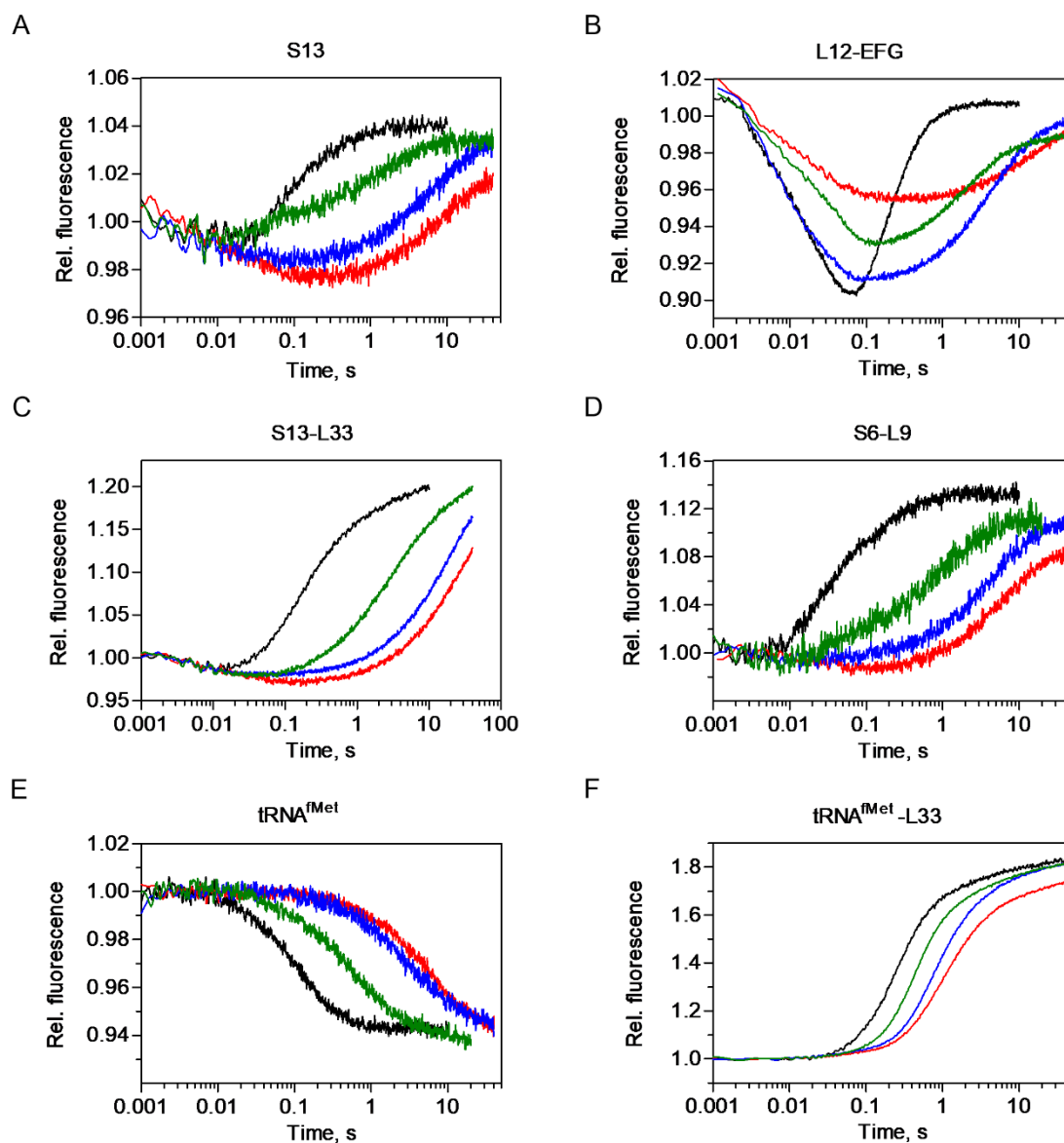


**Figure 2-13. Comparison of different fluorescence reporters for different EF-G mutants**  
Shown are fluorescence traces obtained at the highest EF-G concentration (4  $\mu$ M). Wt EF-G is denoted by black, EF-G Q507D is red, EF-G H583K is blue, and EF-G H583A is green.



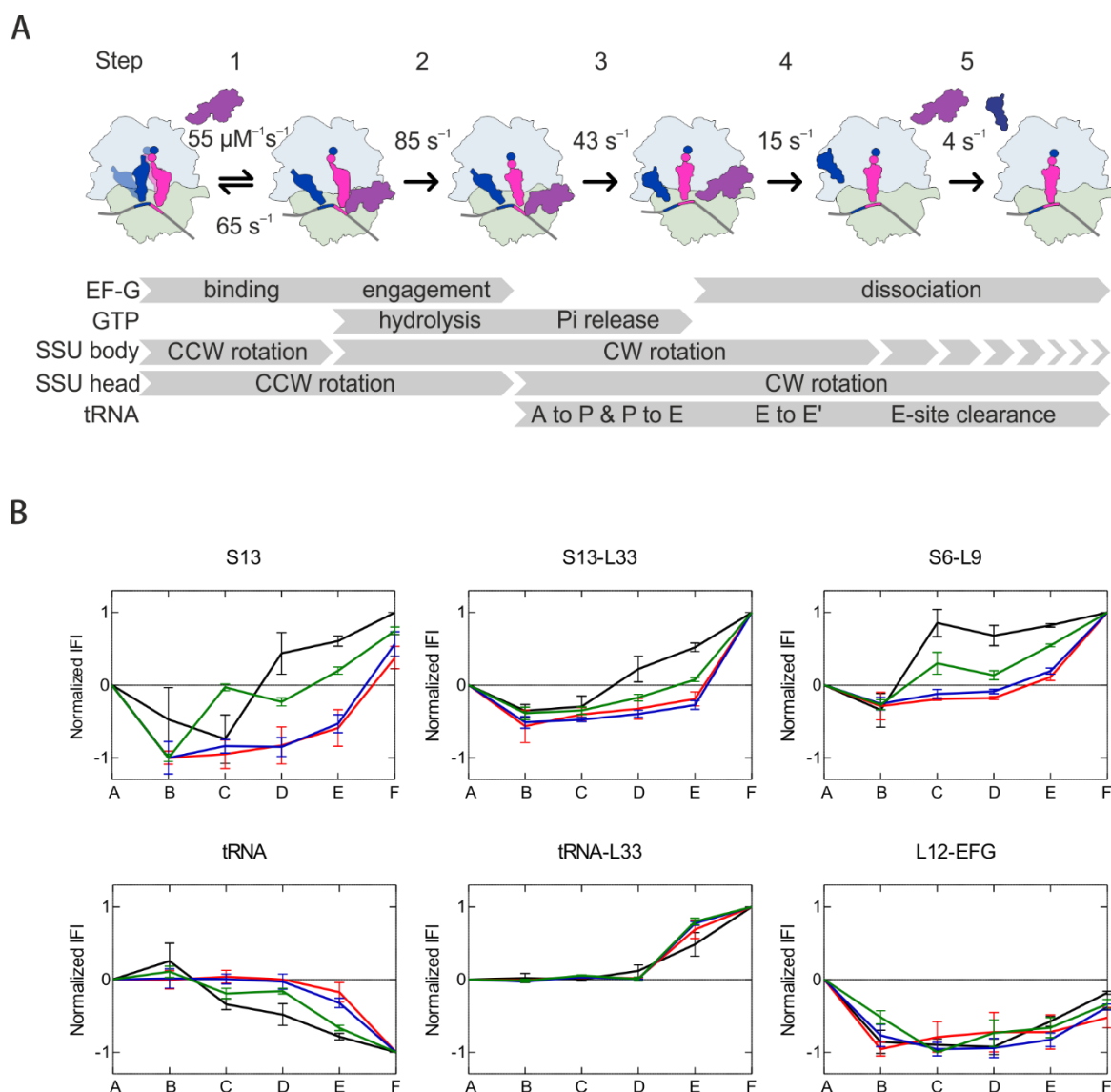


**Figure 2-14. Summary of the effects of mutations in domain 4 of EF-G on translocation.** (A) Scheme of 5-step kinetic model of translocation in the presence of wt EF-G. In step 1, binding of EF-G is reversible and induces a CCW rotation of the SSU body and head. In step 2, GTP is hydrolyzed by EF-G. The SSU body starts to rotate in the CW direction while the SSU head still moves to the CCW direction. In step 3, the inorganic phosphate (Pi) is released from EF-G. The SSU head also rotates in the backward CW direction. The movements of two tRNAs and mRNA from A and P sites to P and E sites are promoted by the EF-G. In step 4 and 5, EF-G dissociates from L12 and leaves the ribosome. The SSU body and head rotate continually in the CW direction still the end of translocation. The E site tRNA moves into the E' state and eventually leaves the ribosome (Belardinelli et al., 2016a). (B) Comparison of fluorescence signatures shown in normalized IFIs. The wt EF-G, EF-G H583A, EF-G H583K, and EF-G Q507D are indicated in black, green, blue, and red. Error bars represented standard deviation (SD) obtained from at least three independent experiments.



### 3. Discussion

#### 3.1. Maintenance of reading frame during translation

The data presented in this study provide a new insight into the ability of the ribosome to move along the mRNA and the role of EF-G in reading frame maintenance. Our work redefines the contributions of the ribosome and of EF-G. Previous studies indicate that all three tRNA-binding sites on the ribosome, the A, P, and E sites, contribute to maintaining the reading frame during translation. Mutations and deletions at these three tRNA binding sites result in +1 or -1 frameshifting (Bocchetta et al., 2001; Devaraj et al., 2009; Kubarenko et al., 2006; Näsvalld et al., 2009; O'Connor et al., 1997; Sanders et al., 2008; Sergiev et al., 2005; Wilson and Nierhaus, 2006). Although interactions between the ribosome and the mRNA-tRNA complex are essential and crucial for reading frame maintenance, we found that the ribosome itself is prone to frameshifting on slippery sequences and thus, the ribosome alone is not capable of maintaining the correct reading. This observation is relevant *in vivo*, as tetrameric slippery motifs (X\_XX.Y) occurs frequently in cellular mRNAs. For instance, an A base preceding lysine codons AAA or AAG is common in open reading frames of the *E. coli* genome. With about 10,800 sites, the number is even slightly overrepresented compared to the statistically expected probability (10,200 sites) (Dr. Iakov Davydov, personal communication). The heptameric slippery motif (X\_XX.Y\_YY.Z) is also common in the genome (Antonov et al., 2013; Gurvich et al., 2003; Moon et al., 2004; Sharma et al., 2014).

Previous work on the mechanism of programmed ribosomal frameshifting indicated that ribosomes can slip into the -1-frame during translocation or when the A-site remains vacant for a prolonged time, e.g. during starvation (Caliskan et al., 2014; Chen et al., 2014; Kim and Tinoco, 2017). Notably, those mechanisms operate also when one of the regulatory elements of programmed ribosome frameshifting, e.g. an mRNA secondary structure, is removed. The only element essential for frameshifting is an mRNA slippery sequence. This work suggests yet another mechanism of frameshifting, which occurs when two tRNAs are bound to the ribosome (a deacylated-tRNA in the P site and a peptidyl-tRNA in the A site) and prior to binding of EF-G. In this case, ribosome slippage might be triggered by spontaneous fluctuations of the ribosome. The shifting of the mRNA reading frame at this stage is reversible. The population of 0- and -1-frame may depend on the thermodynamic preference of the tRNAs for binding to the 0- and -1-frame codons on the mRNA (Figure 3-1, ①).

It is unlikely that ribosomal slippage prior to translocation is prevalent *in vivo*, because there is enough EF-G for translocation in the cells. However, the reading frame might still change during translocation (Figure 3-1, ②) in the presence of EF-G. The mutations in EF-G domain IV studied here lead to increased frameshifting (Figure 2-3). Structure studies suggest potential interactions between the tip loops of domain IV of EF-G with residues Q507 and H583, and the peptidyl-tRNA which might have a role in reading frame maintenance during translocation (Gao et al., 2009; Ramrath et al., 2013). The experimental data in this study show that the disruption of these interactions in the EF-G mutants affects frame maintenance. Higher frameshifting was observed with all EF-G mutants on both model mRNAs with either the tetrameric or the heptameric slippery motif. There are two potential explanations for the role of EF-G in reading frame maintenance during translocation, one role is an active one and the other is a passive one. EF-G might actively stabilize the positioning of the tRNAs in the correct frame with the help of interactions between Q507, H583 and the peptidyl-tRNA. Alternatively, EF-G passively prevents frameshifting by accelerating the process of translocation. Strong correlation between the rate of translocation and the extent of frameshifting suggests that slow translocation might open the kinetic time window for the ribosome to slip into an alternative reading frame.

Structural studies of EF-G with the 70S ribosome show interactions between EF-G and the peptidyl-tRNA, but a recent structural study on eEF2, which is the homolog of EF-G in eukaryotes, shows a direct interaction between the modification of His699 (yeast) at the tip of domain IV of eEF2 and the mRNA (Pellegrino et al., 2018). Diphthamide is a unique post-translational modification of this conserved histidine residue (Jorgensen et al., 2002; Ortiz et al., 2006). In the absence of the diphthamide modification -1 frameshifting is increased and the resistance to diphtheria toxin is reduced (Liu et al., 2012; Ortiz et al., 2006). Pellegrino *et al.* observed that the diphthamide modification of eEF2 points towards the mRNA and interacts with the sugar-backbone moiety at position +4 of the mRNA. The modification might function as a “pawl” maintaining the reading frame during translocation. The diphthamide modification of eEF2 might also prevent spontaneous back rotation of the SSU head domain, thereby avoiding slippage of the reading frame and ensuring fidelity of translation (Pellegrino et al., 2018).

Although the diphthamide modification is not present in bacterial, the finding that eEF2 could directly interact with mRNA might points towards potential interactions of EF-G. The details of the mechanism by which EF-G affects reading frame maintenance during translocation

remain unclear. The EF-G H583K and the EF-G Q507D mutant show a reduction of the rate of translocation to the same extent, to about  $1 \text{ s}^{-1}$ , but the H583K mutant shows less effects on reading frame maintenance. The EF-G Q507D mutant is a particular case, because the level of frameshifting does not change with or without its presence. It is possible that the conserved glutamine residue might have an unexpected role during translation. Meanwhile, the possibility that the EF-G mutants induce frameshifting cannot be completely excluded. EF-G might play both active and passive role in reading frame maintenance during translocation. Further studies are required for understanding the role of the tip loops of domain IV of EF-G in reading frame maintenance and translocation in general.

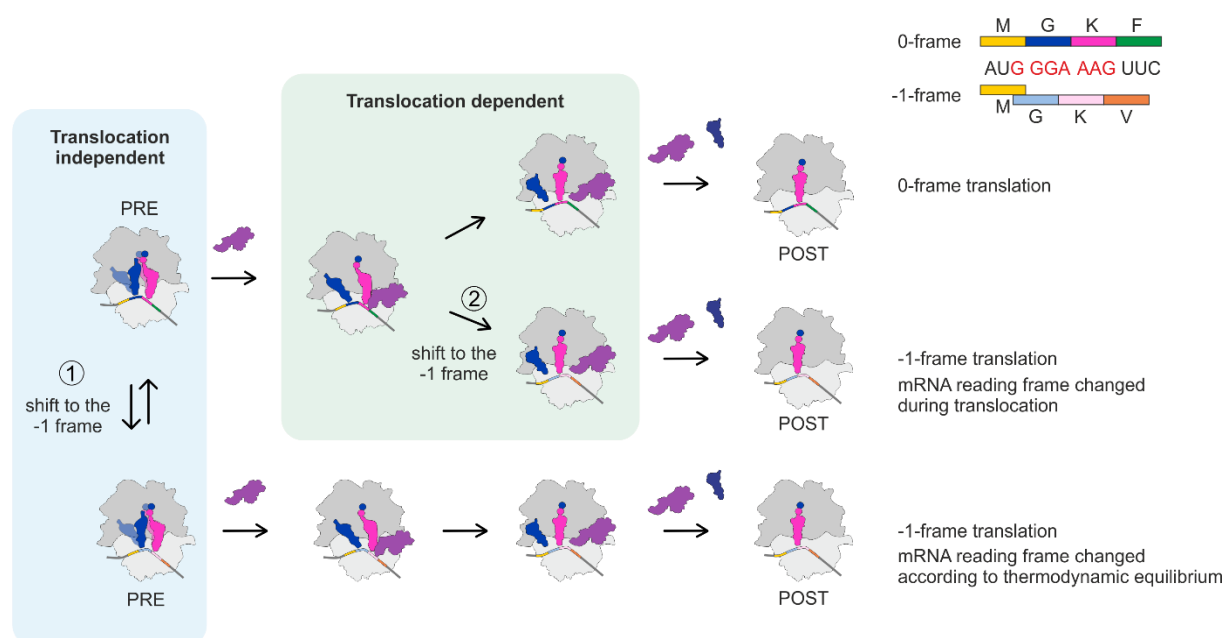


### Figure 3-1. Potential pathways for the divergences of the reading frame

The mRNA reading frame can slip to the -1-frame in two different ways when the ribosome encounters slippery motif during translation. The model mRNA (mRNA7S) used in this study is shown in the top right. The slippery motif of the mRNA is denoted in red and the encoded 0- and -1-frame peptides are shown next to the nucleotide sequence in different colors for the respective codes. The first potential pathway, ①, is translocation independent and according to the thermodynamic equilibrium. The reading frame might shift to the -1-frame while the ribosome is waiting for the binding of EF-G. The change of reading frame at this stage is reversible and depends on the thermodynamic preference of mRNA and tRNAs for the A, P, and E site. The mRNA reading frame might also shift during translocation, ②, which results in -1-frame translation. Details of how the reading frame alters during translocation remain unclear yet.

### 3.2. Effects of EF-G mutants on the SSU dynamics

The kinetic results obtained using several different fluorescence reporters were analysed by global fitting to the 5-step model of translocation used previously. This model describes the mechanism of translocation in the presence of wt EF-G. This analysis provides insights not only into the kinetic mechanism, but also delineates the trajectories of each reporter by revealing how the distances between labeled positions change along the reaction coordinate. Mutations in EF-G not only have strong effects on the elemental rates of the late translocation events,  $k_4$  and  $k_5$  (Table 2-4), but also alter the fluorescence signatures that describe the dynamics of the ribosome during translocation.

The SSU head swiveling and the SSU body rotation are the most important motions of the ribosome in early translocation. The head and the body of the SSU move synchronously in the forward (counter clockwise) direction after EF-G binding. During EF-G engagement and GTP hydrolysis, the SSU head still moves forward whereas the SSU body starts to rotate in the backward (clockwise) direction. The uncoupled movement of the SSU head and body leads to the “unlocking” of the ribosome which alleviates the physical hurdles for the movement of the tRNAs (Belardinelli et al., 2016a; Belardinelli et al., 2016b). Replacement of GTP with GTP $\gamma$ S, a slowly hydrolysable GTP analogue, slows down the backward rotation of the body of the SSU. The backward swiveling of the SSU head is delayed until the last step, step 5. The rates of steps 3 and 5 are reduced by factors of 40 and 20, respectively (Belardinelli et al., 2016a). The antibiotic fusidic acid, which inhibits the dissociation of EF-G-GDP from the ribosome, does not affect the forward and backward rotation of the SSU body and the forward swiveling of the SSU head domain. However, the backward movement of the SSU head and the rates of late translocation events were changed (Belardinelli and Rodnina, 2017).

There are similarities and differences to the results observed with the EF-G tip mutants. The rates of steps 4 and 5 were reduced by factors of 15 and 40, respectively, in translocation promoted by EF-G Q507D (Table 2-4). The backward rotation of the SSU body domain begins much later with the EF-G mutants than with wt EF-G: it is essentially completed at step 2 with wt EF-G, but continues until the end of step 5 with the mutants. The forward swiveling of the head domain of the SSU was observed with both wt EF-G and EF-G mutants. However, the backward swiveling that is observed with wt EF-G at step 3 (intermediate C to D) is delayed.

Previous research indicated that the uncoupled movements of the head and body domains of the SSU at step 2 reduce the interactions between mRNA, tRNAs and the ribosome allowing the movement of the mRNA-tRNA complex (Belardinelli et al., 2016b). In contrast to wt EF-G, when translocation is promoted by EF-G Q507D or EF-G H583K, the SSU body domain moves synchronously with the SSU head domain (Figure 3-2). The synchronous movements of SSU head and body result in an incomplete “unlocking” of the ribosome. The altered dynamics of the SSU also affects the rates of the late step of translocation, such as the dissociation of tRNA and EF-G.

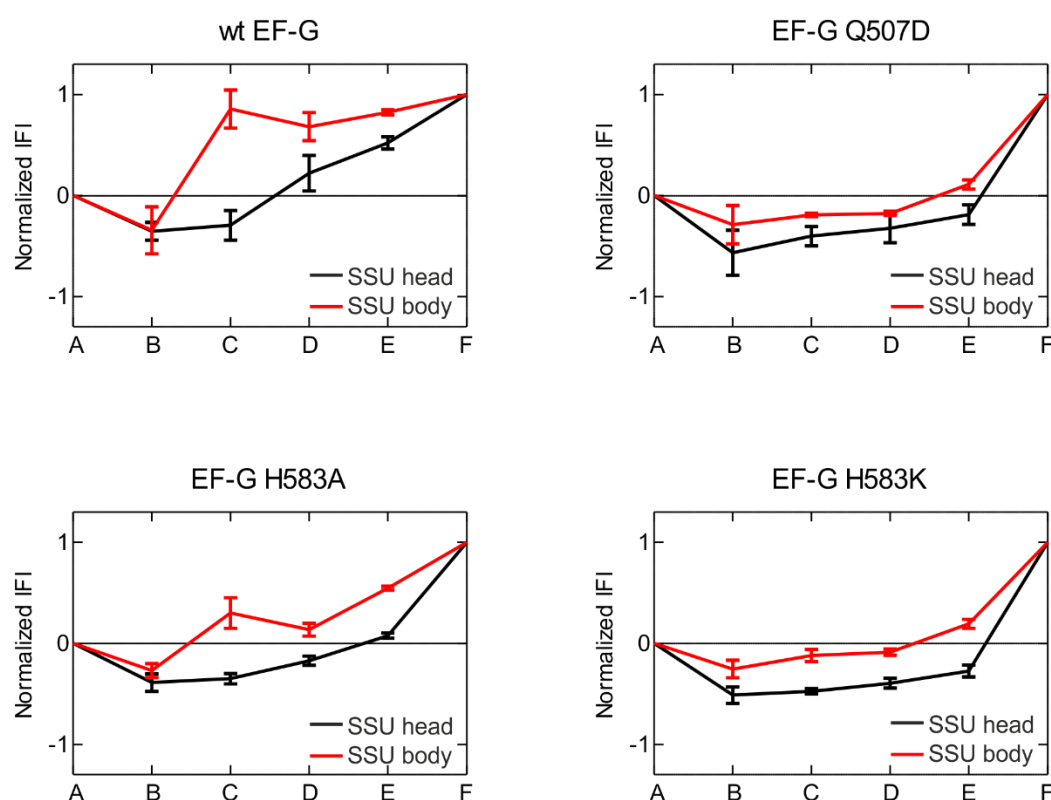


**Figure 3-2. Comparison of the dynamics of SSU head and body with variants of EF-G** Fluorescence signatures are shown as normalized IFIs. The trajectories of SSU head and SSU body are in black and red, respectively.

### 3.3. Conclusion and perspective

In summary, this work investigates the role of EF-G in reading frame maintenance during translation. The ribosome is prone to spontaneous frameshifting on slippery sequences. EF-G rapidly converts PRE complex to the POST complex, preventing the ribosomes from frameshifting at a slippery sequence. EF-G limitation prior to translocation might lead to frameshifting due to the spontaneous fluctuation of the ribosome and the potential thermodynamic preference for the  $-1$ -frame base pairing. Mutations in the tip loops of EF-G domain IV reduce the rate of translocation and increase frameshifting. The ability of EF-G to prevent frameshifting correlates with the rate of translocation. Mutations of domain IV of EF-G also change the motions of the head and body domains of the SSU, which alters the dynamics of the complex during translocation. However, the details of the mechanism by which domain IV of EF-G affects reading frame maintenance remains unclear. Does EF-G maintain the reading frame actively through the specific interactions with the tRNA (and mRNA) or passively by avoiding ribosome slippage by the acceleration of the translocation process? To better interpret the role of EF-G, particularly of the potential interactions between the tip loops of domain IV and the mRNA-tRNA complex, rapid kinetic analysis of the stepwise addition of amino acids into the nascent peptide on a slippery mRNA (mRNA7S) is required to identify the timing of reading frame slippage. Alternatively, the single molecule fluorescence resonance energy transfer (smFRET) technique may provide more information about the way translocation is affected by the mutations in EF-G. Of course, structures of an EF-G mutant-ribosome complex during translocation could be very helpful for understanding the details of the network of interactions.



## 4. Materials and Methods

### 4.1. Chemicals

Chemicals were purchased from Sigma-Aldrich (Steinheim, Germany), Roche Diagnostics (Mannheim, Germany), Merck (Darmstadt, Germany), Carl Roth (Karlsruhe, Germany), and Serva (Heidelberg, Germany), unless stated otherwise. GTP was from Jena Bioscience (Jena, Germany) and kits for plasmid DNA purification were from Macherey-Nagel (Düren, Germany). The centrifugal concentrators, cellulose citrate filters, and syringe filters were from Sartorius Biolab (Göttingen, Germany). The mRNAs were synthesized by IBA (Göttingen, Germany). Fluorophores were from Life Technologies (Darmstadt, Germany). Radioactive compounds were from Hartmann Analytic (Braunschweig, Germany) and PerkinElmer (Massachusetts, USA). Scintillation cocktail Lumasafe plus and Quickzint 361 were obtained from PerkinElmer (Massachusetts, USA) and Zinsser analytic (Frankfurt, Germany), respectively.

### 4.2. Buffers and Media

#### Reaction Buffer

---

1x TAKM <sub>7</sub>	50 mM	Tris-HCl, pH 7.5 at 37°C
	70 mM	NH <sub>4</sub> Cl
	30 mM	KCl
	7 mM	MgCl <sub>2</sub>

#### Protein purification buffers

---

EF-G purification buffer A	20 mM	Tris-HCl, pH 8.5 at 4°C
	300 mM	NaCl
	5 mM	2-mercaptomethanol (add freshly)
	15%	Glycerol

## Materials and Methods

---

EF-G purification buffer B	20 mM	Tris-HCl, pH 8.5 at 4°C
	300 mM	NaCl
	5 mM	2-mercaptomethanol (added freshly)
	15%	glycerol
	250 mM	imidazole
L7/12 opening buffer	50 mM	Tris-HCl, pH 7.4 at RT
	10 mM	MgCl <sub>2</sub>
L7/12 elution buffer	50 mM	Tris-HCl, pH 8.0 at RT
	10 mM	reduced glutathion
Factor Xa cleavage buffer	50 mM	Tris-HCl, pH 8.0 at RT
	100 mM	NaCl
	1 mM	CaCl <sub>2</sub>
L7/12 purification buffer A (HiTrap Q HP)	50 mM	Tris-HCl, pH 7.5 at RT
	10 mM	MgCl <sub>2</sub>
	2 mM	2-mercaptomethanol (added freshly)
L7/12 purification buffer B (HiTrap Q HP)	50 mM	Tris-HCl, pH 7.5 at RT
	10 mM	MgCl <sub>2</sub>
	2 mM	2-mercaptomethanol (added freshly)
	1M	KCl
GST-4B buffer A	100 mM	Tris-HCl, pH 8.5 at RT
	500 mM	NaCl
GST-4B buffer B	100 mM	Sodium acetate, pH 4.5 at RT
	500 mM	NaCl

---

S6 or L9 purification buffer	50 mM	HEPES, pH 7.25 at RT
(Gel filtration chromatography)	400 mM	KCl
	6 M	urea
	6 mM	2-mercaptomethanol

### **Depletion buffers**

---

L7/12 depletion buffer A	20 mM	Tris-HCl, pH 7.5 at RT
	20 mM	MgCl <sub>2</sub>
	0.6 M	NH <sub>4</sub> Cl
	5 mM	2-mercaptomethanol

L7/12 depletion buffer B	50 mM	Tris-HCl, pH 7.5 at RT
	7 mM	MgCl <sub>2</sub>
	30 mM	KCl
	1 mM	2-mercaptomethanol

L7/12 depletion buffer C	50 mM	Tris-HCl, pH 7.5 at RT
	7 mM	MgCl <sub>2</sub>
	30 mM	KCl
	1 mM	2-mercaptomethanol
	50%	Glycerol

### **Labeling and reconstitution buffers**

---

EF-G labeling buffer	20 mM	Tris-HCl, pH 7.0-7.5 at 4°C
	300 mM	NaCl

L7/12 labeling buffer	TAKM <sub>7</sub> reaction buffer
-----------------------	-----------------------------------



**SDS-PAGE buffers**

10x SDS running buffer	250 mM	Tris base
	1.92 M	glycine
	1%	SDS
4x SDS-PAGE loading buffer	200 mM	Tris-HCl, pH 6.8 at RT
	8%	SDS
	40%	glycerol
	< 0.4%	bromophenol blue (optional)
	400 mM	2-mercaptomethanol (add freshly)
Stacking gel solution	125 mM	1 M Tris-HCl, pH 6.8 at RT
	5%	acrylamide solution 40% (29:1)
	0.1%	SDS
	0.1%	TEMED (polymerization)
	0.1%	APS (polymerization)
Resolving gel solution	375 mM	1.5 M Tris-HCl, pH 6.8 at RT
	0.1%	SDS
	10-18%	acrylamide solution 40% (29:1)
	0.1%	TEMED (polymerization)
	0.1%	APS (polymerization)
Coomassie Blue solution	1%	Coomassie blue, in ethanol
Staining solution	10%	ethanol
	5%	acetic acid
	1 mL	coomassie blue solution

Destaining solution	10% ethanol
	5% acetic acid

### 4.3. Cell culture media

LB broth	10 g/L tryptone
	10 g/L NaCl
	5 g/L yeast extract
LB agar	10 g/L tryptone
	10 g/L NaCl
	5 g/L yeast extract
	15 g/L agar

### 4.4. mRNAs

The start AUG codon are in bold. The slippery motif is underlined. The mRNA contained the tetrameric and heptameric slippery motif are called mRNA4S and mRNA7S, respectively.

mRNA4S	5' – GUU AACAGGUAUACA UACUA <b>AUGG</b> <u>AAAAG</u> UUCAUUACC UAA - 3'
mRNA7S	5' – GUU AACAGGUAUACA UACUA <b>AUGGG</b> <u>AAAAG</u> UUCAUUACC UAA - 3'
mMF	5' – GUU AACAGGUAUACA UACUA <b>AUGG</b> UGUUCAUUAC - 3'
mMF+14Alx405	5' – GUU AACAGGUAUACA UACUA <b>AUGG</b> UGUUCAUUAC-Alx405 - 3'

### 4.5. DNA primers

Forward primer:

BP_Q507D_F	5' – GAAGGTAAACACGCGAAAGATTCTGGTGGTCGTGGTCAG - 3'
BP_Q507E_F	5' – GAAGGTAAACACGCGAAAGAATCTGGTGGTCGTGGTCAG - 3'
BP_Q507F_F	5' – GAAGGTAAACACGCGAAATTTTCTGGTGGTCGTGGTCAG - 3'
BP_Q507N_F	5' – GAAGGTAAACACGCGAAAACTCTGGTGGTCGTGGTCAG - 3'

BP\_H583A\_F 5'-GTCTGCACTTCGGTTCTTACGCTGACGTTGACTCCTCTG-3'

Reverse primer:

BP\_Q507\_R 5'-AACATCGGTAACCTTCTGGCGGATAGTTTCACG-3'

BP\_H583A\_R 5'-GAATACCCATGTCTACTACCGGGTAGCCTGC-3'

#### 4.6. Fluorophores

Alexa 488 maleimide (Alx488)	Life Technologies, Darmstadt, Germany
Alexa 568 maleimide (Alx568)	Life Technologies, Darmstadt, Germany
Atto 540Q maleimide (Atto540Q)	Atto-tec, Siegen, Germany
QSY9 C5-Maleimide	Life Technologies, Darmstadt, Germany
Fluorescein	Sigma-Aldrich, Steinheim, Germany

#### 4.7. Instruments and software

Milli-Q Advantage A10	Merck, Darmstadt, Germany
Lab pH meter inoLab® pH 720	WTW, Weilheim, Germany
Water bath RE104 and E100	Lauda-Brinkmann, Delran, USA
Centrifuge 5415R	Eppendorf AG, Hamburg, Germany
Centrifuge 5810R (F3Y-6-30 rotor)	Eppendorf AG, Hamburg, Germany
PCR thermocycler Peqstar	VWR International, Darmstadt, Germany
Nanodrop 2000x UV-Vis spectrophotometer	VWR International, Darmstadt, Germany
Emulsiflex C-3 homogenizer	Avestin, Ottawa, Canada
Phosphorimager FujiFilm 7000	FUJIFILM Europe, Düsseldorf, Germany
Plates incubator INE600	Memmert, Schwabach, Germany
Incubator shaker series Innova	Eppendorf AG, Hamburg, Germany
ÄKTA FPLC Äkta Purifier Plus	GE Healthcare, Braunschweig, Germany
Liquid scintillation counter	PerkinElmer, Massachusetts, USA

RQF-3 Rapid Quench-Flow	KinTek, Texas, USA
Electrophoresis chamber	BIORAD, California, USA
HPLC	Waters, Massachusetts, USA
Milli-Q water purification system	Merck KGaA, Darmstadt, Germany
Optima Tm L-100 XP ultracentrifuge	Beckman Coulter, Krefeld, Germany
Optima Tm MAX-XP ultracentrifuge	Beckman Coulter, Krefeld, Germany
Peqlab UV transilluminator	VWR International, Darmstadt, Germany
Spectrophotometer	PerkinElmer, Massachusetts, USA
SX-20MV stopped-flow apparatus	Applied Photophysics, Leatherhead, UK
Thermomixer comfort	Eppendorf AG, Hamburg, Germany
Vortex Genie 2	Scientific Industries Inc., New York, USA
Rotors:	
50.2 Ti	Beckmann Coulter, California, USA
JLA 8.1000	Beckmann Coulter, California, USA
TLS 55	Beckmann Coulter, California, USA
Softwares:	
GraphPad Prism	GraphPad software, California, USA
KinTek Explorer	KinTek, Texas, USA
Multigauge	Fujifilm, Tokyo, Japan
Prodata viewer	Applied photophysics, Leatherhead, UK
TableCurve	Systat Software GmbH, Erkrath, Germany
UCSF Chimera	RBVI, University of California, California, USA
Scientist Micromath	Micromath, Missouri, USA



## 4.8. Preparation of EF-G

### 4.8.1. Expression and purification of EF-G

The gene coding for EF-G was cloned into pET24 which has a T7 expression system and a C-terminal histidine tag for affinity purification. The mutations were introduced into plasmid by site-directed mutagenesis and all sequences were verified by DNA sequencing. The plasmids were transformed to *E. coli* BL21(DE3) and inoculated into the LB medium supplemented with kanamycin (30 µg/mL, all concentration reported are the final concentration in the reaction) to a starting OD<sub>600</sub> of 0.1 and grown at 37°C. The expression of EF-G was induced by the addition of IPTG (1 mM) at OD<sub>600</sub> values of 0.6 to 1.0 and incubated for another 3 hours. Cells were harvested by centrifugation at 5,000 rpm (JLA 8.1 rotor) for 20 min at 4°C. The cell pellets were dissolved in EF-G purification buffer A with the addition of Complete Protease Inhibitor and trace amount of DNaseI. Cells were then opened by Emulsiflex apparatus and the cell debris was removed by centrifugation at 30,000 rpm (JA30.50 rotor) for 1 hour.

The EF-G proteins were purified by affinity purification using the C-terminal histidine tag which facilitates rapid and efficient purification. The Protino (Ni-IDA) gravity flow column was equilibrated with EF-G purification buffer A before loading the cell to the column. For better protein purity, the column was washed several times with purification buffer A to remove the proteins that bind unspecifically. EF-G was then eluted with the purification buffer B and concentrated by membrane filtration (Vivaspin 20, 30,000 MWCO). For long-term storage at -80°C, the buffer was exchanged to 2x TAKM<sub>7</sub> by dialysis or membrane filtration and diluted to 1x by the addition of one volume of glycerol. The efficiency of expression, the quality of purification, and the concentration of EF-G proteins were determined by 12% SDS PAGE

### 4.8.2. Labeling of EF-G

In order to label EF-G with QSY9 C5-maleimide, , the three natural cysteines were replaced with corresponding amino acids residues found in other bacterial EF-G sequences (C113D, C265A, and C397S) and a cysteine was introduced at position 209 (Ala to Cys mutation) by site-directed mutagenesis. The activity of cysteine-less EF-G is indistinguishable from the wild

type EF-G. (Wilson and Noller, 1998). The cysteine-less EF-G mutants were constructed, expressed, purified, and concentrated as described above. EF-G proteins were labeled in the presence of a 5-fold molar excess of the dye in 1x EF-G labeling buffer under light protection overnight at 4°C. As QSY9 was dissolved in 100% DMSO, it was necessary to adjust the volume of the labeling mixture to have the final concentration of DMSO no more than 10%. The labeled EF-G were purified and quantified as described above.

### **4.9. Preparation of fluorescence-labeled ribosome**

#### **4.9.1. Expression and purification of L7/12**

Protein L7/12 was expressed in *E. coli* BL21(DE3) from plasmid pGEX-5x-3-L7/12 containing the gene for glutathione-S-transferase (GST) fused to the gene L7/12. A XXX residue at position 118 was mutated to Cys; the mutation was verified by DNA sequencing processes. Cells were grown in LB medium supplemented with ampicillin or carbenicillin (50 µg/mL) with starting OD600 of 0.1 and induced by the addition of IPTG (1 mM) at the OD600 value around 0.8. After 3 hours incubation, cells were harvested by centrifugation at 5,000 rpm (JLA 8.1 rotor) for 20 min at 4°C. The cell pellet was dissolved in L7/12 opening buffer with the addition of Triton X-100 (1%), Complete Protease Inhibitor, and trace amount of DNaseI. Cells were opened by Emulsiflex apparatus and the cell debris was removed by centrifugation at 30,000 rpm (JA30.50 rotor) for 1 hour.

The GST fusion L7/12 (GST-L7/12) protein was purified via gravity flow column with Glutathione Sepharose 4B as affinity medium. The Glutathione Sepharose 4B was preserved as 50% slurry in 20% EtOH at 4°C. The column was equilibrated with at least five times volume of opening/binding buffer before loading the cell lysate. After 30 min incubation at room temperature (RT) for protein binding, the column was then washed with opening buffer at least five times to remove unspecifically binding proteins. The GST-L7/12 protein was eluted twice by incubation with elution buffer (1 mL resin requires 0.5 mL buffer) at RT for 10 min and concentrated by membrane filtration (Vivaspin 20, 5,000 MWCO). The protein buffer was exchanged to TAKM<sub>7</sub> with 10% glycerol for long term storage at -80°C or to Factor Xa cleavage buffer for GST tag cleavage. The GST-tag was removed by incubation with Factor Xa at RT. It

is important to perform a pre-cleavage test to determine the cleavage time for Factor Xa. The cleavage reaction was stopped by adding phenylmethanesulfonyl (0.5 mM,) and the pH value of cleavage mixture was adjusted by adding opening/binding buffer in order to have a proper condition for efficient binding.

The column medium was regenerated by incubating twice with elution buffer at RT for 10 min to remove all the binding proteins and washing with glutathione sepharose 4B column buffer A and B sequentially several times. The regenerated column was equilibrated and the cleavage mixture was incubated as described above. The GST tag was bound to the medium and the cleaved L7/12 was collected in the flow-through. The column was washed several times with opening/binding buffer to ensure the L7/12 protein was fully washed out. The fractions that contain L7/12 were gathered and concentrated by membrane filtration (Vivaspin 20, 5,000 MWCO). The concentrated L7/12 protein was stored in TAKM<sub>7</sub> with 10% glycerol at -80°C. The efficiency of expression, the quality of purification, and the concentration of GST-L7/12 and L7/12 proteins were determined by 15% SDS PAGE.

#### **4.9.2. Labeling and purification of L7/12**

The cysteine-less L7/12 was labeled with Alexa Fluor 488 C5-maleimide by incubating protein with a 5-fold excess of dye in TAKM<sub>7</sub> at RT for 2 hours in the dark. The reaction volume was adjusted with TAKM<sub>7</sub> to dilute DMSO <10% final concentration. The purification of labeled protein was carried out by using HiTrap Q HP anion exchange chromatography column using a 0-100% KCl (0 - 1 M KCl) gradient in L7/12 purification buffer A. The excess dye was washed out with 5% KCl (50 mM) and the Alexa 488-labeled L7/12 was eluted with a 30-35% KCl (300 – 350 mM). The collected flow-through samples were checked by 15% SDS-PAGE. The fractions containing labeled protein were pooled and concentrated by membrane filtration (Vivaspin 20, 5,000 MWCO). Buffer was exchanged to TAKM<sub>7</sub> with 10% glycerol for long term storage at -80°C. The concentration of protein was determined by 15% SDS-PAGE.

### 4.9.3. Depletion and reconstitution

Since the L7/12 proteins are essential for cell survival, it is impossible to construct the L7/12 knock-out ribosome mutant strain ( $\Delta$ L7/12 ribosome). The fluorescence-labeled L7/12 was introduced by the specific depletion of the wild type ribosome of the native L7/12 proteins and the reconstitution with labeled L7/12. The depletion of L7/12 was carried out by  $\text{NH}_4\text{Cl}$ /ethanol treatment with modifications (Mohr et al., 2002; Tokimatsu et al., 1981). About 350 pmol sample of purified 70S ribosomes was incubated in 450  $\mu\text{L}$  of depletion buffer A on ice for 10 min. The mixture was mixed with 250  $\mu\text{L}$  of cold ethanol and stirred on ice for 10 min. Afterwards, another 250  $\mu\text{L}$  of cold ethanol was added and stirred on ice for 10 min. The  $\Delta$ L7/12 ribosome was precipitated by centrifugation at 13,200 rpm, for 30 min at 4°C. The procedure was repeated to improve the efficiency of depletion. The ribosome pellet was resolved in 80  $\mu\text{L}$  depletion buffer B by incubating on ice for 30 min. To store the  $\Delta$ L7/12 ribosome at -80°C, 110  $\mu\text{L}$  of depletion buffer C was added and the ribosome was quickly frozen by liquid nitrogen. The concentration of  $\Delta$ L7/12 ribosome was determined by the absorbance of  $\text{OD}_{260}$ .

The reconstitution was performed by incubating roughly 4-fold molar excess of labeled L7/12 protein over deficient ribosome at 37°C for 40 min. The 4-fold is necessary, because L12 stalk contains 4 copies of L7/12 protein on each natural *E. coli* ribosome. The reconstituted ribosome was purified via centrifugation through a 1.1 M sucrose cushion in TAKM<sub>21</sub> at 55,000 rpm (TLS 55 rotor) for 2 hours at 4°C. The pellet was dissolved in TAKM<sub>21</sub> and frozen with liquid nitrogen. The success of reconstitution was checked by GTPase assay and the concentration of ribosome was determined by the absorbance of  $\text{OD}_{260}$ .

### 4.10. Turnover GTP hydrolysis

The multiple turnover of GTP hydrolysis was tested by incubating vacant ribosome (0.5  $\mu\text{M}$ ) and EF-G (1  $\mu\text{M}$ ) together with 1 mM GTP which has a trace amount of [ $\gamma^{32}\text{P}$ ]GTP at RT. Reaction was quenched by adding same volume of 40% formic acid. Samples were analyzed via thin-layer chromatography using 0.5 M potassium phosphate (pH 3.5) as mobile phase. The radioactivity was detected by the phosphor screen and analyzed by phosphorimager.

#### 4.11. Preparation of ribosome complexes

Ribosomes from *E. coli*, f[<sup>3</sup>H]Met-tRNA<sup>Met</sup>, [<sup>14</sup>C]Phe-tRNA<sup>Phe</sup>, [<sup>14</sup>C]Lys-tRNA<sup>Lys</sup>, Glu-tRNA<sup>Glu</sup>, Gly-tRNA<sup>Gly</sup>, Phe-tRNA<sup>Phe</sup>, Val-tRNA<sup>Val</sup>, initiation factors, and EF-Tu were prepared as described (Milon et al., 2007; Rodnina and Wintermeyer, 1995). To prepare initiation complex, the 70S ribosomes were incubated with a 2-fold excess of corresponding mRNA, 1.7-fold excess of initiation factors, 3-fold excess of f[<sup>3</sup>H]Met-tRNA<sup>Met</sup>, and 1 mM GTP in TAKM<sub>7</sub> for 30 minutes at 37°C. Ternary complex was prepared by incubating a 3-fold molar excess of EF-Tu over tRNA with 1 mM GTP, 3 mM phosphoenol pyruvate, and 0.5% pyruvate kinase in TAKM<sub>7</sub> for 15 min at 37°C. Afterwards, 2-5 fold molar excess of corresponding tRNAs over ribosome were added to the EF-Tu mixture for an additional minute. The pre-translocation (PRE) complex was formed by mixing equal volumes of initiation complex and ternary complex. Purification of initiation and PRE-complexes were performed by centrifugation through a 1.1 M sucrose cushion in TAKM<sub>21</sub> at 55,000 rpm (TLS 55 rotor) for 2 hours at 4°C. Pellet was dissolved in TAKM<sub>21</sub> and the concentration of purified complex was determined by nitrocellulose filtration (Savelsbergh et al., 2000). Post-translocation (POST) complex for time resolved Pmn assay was freshly prepared by incubating purified PRE-complex and EF-G (4 μM) for a minute at 37°C. The magnesium concentration was adjusted to working concentration before use. The following experiments were carried out in TAKM<sub>7</sub> unless stated otherwise.

#### 4.12. Reading frame maintenance assay

The effects of EF-G on reading frame maintenance was examined by translating the mRNAs which contain the slippery motif for spontaneous frameshifting. The tetrameric mRNA has a tetrameric slippery motif (X\_XX.Y) and the heptameric mRNA has a heptameric slippery motif (X\_XX.Y\_YY.Z). If the ribosome loses the mRNA reading frame during translation, the translated peptides will be the -1 frame peptide (MEKV or MGKV) instead of the 0 frame peptide (MEKF or MGKF).

The preparation of purified IC that contains tetrameric or heptameric mRNA and TC with corresponding tRNAs (Glu-tRNA<sup>Glu</sup>/ Gly-tRNA<sup>Gly</sup>, [<sup>14</sup>C]Lys-tRNA<sup>Lys</sup>, Phe-tRNA<sup>Phe</sup>, and Val-tRNA<sup>Val</sup>) were performed as previously described. The translation was carried out by incubating

the purified IC, TC, and EF-G (1 nM-2  $\mu$ M) at 37°C for 5 min. Translation was quenched with KOH (0.5 M) and the peptides were released by hydrolysis at 37°C for 30 min. Samples were neutralized by adding one tenth volume of glacial acetic acid and analyzed by reversed-phase HPLC (LiChroSpher100 RP-8 HPLC column, Merck) using a 0-65% acetonitrile gradient in 0.1% trifluoroacetic acid. The 0 frame and -1 frame products were quantified by scintillation counting according to [<sup>3</sup>H]Met and [<sup>14</sup>C]Lys radioactivity labels.

### **4.13. Rapid kinetics assay**

#### **4.13.1. mRNA translocation**

The movement of the mRNA on the 30S subunit was monitored by the fluorescence Alexa 405 attached to the 3' end of the mRNA. The purified PRE-complex using the mMF-A1x405 were prepared as describe above. The experiment was performed by mixing equal volumes of PRE-complex (0.05  $\mu$ M) and EF-G (4  $\mu$ M) in stopped-flow apparatus at 37°C. A1x405 fluorescence was excited at 400 nm and measured after passing a KV418 cut-off filter. The changes of fluorescence signals were determined by exponential fitting using TableCurve software to obtain the mRNA translocation rate.

#### **4.13.2. Time-resolved puromycin assay**

The velocity of tRNA translocation of EF-G was examined by time-resolved puromycin (Pmn) reaction. The purified PRE and POST complexes containing the mMF mRNA were prepared as described above. The experiment was performed by rapidly mixing PRE or POST (0.2  $\mu$ M) with EF-G (4  $\mu$ M) and Pmn (10 mM) in a quench-flow apparatus. The reaction was quenched after a specific period of time with KOH (0.5  $\mu$ M) and the products were released from ribosome at 37°C at 30 min. Samples were then neutralized with glacial acetic acid and analyzed by reversed-phase HPLC (Chromolith®RP-8e column, Merck) using a 0-65% acetonitrile gradient in 0.1% trifluoroacetic acid. The amount of reacted and unreacted peptides were quantified by [<sup>3</sup>H]Met and [<sup>14</sup>C]Phe radioactivity counting. The apparent rates of pmn reaction

of PRE ( $k_{\text{PRE}}$ ) and POST ( $k_{\text{POST}}$ ) were determined by one-exponential fitting using GraphPad Prism. The rate of tRNA translocation ( $k_{\text{TL}}$ ) was calculated according to the rate of PRE ( $k_{\text{PRE}}$ ) and the rate of POST ( $k_{\text{POST}}$ ). The time required for PRE includes Pmn reaction and tRNA translocation while for POST only Pmn reaction is required. Deconvolution of the apparent rates from PRE and POST gives the rate of tRNA translocation ( $1/k_{\text{TL}}=1/k_{\text{PRE}}-1/k_{\text{POST}}$ ). (Holtkamp et al., 2014a).

### 4.13.3. Global fitting of translocation

Six fluorescence reporters and FRET pairs were combined for the global fitting to a linear 5-step kinetic model (Belardinelli et al., 2016a). The binding and dissociation of EF-G, small subunit (SSU) dynamic, SSU head swiveling, SSU rotation relative to the large subunit (LSU), and the P-site tRNA movements were respectively monitored by FRET between L12 and EF-G, r-protein S13, FRET between S13 and L33, FRET between S6 and L9, FRET between P-site tRNA and L33, and P-site tRNA in real time. Dr. Riccardo Belardinelli provided the ribosome subunits containing fluorescence reporters at S13 and L33 and Olaf Geintzer provided the fluorescein-labeled tRNA<sup>fMet</sup>. The labeled L12 and EF-G were prepared as described above. The ribosomal subunits with fluorescence reporters at S6 and L9 were produced as described (Sharma et al., 2016).

Labeled 30S subunit was heat-activated in TAKM<sub>20</sub> at 37°C for 30 min and then incubated with rest initiation components for an additional minute at RT. The 70S initiation complex was formed by incubating activated 30S initiation complex with a 1.5-fold molar excess of large subunit at 37°C for 30 min in TAKM<sub>7</sub>. The mMF mRNA was used for all reporters. The preparation and purification of PRE-complex were carried out as described above. The purified PRE-complex was mixed with different EF-G mutants in the stopped-flow apparatus at 37°C and the changes in fluorescence/FRET were recorded with time. Fluorescence traces were analyzed by numerical integration with KinTeK Explorer (Johnson, 2009) which gives the information about intrinsic fluorescence intensities (IFIs) of each reporter and rate constants of each step.





## 5. References

- Adio, S., Senyushkina, T., Peske, F., Fischer, N., Wintermeyer, W., and Rodnina, M.V. (2015). Fluctuations between multiple EF-G-induced chimeric tRNA states during translocation on the ribosome. *Nature Communications* 6, 7442.
- Aevarsson, A., Brazhnikov, E., Garber, M., Zheltonosova, J., Chirgadze, Y., al-Karadaghi, S., Svensson, L.A., and Liljas, A. (1994). Three-dimensional structure of the ribosomal translocase: elongation factor G from *Thermus thermophilus*. *The EMBO Journal* 13, 3669-3677.
- Agirrezabala, X., Lei, J., Brunelle, J.L., Ortiz-Meoz, R.F., Green, R., and Frank, J. (2008). Visualization of the hybrid state of tRNA binding promoted by spontaneous ratcheting of the ribosome. *Mol Cell* 32, 190-197.
- Amunts, A., Brown, A., Toots, J., Scheres, S.H.W., and Ramakrishnan, V. (2015). Ribosome. The structure of the human mitochondrial ribosome. *Science* 348, 95-98.
- Antonov, I., Baranov, P., and Borodovsky, M. (2013). GeneTack database: genes with frameshifts in prokaryotic genomes and eukaryotic mRNA sequences. *Nucleic Acids Research* 41, D152-D156.
- Atkins, J.F., Loughran, G., Bhatt, P.R., Firth, A.E., and Baranov, P.V. (2016). Ribosomal frameshifting and transcriptional slippage: From genetic steganography and cryptography to adventitious use. *Nucleic Acids Research* 44, 7007-7078.
- Ban, N., Nissen, P., Hansen, J., Moore, P.B., and Steitz, T.A. (2000). The Complete Atomic Structure of the Large Ribosomal Subunit at 2.4 Å Resolution. *Science* 289, 905.
- Belardinelli, R., and Rodnina, M.V. (2017). Effect of Fusidic Acid on the Kinetics of Molecular Motions During EF-G-Induced Translocation on the Ribosome. *Sci Rep* 7, 10536.
- Belardinelli, R., Sharma, H., Caliskan, N., Cunha, C.E., Peske, F., Wintermeyer, W., and Rodnina, M.V. (2016a). Choreography of molecular movements during ribosome progression along mRNA. *Nat Struct Mol Biol* 23, 342-348.
- Belardinelli, R., Sharma, H., Peske, F., Wintermeyer, W., and Rodnina, M.V. (2016b). Translocation as continuous movement through the ribosome. *RNA Biology* 13, 1197-1203.
- Beringer, M., Adio, S., Wintermeyer, W., and Rodnina, M. (2003). The G2447A mutation does not affect ionization of a ribosomal group taking part in peptide bond formation. *RNA* 9, 919-922.
- Beringer, M., Bruell, C., Xiong, L., Pfister, P., Bieling, P., Katunin, V.I., Mankin, A.S., Bottger, E.C., and Rodnina, M.V. (2005). Essential mechanisms in the catalysis of peptide bond formation on the ribosome. *J Biol Chem* 280, 36065-36072.

Bieling, P., Beringer, M., Adio, S., and Rodnina, M.V. (2006). Peptide bond formation does not involve acid-base catalysis by ribosomal residues. *Nature Structural & Molecular Biology* *13*, 423.

Bjork, G.R., Durand, J.M., Hagervall, T.G., Leipuviene, R., Lundgren, H.K., Nilsson, K., Chen, P., Qian, Q., and Urbonavicius, J. (1999). Transfer RNA modification: influence on translational frameshifting and metabolism. *FEBS Lett* *452*, 47-51.

Blanchard, S.C., Kim, H.D., Gonzalez, R.L., Jr., Puglisi, J.D., and Chu, S. (2004). tRNA dynamics on the ribosome during translation. *Proc Natl Acad Sci U S A* *101*, 12893-12898.

Bocchetta, M., Xiong, L., Shah, S., and Mankin, A.S. (2001). Interactions between 23S rRNA and tRNA in the ribosomal E site. *RNA* *7*, 54-63.

Bock, L.V., Blau, C., Schröder, G.F., Davydov, I.I., Fischer, N., Stark, H., Rodnina, M.V., Vaiana, A.C., and Grubmüller, H. (2013). Energy barriers and driving forces in tRNA translocation through the ribosome. *Nature Structural & Molecular Biology* *20*, 1390.

Bremer, H., and Dennis, P. (2008). Modulation of Chemical Composition and Other Parameters of the Cell at Different Exponential Growth Rates. *EcoSal Plus*.

Brierley, I., Digard, P., and Inglis, S.C. (1989). Characterization of an efficient coronavirus ribosomal frameshifting signal: Requirement for an RNA pseudoknot. *Cell* *57*, 537-547.

Brierley, I., and Dos Ramos, F.J. (2006). Programmed ribosomal frameshifting in HIV-1 and the SARS-CoV. *Virus Res* *119*, 29-42.

Brierley, I., Gilbert, R.J.C., and Pennell, S. (2010). Pseudoknot-Dependent Programmed —1 Ribosomal Frameshifting: Structures, Mechanisms and Models. In *Recoding: Expansion of Decoding Rules Enriches Gene Expression*, J.F. Atkins, and R.F. Gesteland, eds. (New York, NY: Springer New York), pp. 149-174.

Brilot, A.F., Korostelev, A.A., Ermolenko, D.N., and Grigorieff, N. (2013). Structure of the ribosome with elongation factor G trapped in the pretranslocation state. *Proc Natl Acad Sci U S A* *110*, 20994-20999.

Caliskan, N., Katunin, V.I., Belardinelli, R., Peske, F., and Rodnina, M.V. (2014). Programmed -1 frameshifting by kinetic partitioning during impeded translocation. *Cell* *157*, 1619-1631.

Caliskan, N., Wohlgenuth, I., Korniy, N., Pearson, M., Peske, F., and Rodnina, M.V. (2017). Conditional Switch between Frameshifting Regimes upon Translation of dnaX mRNA. *Molecular Cell* *66*, 558-567.e554.

Cantara, W.A., Crain, P.F., Rozenski, J., McCloskey, J.A., Harris, K.A., Zhang, X., Vendeix, F.A., Fabris, D., and Agris, P.F. (2011). The RNA Modification Database, RNAMDB: 2011 update. *Nucleic Acids Res* *39*, D195-201.

- Chen, J., Petrov, A., Johansson, M., Tsai, A., O'Leary, S.E., and Puglisi, J.D. (2014). Dynamic pathways of -1 translational frameshifting. *Nature* *512*, 328-332.
- Cornish, P.V., Ermolenko, D.N., Noller, H.F., and Ha, T. (2008). Spontaneous intersubunit rotation in single ribosomes. *Mol Cell* *30*, 578-588.
- Cornish, P.V., Ermolenko, D.N., Staple, D.W., Hoang, L., Hickerson, R.P., Noller, H.F., and Ha, T. (2009). Following movement of the L1 stalk between three functional states in single ribosomes. *Proceedings of the National Academy of Sciences of the United States of America* *106*, 2571-2576.
- Cunha, C.E., Belardinelli, R., Peske, F., Holtkamp, W., Wintermeyer, W., and Rodnina, M.V. (2013). Dual use of GTP hydrolysis by elongation factor G on the ribosome. *Translation* *1*, e24315.
- Davydov, II, Wohlgemuth, I., Artamonova, II, Urlaub, H., Tonevitsky, A.G., and Rodnina, M.V. (2013). Evolution of the protein stoichiometry in the L12 stalk of bacterial and organellar ribosomes. *Nat Commun* *4*, 1387.
- Devaraj, A., Shoji, S., Holbrook, E.D., and Fredrick, K. (2009). A role for the 30S subunit E site in maintenance of the translational reading frame. *RNA* *15*, 255-265.
- Diaconu, M., Kothe, U., Schlunzen, F., Fischer, N., Harms, J.M., Tonevitsky, A.G., Stark, H., Rodnina, M.V., and Wahl, M.C. (2005). Structural basis for the function of the ribosomal L7/12 stalk in factor binding and GTPase activation. *Cell* *121*, 991-1004.
- Doerfel, L.K., Wohlgemuth, I., Kothe, C., Peske, F., Urlaub, H., and Rodnina, M.V. (2013). EF-P Is Essential for Rapid Synthesis of Proteins Containing Consecutive Proline Residues. *Science* *339*, 85.
- Doerfel, L.K., Wohlgemuth, I., Kubyskin, V., Starosta, A.L., Wilson, D.N., Budisa, N., and Rodnina, M.V. (2015). Entropic Contribution of Elongation Factor P to Proline Positioning at the Catalytic Center of the Ribosome. *Journal of the American Chemical Society* *137*, 12997-13006.
- Drummond, D.A., and Wilke, C.O. (2009). The evolutionary consequences of erroneous protein synthesis. *Nat Rev Genet* *10*, 715-724.
- Dunkle, J.A., and Cate, J.H. (2010). Ribosome structure and dynamics during translocation and termination. *Annu Rev Biophys* *39*, 227-244.
- Dunkle, J.A., Vinal, K., Desai, P.M., Zelinskaya, N., Savic, M., West, D.M., Conn, G.L., and Dunham, C.M. (2014). Molecular recognition and modification of the 30S ribosome by the aminoglycoside-resistance methyltransferase NpmA. *Proc Natl Acad Sci U S A* *111*, 6275-6280.

- Elgamal, S., Katz, A., Hersch, S.J., Newsom, D., White, P., Navarre, W.W., and Ibba, M. (2014). EF-P Dependent Pauses Integrate Proximal and Distal Signals during Translation. *PLOS Genetics* *10*, e1004553.
- Farabaugh, P.J., and Björk, G.R. (1999). How translational accuracy influences reading frame maintenance. *The EMBO Journal* *18*, 1427-1434.
- Fayet, O., and Prère, M.-F. (2010). Programmed Ribosomal  $-1$  Frameshifting as a Tradition: The Bacterial Transposable Elements of the IS3 Family. In *Recoding: Expansion of Decoding Rules Enriches Gene Expression*, J.F. Atkins, and R.F. Gesteland, eds. (New York, NY: Springer New York), pp. 259-280.
- Fijalkowska, I.J., Schaaper, R.M., and Jonczyk, P. (2012). DNA replication fidelity in *Escherichia coli*: a multi-DNA polymerase affair. *FEMS Microbiol Rev* *36*, 1105-1121.
- Fischer, N., Konevega, A.L., Wintermeyer, W., Rodnina, M.V., and Stark, H. (2010). Ribosome dynamics and tRNA movement by time-resolved electron cryomicroscopy. *Nature* *466*, 329-333.
- Fischer, N., Neumann, P., Bock, L.V., Maracci, C., Wang, Z., Paleskava, A., Konevega, A.L., Schroder, G.F., Grubmuller, H., Ficner, R., *et al.* (2016). The pathway to GTPase activation of elongation factor SelB on the ribosome. *Nature* *540*, 80-85.
- Frank, J. (2017). The translation elongation cycle—capturing multiple states by cryo-electron microscopy. *Philosophical Transactions of the Royal Society B: Biological Sciences* *372*, 20160180.
- Fredrick, K., and Noller, H.F. (2003). Catalysis of Ribosomal Translocation by Sparsomycin. *Science* *300*, 1159.
- Gamper, H.B., Masuda, I., Frenkel-Morgenstern, M., and Hou, Y.M. (2015). Maintenance of protein synthesis reading frame by EF-P and m(1)G37-tRNA. *Nat Commun* *6*, 7226.
- Gao, Y.G., Selmer, M., Dunham, C.M., Weixlbaumer, A., Kelley, A.C., and Ramakrishnan, V. (2009). The structure of the ribosome with elongation factor G trapped in the posttranslocational state. *Science* *326*, 694-699.
- Gesteland, R.F., and Atkins, J.F. (1996). *Recoding: Dynamic Reprogramming of Translation*. *Annual Review of Biochemistry* *65*, 741-768.
- Greber, B.J., and Ban, N. (2016). Structure and Function of the Mitochondrial Ribosome. *Annu Rev Biochem* *85*, 103-132.
- Gromadski, K.B., Daviter, T., and Rodnina, M.V. (2006). A Uniform Response to Mismatches in Codon-Anticodon Complexes Ensures Ribosomal Fidelity. *Molecular Cell* *21*, 369-377.

- Gromadski, K.B., and Rodnina, M.V. (2004). Kinetic Determinants of High-Fidelity tRNA Discrimination on the Ribosome. *Molecular Cell* 13, 191-200.
- Gualerzi, C.O., and Pon, C.L. (2015). Initiation of mRNA translation in bacteria: structural and dynamic aspects. *Cell Mol Life Sci* 72, 4341-4367.
- Gurvich, O.L., Baranov, P.V., Zhou, J., Hammer, A.W., Gesteland, R.F., and Atkins, J.F. (2003). Sequences that direct significant levels of frameshifting are frequent in coding regions of *Escherichia coli*. *The EMBO Journal* 22, 5941-5950.
- Harms, J., Schlutzenzen, F., Zarivach, R., Bashan, A., Gat, S., Agmon, I., Bartels, H., Franceschi, F., and Yonath, A. (2001). High resolution structure of the large ribosomal subunit from a mesophilic eubacterium. *Cell* 107, 679-688.
- Hiller, D.A., Singh, V., Zhong, M., and Strobel, S.A. (2011). A two-step chemical mechanism for ribosome-catalysed peptide bond formation. *Nature* 476, 236-239.
- Holtkamp, W., Cunha, C.E., Peske, F., Konevega, A.L., Wintermeyer, W., and Rodnina, M.V. (2014a). GTP hydrolysis by EF-G synchronizes tRNA movement on small and large ribosomal subunits. *EMBO J* 33, 1073-1085.
- Holtkamp, W., Wintermeyer, W., and Rodnina Marina, V. (2014b). Synchronous tRNA movements during translocation on the ribosome are orchestrated by elongation factor G and GTP hydrolysis. *BioEssays* 36, 908-918.
- Howard, M.T., Gesteland, R.F., and Atkins, J.F. (2004). Efficient stimulation of site-specific ribosome frameshifting by antisense oligonucleotides. *RNA* 10, 1653-1661.
- Jacks, T., Madhani, H.D., Masiarz, F.R., and Varmus, H.E. (1988). Signals for ribosomal frameshifting in the rous sarcoma virus gag-pol region. *Cell* 55, 447-458.
- Jenner, L., Romby, P., Rees, B., Schulze-Briese, C., Springer, M., Ehresmann, C., Ehresmann, B., Moras, D., Yusupova, G., and Yusupov, M. (2005). Translational Operator of mRNA on the Ribosome: How Repressor Proteins Exclude Ribosome Binding. *Science* 308, 120.
- Jenner, L.B., Demeshkina, N., Yusupova, G., and Yusupov, M. (2010). Structural aspects of messenger RNA reading frame maintenance by the ribosome. *Nat Struct Mol Biol* 17, 555-560.
- Johnson, K.A. (2009). Fitting enzyme kinetic data with KinTek Global Kinetic Explorer. *Methods Enzymol* 467, 601-626.
- Jorgensen, F., Adamski, F.M., Tate, W.P., and Kurland, C.G. (1993). Release factor-dependent false stops are infrequent in *Escherichia coli*. *J Mol Biol* 230, 41-50.

Jorgensen, R., Carr-Schmid, A., Ortiz, P.A., Kinzy, T.G., and Andersen, G.R. (2002). Purification and crystallization of the yeast elongation factor eEF2. *Acta Crystallogr D Biol Crystallogr* *58*, 712-715.

Julian, P., Konevega, A.L., Scheres, S.H., Lazaro, M., Gil, D., Wintermeyer, W., Rodnina, M.V., and Valle, M. (2008). Structure of ratcheted ribosomes with tRNAs in hybrid states. *Proc Natl Acad Sci U S A* *105*, 16924-16927.

Katunin, V.I., Savelsbergh, A., Rodnina, M.V., and Wintermeyer, W. (2002). Coupling of GTP hydrolysis by elongation factor G to translocation and factor recycling on the ribosome. *Biochemistry* *41*, 12806-12812.

Kim, H.-K., Liu, F., Fei, J., Bustamante, C., Gonzalez, R.L., and Tinoco, I. (2014). A frameshifting stimulatory stem loop destabilizes the hybrid state and impedes ribosomal translocation. *Proceedings of the National Academy of Sciences of the United States of America* *111*, 5538-5543.

Kim, H.-K., and Tinoco, I. (2017). EF-G catalyzed translocation dynamics in the presence of ribosomal frameshifting stimulatory signals. *Nucleic Acids Research* *45*, 2865-2874.

Koh, C.S., and Sarin, L.P. (2018). Transfer RNA modification and infection – Implications for pathogenicity and host responses. *Biochimica et Biophysica Acta (BBA) - Gene Regulatory Mechanisms* *1861*, 419-432.

Konevega, A.L., Fischer, N., Semenov, Y.P., Stark, H., Wintermeyer, W., and Rodnina, M.V. (2007). Spontaneous reverse movement of mRNA-bound tRNA through the ribosome. *Nature Structural & Molecular Biology* *14*, 318.

Korobeinikova, A.V., Garber, M.B., and Gongadze, G.M. (2012). Ribosomal proteins: structure, function, and evolution. *Biochemistry (Mosc)* *77*, 562-574.

Kothe, U., and Rodnina, M.V. (2007). Codon Reading by tRNA<sup>Ala</sup> with Modified Uridine in the Wobble Position. *Molecular Cell* *25*, 167-174.

Kothe, U., Wieden, H.J., Mohr, D., and Rodnina, M.V. (2004). Interaction of helix D of elongation factor Tu with helices 4 and 5 of protein L7/12 on the ribosome. *J Mol Biol* *336*, 1011-1021.

Kramer, E.B., and Farabaugh, P.J. (2007). The frequency of translational misreading errors in *E. coli* is largely determined by tRNA competition. *RNA* *13*, 87-96.

Kubarenko, A., Sergiev, P., Wintermeyer, W., Dontsova, O., and Rodnina, M.V. (2006). Involvement of helix 34 of 16 S rRNA in decoding and translocation on the ribosome. *J Biol Chem* *281*, 35235-35244.

- Kuhlenkoetter, S., Wintermeyer, W., and Rodnina, M.V. (2011). Different substrate-dependent transition states in the active site of the ribosome. *Nature* *476*, 351-354.
- Kurland, C.G. (1960). Molecular characterization of ribonucleic acid from *Escherichia coli* ribosomes: I. Isolation and molecular weights. *Journal of Molecular Biology* *2*, 83-91.
- Kurland, C.G. (1992). Translational Accuracy and the Fitness of Bacteria. *Annual Review of Genetics* *26*, 29-50.
- Larsen, B., Wills, N.M., Gesteland, R.F., and Atkins, J.F. (1994). rRNA-mRNA base pairing stimulates a programmed -1 ribosomal frameshift. *Journal of Bacteriology* *176*, 6842-6851.
- Li, W., Liu, Z., Koripella, R.K., Langlois, R., Sanyal, S., and Frank, J. (2015). Activation of GTP hydrolysis in mRNA-tRNA translocation by elongation factor G. *Science Advances* *1*.
- Lill, R., Lepier, A., Schwägele, F., Sprinzl, M., Vogt, H., and Wintermeyer, W. (1988). Specific recognition of the 3'-terminal adenosine of tRNA<sup>Phe</sup> in the exit site of *Escherichia coli* ribosomes. *Journal of Molecular Biology* *203*, 699-705.
- Lin, J., Gagnon, M.G., Bulkley, D., and Steitz, T.A. (2015). Conformational Changes of Elongation Factor G on the Ribosome During tRNA Translocation. *Cell* *160*, 219-227.
- Lind, P.A., Berg, O.G., and Andersson, D.I. (2010). Mutational Robustness of Ribosomal Protein Genes. *Science* *330*, 825.
- Ling, C., and Ermolenko, D.N. (2016). Structural insights into ribosome translocation. *Wiley Interdisciplinary Reviews RNA* *7*, 620-636.
- Liu, G., Song, G., Zhang, D., Zhang, D., Li, Z., Lyu, Z., Dong, J., Achenbach, J., Gong, W., Zhao, X.S., *et al.* (2014). EF-G catalyzes tRNA translocation by disrupting interactions between decoding center and codon-anticodon duplex. *Nature Structural & Molecular Biology* *21*, 817.
- Liu, S., Bachran, C., Gupta, P., Miller-Randolph, S., Wang, H., Crown, D., Zhang, Y., Wein, A.N., Singh, R., Fattah, R., *et al.* (2012). Diphthamide modification on eukaryotic elongation factor 2 is needed to assure fidelity of mRNA translation and mouse development. *Proceedings of the National Academy of Sciences of the United States of America* *109*, 13817-13822.
- Loveland, A.B., Demo, G., Grigorieff, N., and Korostelev, A.A. (2017). Ensemble cryo-EM elucidates the mechanism of translation fidelity. *Nature* *546*, 113-117.
- Miller, W.A., and Giedroc, D.P. (2010). Ribosomal Frameshifting in Decoding Plant Viral RNAs. In *Recoding: Expansion of Decoding Rules Enriches Gene Expression*, J.F. Atkins, and R.F. Gesteland, eds. (New York, NY: Springer New York), pp. 193-220.

- Milon, P., Konevega, A.L., Peske, F., Fabbretti, A., Gualerzi, C.O., and Rodnina, M.V. (2007). Transient kinetics, fluorescence, and FRET in studies of initiation of translation in bacteria. *Methods Enzymol* *430*, 1-30.
- Milon, P., Maracci, C., Filonava, L., Gualerzi, C.O., and Rodnina, M.V. (2012). Real-time assembly landscape of bacterial 30S translation initiation complex. *Nat Struct Mol Biol* *19*, 609-615.
- Moazed, D., and Noller, H.F. (1989). Intermediate states in the movement of transfer RNA in the ribosome. *Nature* *342*, 142.
- Mohr, D., Wintermeyer, W., and Rodnina, M.V. (2002). GTPase activation of elongation factors Tu and G on the ribosome. *Biochemistry* *41*, 12520-12528.
- Moine, H., and Dahlberg, A.E. (1994). Mutations in Helix 34 of Escherichia coli 16 S Ribosomal RNA Have Multiple Effects on Ribosome Function and Synthesis. *Journal of Molecular Biology* *243*, 402-412.
- Moon, S., Byun, Y., Kim, H.-J., Jeong, S., and Han, K. (2004). Predicting genes expressed via -1 and +1 frameshifts. *Nucleic Acids Research* *32*, 4884-4892.
- Näsvall, S.J., Nilsson, K., and Björk, G.R. (2009). The Ribosomal Grip of the Peptidyl-tRNA is Critical for Reading Frame Maintenance. *Journal of Molecular Biology* *385*, 350-367.
- O'Connor, M., Thomas, C.L., Zimmermann, R.A., and Dahlberg, A.E. (1997). Decoding fidelity at the ribosomal A and P sites: influence of mutations in three different regions of the decoding domain in 16S rRNA. *Nucleic Acids Research* *25*, 1185-1193.
- Ogle, J.M., Brodersen, D.E., Clemons, W.M., Jr., Tarry, M.J., Carter, A.P., and Ramakrishnan, V. (2001). Recognition of cognate transfer RNA by the 30S ribosomal subunit. *Science* *292*, 897-902.
- Ortiz, P.A., Ulloque, R., Kihara, G.K., Zheng, H., and Kinzy, T.G. (2006). Translation elongation factor 2 anticodon mimicry domain mutants affect fidelity and diphtheria toxin resistance. *J Biol Chem* *281*, 32639-32648.
- Pape, T., Wintermeyer, W., and Rodnina, M. (1999). Induced fit in initial selection and proofreading of aminoacyl-tRNA on the ribosome. *EMBO J* *18*, 3800-3807.
- Pavlov, M.Y., Watts, R.E., Tan, Z., Cornish, V.W., Ehrenberg, M., and Forster, A.C. (2009). Slow peptide bond formation by proline and other <em>N</em>-alkylamino acids in translation. *Proceedings of the National Academy of Sciences* *106*, 50.



- Pellegrino, S., Demeshkina, N., Mancera-Martinez, E., Melnikov, S., Simonetti, A., Myasnikov, A., Yusupov, M., Yusupova, G., and Hashem, Y. (2018). Structural insights into the role of diphthamide on elongation factor 2 in messenger RNA reading frame maintenance. *Journal of Molecular Biology*.
- Peske, F., Savelsbergh, A., Katunin, V.I., Rodnina, M.V., and Wintermeyer, W. (2004). Conformational changes of the small ribosomal subunit during elongation factor G-dependent tRNA-mRNA translocation. *J Mol Biol* 343, 1183-1194.
- Prescott, C.D., and Kornau, H.C. (1992). Mutations in E.coli 16s rRNA that enhance and decrease the activity of a suppressor tRNA. *Nucleic Acids Research* 20, 1567-1571.
- Ramakrishnan, V. (2014). The ribosome emerges from a black box. *Cell* 159, 979-984.
- Ramrath, D.J., Lancaster, L., Sprink, T., Mielke, T., Loerke, J., Noller, H.F., and Spahn, C.M. (2013). Visualization of two transfer RNAs trapped in transit during elongation factor G-mediated translocation. *Proc Natl Acad Sci U S A* 110, 20964-20969.
- Rodnina, M.V. (2012). Quality control of mRNA decoding on the bacterial ribosome. *Adv Protein Chem Struct Biol* 86, 95-128.
- Rodnina, M.V. (2013). The ribosome as a versatile catalyst: reactions at the peptidyl transferase center. *Current Opinion in Structural Biology* 23, 595-602.
- Rodnina, M.V. (2016). The ribosome in action: Tuning of translational efficiency and protein folding. *Protein Sci* 25, 1390-1406.
- Rodnina, M.V., Savelsbergh, A., Katunin, V.I., and Wintermeyer, W. (1997). Hydrolysis of GTP by elongation factor G drives tRNA movement on the ribosome. *Nature* 385, 37-41.
- Rodnina, M.V., and Wintermeyer, W. (1995). GTP consumption of elongation factor Tu during translation of heteropolymeric mRNAs. *Proc Natl Acad Sci U S A* 92, 1945-1949.
- Rodnina, M.V., and Wintermeyer, W. (2001). Fidelity of aminoacyl-tRNA selection on the ribosome: kinetic and structural mechanisms. *Annu Rev Biochem* 70, 415-435.
- Rodnina, M.V., and Wintermeyer, W. (2009). Recent mechanistic insights into eukaryotic ribosomes. *Current Opinion in Cell Biology* 21, 435-443.
- Rodnina, Marina V., and Wintermeyer, W. (2011). The ribosome as a molecular machine: the mechanism of tRNA-mRNA movement in translocation. *Biochemical Society Transactions* 39, 658-662.
- Rodnina, M.V., and Wintermeyer, W. (2016). Protein Elongation, Co-translational Folding and Targeting. *J Mol Biol* 428, 2165-2185.

- Salsi, E., Farah, E., Netter, Z., Dann, J., and Ermolenko, D.N. (2015). Movement of Elongation Factor G between Compact and Extended Conformations. *Journal of molecular biology* *427*, 454-467.
- Sanders, C.L., Lohr, K.J., Gambill, H.L., Curran, R.B., and Curran, J.F. (2008). Anticodon loop mutations perturb reading frame maintenance by the E site tRNA. *RNA* *14*, 1874-1881.
- Satterthwait, A.C., and Jencks, W.P. (1974). The mechanism of the aminolysis of acetate esters. *J Am Chem Soc* *96*, 7018-7031.
- Savelsbergh, A., Katunin, V.I., Mohr, D., Peske, F., Rodnina, M.V., and Wintermeyer, W. (2003). An elongation factor G-induced ribosome rearrangement precedes tRNA-mRNA translocation. *Mol Cell* *11*, 1517-1523.
- Savelsbergh, A., Matassova, N.B., Rodnina, M.V., and Wintermeyer, W. (2000). Role of domains 4 and 5 in elongation factor G functions on the ribosome. *J Mol Biol* *300*, 951-961.
- Schluenzen, F., Tocilj, A., Zarivach, R., Harms, J., Gluehmann, M., Janell, D., Bashan, A., Bartels, H., Agmon, I., Franceschi, F., *et al.* (2000). Structure of Functionally Activated Small Ribosomal Subunit at 3.3 Å Resolution. *Cell* *102*, 615-623.
- Semenkov, Y.P., Rodnina, M.V., and Wintermeyer, W. (2000). Energetic contribution of tRNA hybrid state formation to translocation catalysis on the ribosome. *Nature Structural Biology* *7*, 1027.
- Sergiev, P.V., Lesnyak, D.V., Kiparisov, S.V., Burakovsky, D.E., Leonov, A.A., Bogdanov, A.A., Brimacombe, R., and Dontsova, O.A. (2005). Function of the ribosomal E-site: a mutagenesis study. *Nucleic Acids Research* *33*, 6048-6056.
- Sharma, H., Adio, S., Senyushkina, T., Belardinelli, R., Peske, F., and Rodnina, M.V. (2016). Kinetics of Spontaneous and EF-G-Accelerated Rotation of Ribosomal Subunits. *Cell Rep* *16*, 2187-2196.
- Sharma, V., Prere, M.F., Canal, I., Firth, A.E., Atkins, J.F., Baranov, P.V., and Fayet, O. (2014). Analysis of tetra- and hepta-nucleotides motifs promoting -1 ribosomal frameshifting in *Escherichia coli*. *Nucleic Acids Res* *42*, 7210-7225.
- Shoji, S., Walker, S.E., and Fredrick, K. (2006). Reverse Translocation of tRNA in the Ribosome. *Molecular Cell* *24*, 931-942.
- Tinoco, I., Kim, H.-K., and Yan, S. (2013). Frameshifting Dynamics. *Biopolymers* *99*, 1147-1166.
- Tokimatsu, H., strycharz, W.A., and Dahlberg, A.E. (1981). Gel electrophoretic studies on ribosomal proteins L7L12 and the *Escherichia coli* 50 s subunit. *Journal of Molecular Biology* *152*, 397-412.

- Traverse, C.C., and Ochman, H. (2016). Conserved rates and patterns of transcription errors across bacterial growth states and lifestyles. *Proc Natl Acad Sci U S A* *113*, 3311-3316.
- Ude, S., Lassak, J., Starosta, A.L., Kraxenberger, T., Wilson, D.N., and Jung, K. (2013). Translation Elongation Factor EF-P Alleviates Ribosome Stalling at Polyproline Stretches. *Science* *339*, 82.
- Urbonavičius, J., Qian, Q., Durand, J.M.B., Hagervall, T.G., and Björk, G.R. (2001). Improvement of reading frame maintenance is a common function for several tRNA modifications. *The EMBO Journal* *20*, 4863-4873.
- Voorhees, R.M., and Ramakrishnan, V. (2013). Structural basis of the translational elongation cycle. *Annu Rev Biochem* *82*, 203-236.
- Wilson, D.N., and Doudna Cate, J.H. (2012). The structure and function of the eukaryotic ribosome. *Cold Spring Harb Perspect Biol* *4*.
- Wilson, D.N., and Nierhaus, K.H. (2006). The E-site story: the importance of maintaining two tRNAs on the ribosome during protein synthesis. *Cell Mol Life Sci* *63*, 2725-2737.
- Wilson, K.S., and Noller, H.F. (1998). Mapping the position of translational elongation factor EF-G in the ribosome by directed hydroxyl radical probing. *Cell* *92*, 131-139.
- Wimberly, B.T., Brodersen, D.E., Clemons, W.M., Jr., Morgan-Warren, R.J., Carter, A.P., Vornrhein, C., Hartsch, T., and Ramakrishnan, V. (2000). Structure of the 30S ribosomal subunit. *Nature* *407*, 327-339.
- Wohlgemuth, I., Brenner, S., Beringer, M., and Rodnina, M.V. (2008). Modulation of the rate of peptidyl transfer on the ribosome by the nature of substrates. *J Biol Chem* *283*, 32229-32235.
- Wohlgemuth, I., Pohl, C., Mittelstaet, J., Konevega, A.L., and Rodnina, M.V. (2011). Evolutionary optimization of speed and accuracy of decoding on the ribosome. *Philos Trans R Soc Lond B Biol Sci* *366*, 2979-2986.
- Yan, S., Wen, J.-D., Bustamante, C., and Tinoco, I. (2015). Ribosome Excursions during mRNA Translocation Mediate Broad Branching of Frameshift Pathways. *Cell* *160*, 870-881.
- Youngman, E.M., Brunelle, J.L., Kochaniak, A.B., and Green, R. (2004). The Active Site of the Ribosome Is Composed of Two Layers of Conserved Nucleotides with Distinct Roles in Peptide Bond Formation and Peptide Release. *Cell* *117*, 589-599.
- Yu, C.-H., Teulade-Fichou, M.-P., and Olsthoorn, R.C.L. (2014). Stimulation of ribosomal frameshifting by RNA G-quadruplex structures. *Nucleic Acids Research* *42*, 1887-1892.

## References

---

Yusupov, M.M., Yusupova, G.Z., Baucom, A., Lieberman, K., Earnest, T.N., Cate, J.H.D., and Noller, H.F. (2001). Crystal Structure of the Ribosome at 5.5 Å Resolution. *Science* 292, 883.

Zaher, H.S., and Green, R. (2009a). Fidelity at the Molecular Level: Lessons from Protein Synthesis. *Cell* 136, 746-762.

Zaher, H.S., and Green, R. (2009b). Quality control by the ribosome following peptide bond formation. *Nature* 457, 161-166.

Zhou, J., Lancaster, L., Donohue, J.P., and Noller, H.F. (2014). How the ribosome hands the A-site tRNA to the P site during EF-G-catalyzed translocation. *Science* 345, 1188-1191.

## 6. Appendix

### 6.1. Abbreviations

$\mu\text{M}$	micromolar
A site	aminoacyl site
aa-tRNA	aminoacyl-tRNA
Cryo-EM	cryo-Electron microscopy
E site	exit site
EF-G	elongation factor G
EF-Tu	elongation factor Tu
FRET	förster resonance energy transfer
g	gram
GDP	guanosine diphosphate
GTP	guanosine triphosphate
h	hour
IF	initiation factor
IFI	intrinsic fluorescence intensity
LSU	large subunit
M	molar, mole/L
MDa	megadalton
min	minute
mL	milliliter
mM	millimolar
mRNA	messenger RNA
nm	nanometer
nM	nanomolar
OD <sub>260</sub>	absorbance at 260 nm
P site	peptidyl site
PDB	protein data bank
pmol	picomole
POST-complex	post-translocation complex
PRE-complex	pre-translocation complex

RF	release factor
RNA	ribonucleic acid
rpm	rotation per minute
RRF	ribosome recycling factor
rRNA	ribosomal RNA
RT	room temperature
S	svedberg unit
s	second
SSU	small subunit
tRNA	transfer RNA
wt	wild type

## 6.2. List of figures:

Figure 1-1. Structure of the 50S and 30S subunits.....	5
Figure 1-2. Structure of 70S ribosome.....	7
Figure 1-3. Overview of translation cycle.....	8
Figure 1-4. Overview of the elongation cycle.....	10
Figure 1-5. Mechanism of aa-tRNA selection during decoding.....	11
Figure 1-6. Scheme of translocation cycle.....	14
Figure 1-7. Retrospective editing.....	16
Figure 1-8. Kinetic model of programmed -1 ribosomal frameshifting (-1PRF).....	18
Figure 1-9. Mechanisms of induced frameshifting via defective tRNA.....	20
Figure 1-10. The structure of EF-G.....	23
Figure 1-11. Interactions between the loops at the tip of domain IV of EF-G and peptidyl-tRNA.....	24
Figure 2-1. GTP hydrolysis by EF-G.....	29
Figure 2-2. Sequence and HPLC separation profile of mRNA4S and mRNA7S.....	31
Figure 2-3. Effects of EF-G mutants on reading frame maintenance.....	32
Figure 2-4. Dependence of reading frame maintenance on EF-G concentration.....	34
Figure 2-5. Kinetic of mRNA translocation.....	36
Figure 2-6. Kinetics of tRNA translocation.....	38
Figure 2-7. Correlation between the translocation rate and frameshifting.....	40
Figure 2-8. Fluorescence reporters.....	41
Figure 2-9. Fluorescence changes of different reporters with wt EF-G.....	44
Figure 2-10. Fluorescence changes of different reporters with EF-G Q507D.....	45
Figure 2-11. Fluorescence changes of different reporters with EF-G H583K.....	46
Figure 2-12. Fluorescence changes of different reporters with EF-G H583A.....	47

Figure 2-13. Comparison of different fluorescence reporters for different EF-G mutants ..... 48

Figure 2-14. Summary of the effects of mutations in domain 4 of EF-G on translocation..... 49

Figure 3-1. Potential pathways for the divergences of reading frame..... 53

Figure 3-2. Comparison of the dynamics of SSU head and body with variants of EF-G ..... 55



---

### 6.3. List of Tables

Table 1-1. The composition of ribosomes .....	4
Table 2-1. List of EF-G mutations.....	28
Table 2-2. Dependence of frameshifting efficiency on EF-G concentration.....	35
Table 2-3. Apparent rates and translocation rates of variants of EF-G .....	39
Table 2-4. Elemental rate of sub-step of translocation .....	43



## Acknowledgements

First of all, I would like to thank Prof. Dr. Marina V. Rodnina for giving me this opportunity to join the fascinating field of ribosome and the constant support and guidance for the Ph.D. project. I also thank my committee members Prof. Dr. Holgar Stark and Prof. Dr. Ralf Ficner for their time and useful suggestions in the committee meetings. I am happy that I can always answer "I enjoy this project" in the TAC meetings. I also thank Prof. Dr. Wolfgang Wintermeyer, Dr. Alexis Caspar Faesen, and Dr. Juliane Liepe for being a part of the examination board. I would also like to thank GGNB office for organizing the doctoral program and answering all my weird questions very patiently.

I would like to specially thank Dr. Frank Peske for his patience and encouragement throughout my doctoral studies. Every discussion has always benefited me a lot, for both work and life. I also thank Dr. Riccardo Belardinelli for teaching me the amazing KinTek Explorer again and again, this software is probably the best software that I ever used for my doctoral studies. I thank all technical staff for the smooth and easy working environment. Special thanks to Michael, Olaf, and Sandra for the experimental support. I would also like to thank all my wonderful colleagues, Heena, Natalia, Sarah, Marija, Cristina, Ingo, Prajwal, Ole, Michi, Albena, Aki, Sandra, Raffa, Irena, Evan, Tamara, Mani, Namit, Masha, Neva, Katya, Cathie, Sung-Hui, Xiaolin, for the joyous atmosphere in the lab; work will be too boring without you people. Thank you for not only sharing the experimental experiences but also so many wonderful and joyful conversation. Special thanks go to our secretary Dimitra, who helped a lot of administrative work and made things simpler and easier.

It is not easy to live alone abroad and I am so grateful to my friends. Thanks to Xiaozhu, Luping, Jiahe, Gaoyuan, Vivien for the encouragement all the time. Those scientifically irrelevant conversations are really helpful to leave the unsuccessful experiments behind and refresh the minds. Mingdi, since you moved to Berlin, I am not able to find another person who is willing to sing those stupid songs with me, and the quality of my meal is also dropped off dramatically. I miss those days that you, me, and chen chat and play all night long. Thanks to the friends in Taiwan and in different countries, because all of you, I could vent my depressed emotions 24/7 without affecting anybody's working time. I would also like to thank the family of Dr. Wilkening. Without your help and support, I might not be able to come to Germany and study

here. Special thanks go to my boyfriend Pengxiang for the supporting and caring in these two years, especially during the time of writing the thesis.

The last but not the least, I would like to express my deeply grateful to my parents. Live alone abroad is difficult, but to let your child to live alone abroad for so many years is more difficult for parents. I know you have experienced so many sleepless days because of worrying. I would like to send my greatest love to my parents. Thank you for always respecting my decision and supporting me regardless financially or emotionally. I love you more than anything in this world.

In the end, I would like to dedicate my doctoral degree to my parents. Without your support, I could not reach this achievement.

## Curriculum vitae

### **BEE-ZEN PENG**

Max Plank Institute for Biophysical Chemistry  
Am Fassberg 11  
Göttingen 37077, Germany  
Phone: +49 15902280416  
Email: bpeng@mpibpc.mpg.de

### **Education**

---

- 2014-2018      Doctoral studies at the Max Planck Institute for Biophysical Chemistry  
Graduate Program GGNB - Biomolecules: Structure - Function - Dynamics  
Göttingen, Germany
- 2011-2014      M.Sc at the Georg-August-Universität Göttingen  
Microbiology and Biochemistry  
Thesis: Analysis of putative effectors in lineage-specific regions of  
*Verticillium*  
Göttingen, Germany
- 2007-2011      B.Sc at the Georg-August-Universität Göttingen  
Biology  
Thesis: Optimization of sample preparation protocols for mass  
spectrometric analysis of protein-RNA cross-linking  
Göttingen, Germany
- 2004-2007      Bachelor studies at the National Chung Hsing University (Not graduated)  
Entomology  
Taichung, Taiwan

### **Additional Research Experience**

---

- 2005-2007      National Chung Hsing University  
Internship as a laboratory assistant on the subject “The effect of methyl  
jasmonic acid on plant’s induced resistance and subsequently on the  
performance of pests.”

**Professional experience**

---

2009-2011      Max Planck Institute for Biophysical Chemistry  
                    Bioanalytical Mass Spectrometry Laboratory  
                    Working as student assistant

**Personal information**

---

Date of birth    3<sup>rd</sup> May, 1985  
Place of birth   Taichung, Taiwan  
Language        Chinese (Native Language)  
                    English, German